Detection of ligand-gated chloride ion channels on human lymphocytes

Alam, Sabina

Award date:
2004

Awarding institution:
University of Bath

DETECTION OF LIGAND-GATED CHLORIDE ION CHANNELS ON HUMAN LYMPHOCYTES

Submitted by Sabina Alam

for the degree of PhD
of the University of Bath
2004

ProQuest LLC
789 East Eisenhower Parkway
P.O. Box 1346
Ann Arbor, MI 48106-1346

List of Abbreviations

Ab	antibody
APS	ammonium persulphate
ACh	acetylcholine
AChR	acetylcholine receptor
AM	acetoxymethyl ester
BSA	bovine serum albumin
bp	base pairs
° C	degree celcius
Ca^{2+}	calcium ion
$[Ca^{2+}]_i$	intracellular free calcium ion concentration
cDNA	complementary DNA
dd	double distilled
DEPC	diethyl pyrocarbonate
DTT	dithiothreitol
EC_{50}	concentration producing a half maximum response
EDTA	ethylenediaminetetracetic acid
EGTA	ethyleneglycol-bis(β-aminoethyl ether)-N,N,N',N'-tetraacetic acid
FACS	Fluorescence activated cell sorting
FAM	6-carboxy-fluorescein
FBS	fetal bovine serum
FITC	fluorescein isothiocyanate
FLIPR	fluorometric imaging plate reader
fMLP	N-formyl-L-methionyl-L-leucyl-phenylalanine
g	gravitational force
GABA	gamma-amino butyric acid
HEPES	N-[2-hydroxyethyl] piperazine-N' – [2-ethanesulfonic acid]
IC_{50}	concentration producing 50 % inhibition
IP_3	insitol triphosphate
kb	kilobase pairs
kDa	kilo Daltons
LB	(Luria Bertani) Broth
LGIC	ligand-gated ion channel
LPS	lipopolysaccharide
mRNA	messenger RNA
nAChR	nicotinic acetylcholine receptor
PBS	phosphate buffered saline
PBMC	peripheral blood mononuclear cell
PCR	polymerase chain reaction
PFA	paraformaldehyde
PEI	polyethylenimine
pH	$-\log_{10}$ (hydrogen ion concentration)
pH_i	intracellular pH
PMSF	(4-bromo) phenylmethylsulphonyl fluoride
RBC	red blood cell
rRNA	ribosomal RNA

RT	reverse transcriptase
RT-PCR	reverse-transcriptase polymerase chain reaction
SDS	sodium dodecyl sulphate
SDS-PAGE	sodium dodecyl sulphate polyacrylamide gel electrophoresis TBE tris borate EDTA
TEMED	N,N,N'N'-tetramethylethylenediamine
Tween 20	polyoxyethylenesorbitan monolaurate
v/v	volume to volume
w/v	weight per unit volume

List of Figures

List of Tables

Summary

Recently it has been reported that some receptors normally found in the nervous system may also be present on immune cells, including T-cells and neutrophils (Bergeret *et.al.*, 1998; Wheeler *et.al.*, 2000; Froh *et.al.*, 2002). This includes suggestions that these receptors may regulate immune cell activation. Functional data also exists to indicate that $GABA_A$ receptors may be present in mouse T-cells (Tian *et.al.*, 1999). The initial aim of the project was to determine if such receptors might play a similar role in human leukocytes. We used RT-PCR and real-time quantitative TaqMan RT-PCR to screen for receptor subunit mRNAs in human leukocytes. Many of these subunit mRNAs were detected in human PBMC and Jurkat cells, although quantitative studies showed these were expressed at low levels.

$GABA_A$-R α1, α3, β2, δ and ε subunit mRNAs were detected in PBMC and Jurkat cells, while the GlyR β subunit mRNA detected in Jurkat cells only. Functional studies were carried out by studying the effects of GABA and glycine on the increase in intracellular $[Ca^{2+}]$ in response to 1 nM fMLP or 1 mg/ml LPS in rat and human PBMC and neutrophils. Based on the published rat data, GABA and glycine were expected to inhibit this release. However, application of neither GABA nor glycine led to a reduction in the response to either agonist. In rat and human PBMC, some reduction of intracellular $[Ca^{2+}]$ was detected upon application of 1 mM GABA. These results indicate that mammalian neutrophils do not express functional $GABA_A$ or glycine receptors, but that $GABA_A$ receptors are present in mammalian PBMC.

Contents

Acknowledgements

Many, many thanks to my supervisor, Dr. Adrian Wosltenholme for all his advice and moral support over the years, and especially for always making the time to have a quick discussion when it was needed. Also, much gratitude to my industrial supervisor, Dr. David Laughton at AstraZeneca (Loughborough) for always being available to discuss progress on the project and for being more than accommodating when work needed to be carried out at AstraZeneca. Sincere thanks also to Professor Anne Stephenson (London School of Pharmacy), for her kind gift of the $GABA_A$ α1 antibody, without which I would have no protein expression data to discuss!!! I am also extremely indebted to Dr Adrian Wolstenholme, Dr Nathalie Aptel, Dr Adrian Liftschitz, Patty Chen, Alistair Monk and Dr. Sam Boundy for always being more than willing to donate their blood whenever it was needed (which was often!). Also, many thanks to Dr.Verna Lavendar and the nurses at the medical centre for performing the phlebotomies.

Immense gratitude goes towards my parents, Mohammed Shamsul Alam and Rowshan Alam, for their unwavering support and encouragement throughout my life and especially over the last three years, for being so understanding and accommodating, and for the many 'take-away' meals given to me over the last three years. I am also indebted to my father-and mother-in-law, Benjamin and Bertha Muneton for the many trips to and from Bath, and for providing so much emotional support and encouragement. Countless thanks is also extended towards my husband, Roberto Muneton for all his love, understanding and complete support over the years, and particularly over the last few months for putting up with me, for coming to my aid every time my laptop decided to freeze or the printer decided to go to sleep, and also for giving me many cups of tea!

I have gained many wonderful friends during the course of my time at Bath all of whom I have to thank for making coming to work each day a pleasant experience. Dr. Virginia Portillo, Dr. Darran Yates, Kate Ralphs, Patty Chen, Dr. Adrian Rogers and Sandra Barns are all guilty of being my 'comrades', and my love and thanks goes to them for all the light entertainment, the many (sometimes weird) discussions and not least for making the lab such a pleasant place to work in.

The most exciting phrase to hear in science, the one that heralds new discoveries, is not Eureka! (I found it!) but rather, "hmm.... that's funny...."

- Isaac Asimov

Chapter 1

Introduction

1.1 – Interactions between the immune and nervous systems

Recent advances in the study of interactions between the immune and nervous systems has led to increasing experimental and clinical evidence indicating the occurrence of bidirectional communication between the two systems. A vast network of communication exists, as primary (bone marrow and thymus) and secondary (spleen and lymph nodes) lymphoid organs are supplied with an autonomic (mainly sympathetic) efferent innervation and with an afferent sensory innervation (Felten *et al.*, 1985; Cavagnaro, 1986; Fatani *et al.*, 1986; Felten *et al.*, 1988; Artico *et al.*, 2002).

The nervous and immune systems communicate in two different ways: neurohormones and neurotransmitters use anatomical and functional pathways related to the pituitary and autonomic systems, and the immune system is able to modulate some nervous functions via the action of a group of soluble proteins called cytokines (Bongioanni, 1993). Developments in immunohistochemistry have enabled assessment of a differential localisation of intramedullary nerve fibres in bone marrow. In the rat, noradrenergic fibres and spinal nerve branches supply the bone marrow (Felten *et al.*, 1985; Felten *et al.*, 1988; Tabarowski *et al.*, 1996). In mice, immunoreactivity for tyrosine hydroxylase (TH), a marker for sympathetic nerves, was found around large vessels, with occasional TH-positive fibres ending in the bone marrow (Tabarowski *et al.*, 1996). The intimate association between nerve fibres and haematopoietic and stromal cells is considered important for neural modulation of haematopoiesis, including maintenance of the blood-marrow interface, control of peripheral blood cell number and mobilisation of colony forming cells (Tabarowski *et al.*, 1996; Afan *et al.*, 1997).

A functional role for cholinergic innervation of the haematopoietic compartment was also recently proposed in view of the demonstration of choline acetyltransferase (ChAT)-immunoreactive nerve fibre-like structures in rat femur bone marrow around haematopoietic islets (Artico *et al.*, 2002). Also, accessory immune cells (e.g. monocytes and macrophages) and lymphocytes have been

shown to express specific membrane receptors for several neurotransmitters and neuropeptides, including adrenergic, dopamine and cholinergic receptors (Halper *et al.*, 1984; Bering *et al.*, 1987; Maslinski *et al.*, 1992; Costa *et al.*, 1995; Ricci *et al.*, 1995; Bondy *et al.*, 1996; Hiemke *et al.*, 1996; Bany *et al.*, 1999; Tayebati *et al.*, 2002; Wang *et al.*, 2002; Dantzer & Wollman, 2003; Mignini, 2003). These receptors have been shown to respond *in vivo* and *in vitro* to the neural substances and their manipulation can alter immune responses.

Neuromediators and neuropeptides can be found at sites of immune and inflammatory reactions (Nio *et al.,* 1993; Tissot *et al.,* 1988; Kawashima and Fujii, 2000) and modulate immune responses (Goetzl *et al.,* 1990). Changes in immune function can also influence the distribution of nerves and the expression of neural receptors in lymphoid organs (Mignini *et al.* 2003). Therefore, in the immune system, the same transmitter originating from neural and non-neural sources may be involved in the control of immune defences. In humans, acetylcholine and the synthesizing enzyme, choline acetyltransferase (ChAT), have been found in epithelial cells (airways, alimentary tract, urogenital tract, epidermis), mesothelial cells (pleura, pericardium), endothelial cells, muscle and immune cells (mononuclear cells, granulocytes, alveolar macrophages, mast cells). The widespread expression of non-neuronal acetylcholine is accompanied by the ubiquitous presence of cholinesterase and nicotinic and muscarinic receptors (Wessler *et al.*, 2001; Wessler *et al.*, 2003).

1.2 – Leukocytes

Leukocytes or white blood cells, are responsible for both innate and adaptive immune responses. These cells respond to pathogens, cell injury and allergic reactions. In humans there are approximately 7 x 10^6 leukocytes per ml in whole blood (Roitt *et al.,* 1998). Cells of the immune system are present throughout the body. Some are resident within tissues, where they respond to local trauma and alert the defence system, while others circulate in body fluids, from where they are recruited to sites of infection. In defending the body against pathogens, white blood

cells cooperate with each other first to recognise the microorganism as an invader and then to destroy it. Three main types of leukocytes exist which are shown in Figure 1.

Leukocytes all originate in the bone marrow, from where they migrate to develop further and perform their functions. All blood cells are continuously regenerated by the process called hematopoiesis, which is believed to be the function of a single precursor cell called the pluripotent stem cell. These cells then undergo differentiation to give rise to the common myeloid and lymphoid progenitor cells. Lymphocytes are of lymphoid progenitor origin, while phagocytes and monocytes are of myeloid origin (Figure 2).

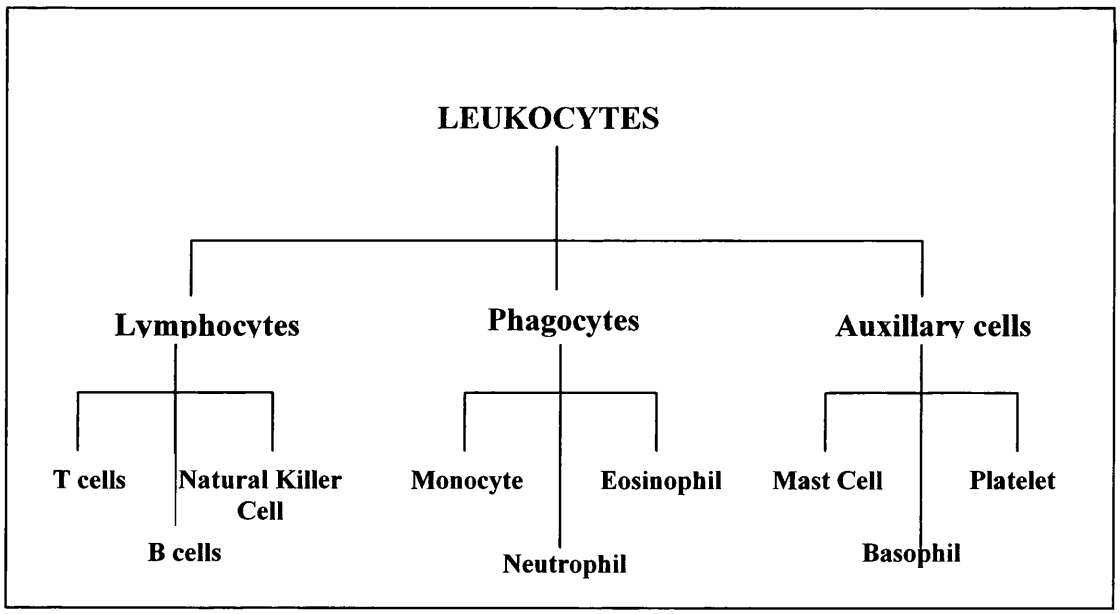

Figure 1: Types of leukocytes present in the immune system (adapted from Roitt *et al.*, 1998).

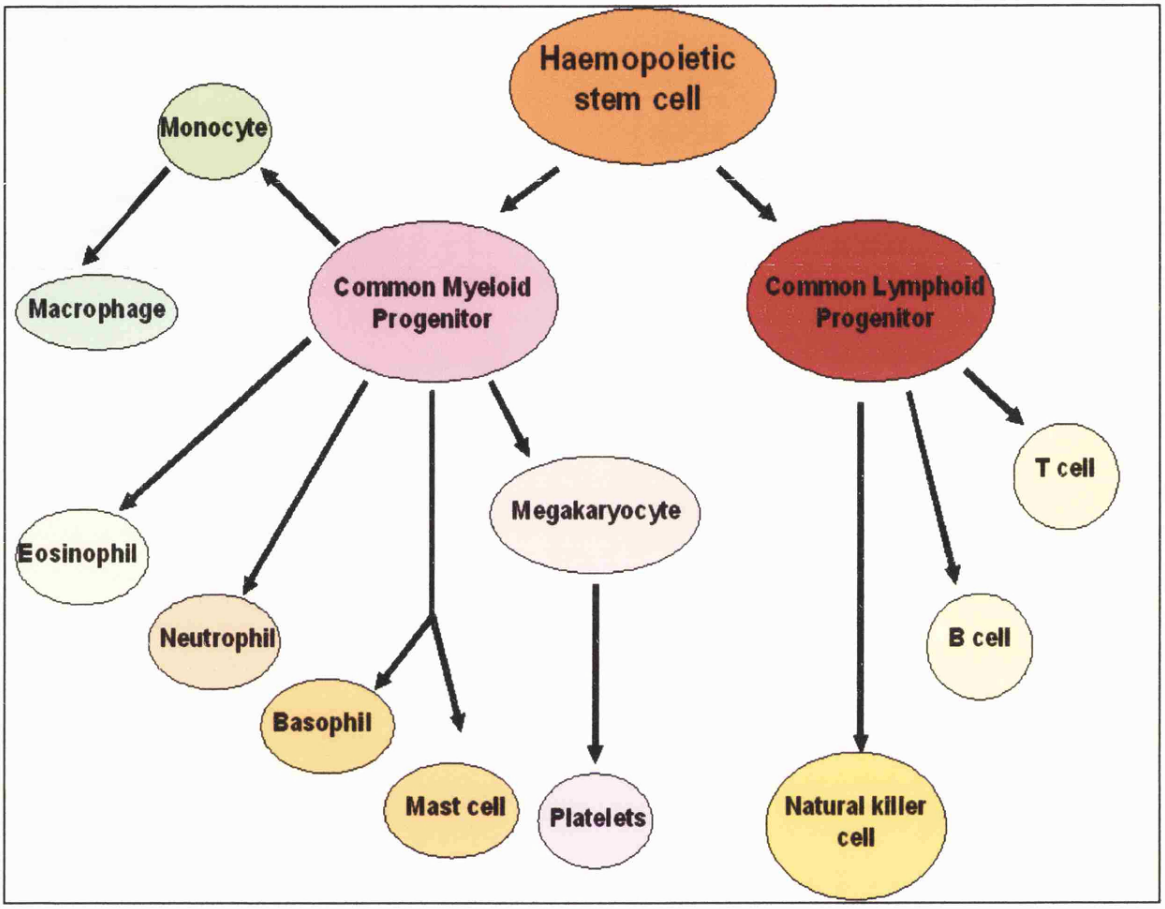

Figure 2: Origin and differentiation of leukocytes (Adapted from Roitt *et al.*, 1998). The haemopoietic cells are derived from pluripotent stem cells. These cells divide and differentiate into the more specialised progenitor cells that give rise to the lymphoid lineage and the myeloid lineage. The common lymphoid progenitor differentiates into T cells, B cells and natural killer cells. The myeloid progenitor cell differentiates to produce the three types of granulocytes: the eosinophil, the neutrophil and the basophil. It also differentiates into the mast cell and the monocyte, which in turn gives rise to the macrophage.

1.2.1 – Lymphocytes: types, structure and function

The lymphocytes make up 20 – 40% of total immune cell population in blood, and are 6 – 8 μm in diameter. These cells are divided into various classes with respect to their recognition molecules and the functions that they are programmed to perform. There are two main types of lymphocytes: the B cells and T cells (Figure 3A). B cells have surface receptors which recognise specific antigens. Upon recognising its specific antigen, B cells multiply and differentiate into plasma cells, which then produce large amounts of antibody (Reth, 1995). On activation by infection, B cells divide and differentiate into plasma cells that make antibodies (Owens, 1988). T cells have more diverse functions, which they perform on interaction with other cells of the immune system and cells infected with intracellular pathogens such as viruses. When activated by infection, T cells differentiate into effector T cells with various functions. One group of T cells interacts with B cells and assists division, differentiation and antibody production, while another group interacts with mononuclear phagocytes (Owens, 1988; Owens, 1991; Springer, 1994). These two groups of cells are the T-helper (Th) cells. A third group of cells are the T-cytotoxic (Tc) cells, which are responsible for the destruction of infected host cells (Roitt *et al.*, 1998; Abbas *et al.*, 2000).

Both B and T cells originate from lymphoid precursors in the bone marrow, but whereas B cells complete their maturation in the bone marrow before entering the circulation, T cells leave at an immature stage and migrate in the blood in the thymus, where they complete their maturation (Germain *et al.*, 2002; Spits, 2002). T- and B cells also take up residence in lymph nodes, the spleen and other tissues where they encounter antigens, continue to divide by mitosis and mature into fully functional cells (Roitt *et al.*, 1998; Abbas *et al.*, 2000; Niiro & Clark, 2002).

In addition to small lymphocytes, the blood contains large granular lymphocytes, also known as natural killer cells (Figure 3C), which function in innate immunity and are important in the defence against viral infections (Lanier *et al*, 1996). These cells make up 1.5 – 2% of leukocytes and have a diameter of ~ 8 – 12 μm. Unlike

the T and B cells, natural killer cells do not express antigen receptors, although they do contain azurophilic granules (Roitt *et al.*, 1998).

1.2.2 – Phagocytes: types, structure and function

Phagocytes mediate innate immune responses by phagocytosing microorganisms, and are the first line of defense against infection. Phagocytes can be divided into two main groups: the agranular phagocytes, which include monocytes and macrophages, and the granular phagocytes, which include neutrophils, eosinophils and basophils. The latter group are also collectively called granulocytes because of their prominent cytoplasmic granules, which contain reactive substances that kill microorganisms and enhance inflammation (Razin *et al.*, 1995).

The most abundant leukocytes are the neutrophils (60 – 70% of leukocytes), which are also the most prominent of phagocytes. These cells are 10 – 12 μm in diameter and possess a very characteristic nucleus, where it is divided into 2 – 8 lobes which are connected by thin strands of chromatin (Figure 3D). However, 1 – 2% of neutrophils have a horse-shoe shaped nucleus. In addition to the usual complement of organelles, they also contain two types of granules. Primary granules (or A granules) contain lysosomal enzymes and secondary granules (or B granules), which are the specific granules of the neutrophils, containing enzymes with strong bactericidal actions (Roitt *et al.*, 1998; Abbas *et al.*, 2000).

Unlike most cells of the body which are associated with specific locations, neutrophils migrate from the blood stream to various parts of the body, including the kidneys, lung and gut (Morris *et al.*, 2001). These cells possess general pathogen-recognition mechanisms, and play a central role in inflammatory processes (Nussler *et al.*, 1999). Large numbers invade sites of infection and begin to phagocytose tissue debris and foreign bodies, e.g. bacteria. These are the first wave of cells invading sites of infection, and their phagocytotic activity is stimulated if invading microorganisms are "tagged" with antibodies.

Eosinophils make up 2 – 5% of leukocytes and are 12 – 15 μm in diameter. The nucleus usually has only two lobes and almost all of the cytoplasm is filled with the

specific granules (Figure 3F). Aside from the usual complement of organelles, eosinophils contain some large rounded vesicles (up to 1 μm) in their cytoplasm. These specific granules contain enzymes that are otherwise found in lysosomes. The granules contain the enzymes, histaminase and sulphatase, which break down histamine and leukotrienes, which may dampen the effects of their release by basophils or mast cells (Wardlaw *et al.*, 1995).

Basophils make up 0.5 – 1% of leukocytes and have a diameter of ~ 14 μm. These cells have a 2 or 3 lobed nucleus. The lobes are usually not as well defined as in neutrophilic granulocytes and the nucleus may appear S-shaped (Figure 3E). The granules are not as numerous as those in eosinophils, and contain heparin, histamine, lysosomal enzymes and leukotrienes. Heparin and histamine are vasoactive substances and therefore facilitate the access of other lymphocytes and of plasma-borne substances of importance for the immune response (e.g. antibodies) to e.g. a site of infection. The release of the contents of the granules of basophils is receptor-mediated. Antibodies produced by plasma cells (activated B-lymphocytes) bind to Fc-receptors on the plasma membrane of basophils. If these antibodies come into contact with their antigens, they induce the release of the contents of the basophil granules (Razin *et al.*, 1995). Mast cells are bone marrow derived cells found in connective tissues. They contain granules containing substances (e.g. histamine) that contribute to inflammation.

The non granular monocytes are larger than granulocytes, make up 3 – 8% of leukocytes and are ~ 12 – 18 μm in diameter. The monocyte has a C-shaped nucleus (Figure 3B) and contains granules which in appearance and content correspond to the primary lysosome granules of neutrophils. Once monocytes enter the connective tissue they differentiate into macrophages. At sites of infection macrophages are the dominant cell type after the death of the invading neutrophils. Tissue macrophages are large cells characterised by an extensive cytoplasm with numerous vacuoles, often containing engulfed materials. They are the general scavenger cells of the body, phagocytosing and disposing of dead cells and cell debris. In both innate and adaptive immune responses, one of their roles is to engulf, kill, and break down microorganisms. Macrophages have mechanisms for recognising and reacting to pathogens, which make them important cells of innate

immunity. They also cooperate with lymphocytes to develop adaptive immune responses.

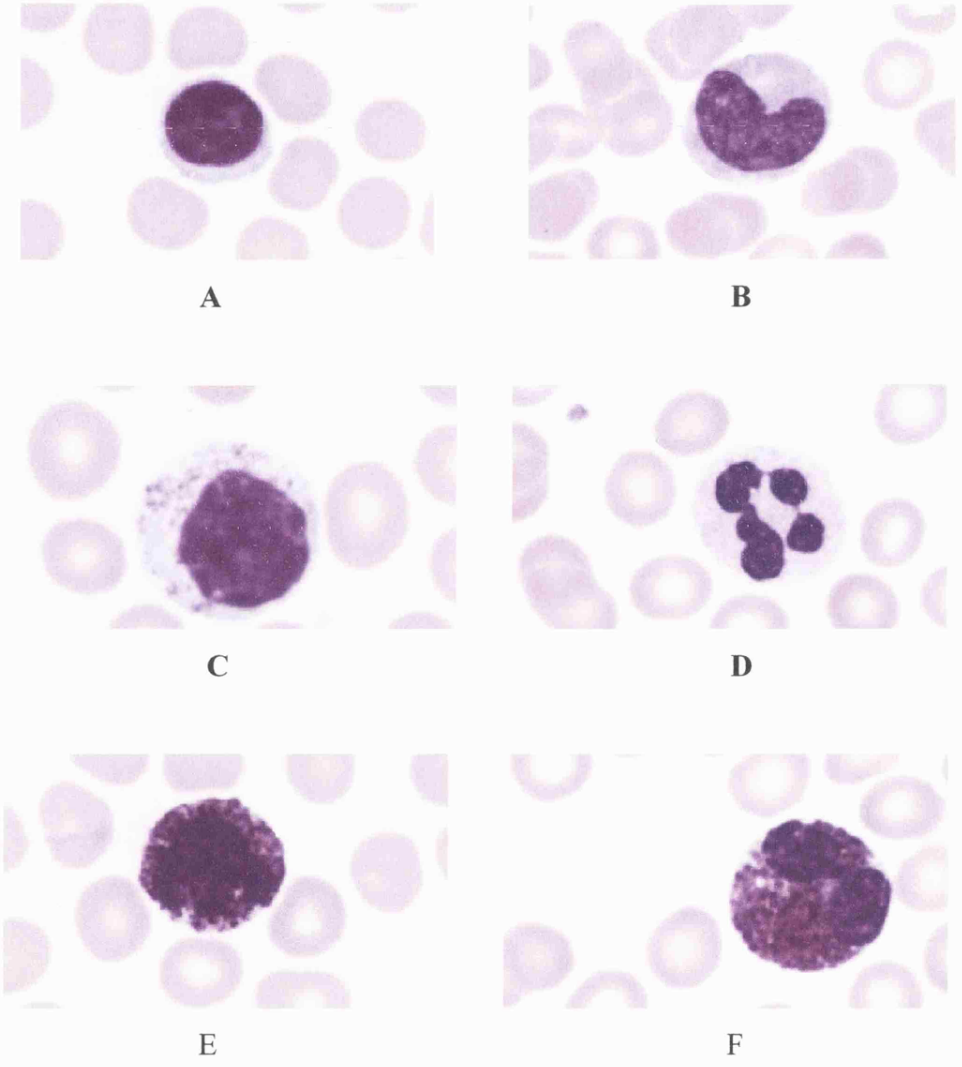

Figure 3: Micrographs of Leishman's stained immune cells. (A) Lymphocyte (T- and B-cells); (B) Monocyte; (C) Natural killer cell; (D) Neutrophil; (E) Basophil and (F) Eosinophil. Adapted from Abbas *et al.* (2000).

Lymphocytes and monocytes are also collectively called agranulocytes or mononuclear cells due to their appearance. These cells can be isolated from other immune cells as a crude preparation called peripheral blood mononuclear cell (PBMC) fraction. This preparation comprises mainly of T and B cells (~ 90%) and is commonly used in studies where lymphocytes in general are of interest.

1.3 – Presence of neurotransmitters in immune cells

Neurotransmitters such as acetylcholine, serotonin and dopamine have all been reported to be present in the blood of several mammals, including humans (Fujii, *et al.,* 1997; Yamada, *et al.,* 1997; Kawashima *et al.,* 1998; Kawashima *et al.*, 2000; McKenna *et al.*, 2002; Wang *et al.*, 2002; Ghosh *et al.*, 2003; Fajardo *et al.*, 2003; Gordon *et al.*, 2003). Acetylcholine, in particular has been detected in the blood and plasma of various mammals and has been suggested to have a role in immune modulation. (Maslinkski, 1989; Rinner and Schauenstein, 1991; Kawashima and Fuji, 2000). Acetylcholine is a main peripheral, autonomic and brain excitatory neurotransmitter, and increasing evidence indicates that mammalian peripheral blood lymphocytes possess a cholinergic system and that ACh acting as an autocrine or paracrine factor may regulate immune cell function (Bany *et al.*, 1999; Fujii and Kawashima, 2001; Wang *et al.*, 2002). Also, ACh and various muscarinic and nicotinic ACh receptor agonists have been shown to modulate lymphocyte function and metabolism (Kawashima & Fujii, 2000). In particular, Fujii and Kawashima (2000), while examining the effects of ACh and muscarinic agonists on the intracellular free Ca^{2+} concentration ($[Ca^{2+}]_i$) in human T-cell (CEM) and B-cell (Daudi) lines, provided the first evidence that ACh released from T-lymphocytes triggers nuclear signalling and upregulation of gene expression in T- and B-lymphocytes via muscarinic receptors. Functional and molecular studies have also established the presence of both the ionotropic nicotinic acetylcholine (nACh) and the metabotropic muscarinic (mACh) receptors in several human immune cell types, particularly in T and B cells (Link *et al.*, 1992; Fujii *et al.*, 1999; Kawashima *et al.*, 1998; Tayebati, *et al.* 2002). The presence of nicotinic ACh receptors on lymphocytes has been demonstrated by radiolabeling, fluorescent labelling and immunocytochemistry (Kawashima & Fujii, 2000). Recent molecular biological

studies revealed the expression of nicotinic receptor α3, α5 and β4 subunits in human thymocytes (Mihovilovic & Roses, 1991; Mihovilovic & Roses, 1993) and the α3 and α4 subunits in human circulating lymphocytes (Hiemke *et al.*, 1996). Also, Skok *et.al.* (2003) showed that functional nicotinic ACh receptors are expressed on B-cell lines.

Enhanced cholinergic stimulation is a well-known phenomenon in patients with bronchial asthma, and acetylcholine might stimulate alveolar macrophages to release neutrophil, monocytes and eosinophil chemotactic factors (Sato *et al.*, 1998). To date, the presence of ACh in human blood and ACh synthesis by choline acetyltransferase (ChAT) has been reported in T and B-cells, granulocytes, macrophages and mast cells (Kawashima and Fujii, 2000; Wessler *et al.,* 2001; Tayebati *et al.*, 2002). The gene encoding ChAT is also expressed in human leukemic T cell lines. This is supported by findings that human T cell lines, but not B cell lines, possess high ChAT activity and high intracellular ACh content (Fujii *et al.,* 1999). Also, the majority of acetylcholinesterase (AChE) activity appears to reside in T cells (Topilko & Caillou, 1985; Szelenyi *et al.*, 1987; Paldi-Harris *et al.*, 1990). Ando *et al.* (1999) detected the expression of mRNAs encoding three different AChE isoforms in human mononuclear lymphocytes (mainly T cells) and leukemic T cell (CEM) and B cell (Daudi) lines using RT-PCR. It has therefore been hypothesised that blood ACh may originate primarily from T cells and interact with ACh receptors on themselves and other blood cells, serving as an immunomodulator (Fujii and Kawashima, 2001). Recent studies on human macrophages by Wang *et al.* (2002) have shown that the nicotinic acetylcholine receptor α7 subunit is necessary for cholinergic inhibition of TNF release, making it an essential regulator of inflammation.

Dopamine, a catecholamine neurotransmitter, has been reported to influence the growth and proliferation of lymphocytes, and pharmacologically relevant doses of dopamine have been shown to modulate T cell functions significantly (Saha *et al.*, 2001). This information correlates with findings that significantly elevated plasma dopamine levels are observed in humans during stress, and suppression of T cell functions during stress is a well-known phenomenon. Saha *et al.* (2001) evaluated

the effect of the dopamine level attained in the plasma of individuals with stress on the proliferation and cytotoxicity of CD4+ and CD8+ T cells *in vitro*. At elevated physiological concentrations, dopamine was found to significantly inhibit the proliferation and cytotoxicity of CD4+ and CD8+ T cells *in vitro*. This dopamine-mediated inhibition of proliferation was more marked on CD8+ T cells than on CD4+ T cells. The underlying mechanism was found to be a D1 class of dopamine-receptor-mediated stimulation of intracellular cAMP. In a similar experiment, Ghosh *et al.* (2003) studied the effects of dopamine on the release of cytokines from activated human T cells. They observed that dopamine inhibited anti-CD3 mAb-induced release of both Th1 and Th2 cytokines, IL2, IFN-gamma and IL4 from T cells. Dopamine was found to suppress non-receptor tyrosine kinases, Lck and Fyn expression. These are the initial and pivotal signalling steps in T cell receptor (TCR) mediated different down stream signalling cascades, leading to cytokine release and subsequent clonal expansion of these immune effector cells. Dopamine D2, D3, D4 and D5 receptor expression on human leukocytes has been identified by flow cytometric techniques (McKenna *et al.*, 2002), radioligand binding assays and immunocytochemistry (Amenta *et al.*, 2002). The studies demonstrated that while B cells and NK cells showed consistently high expression, T cells and monocytes showed low expression of dopamine receptors, whereas neutrophils and eosinophils showed moderate expression.

The monoamine transmitter serotonin (5-hydroxytryptamine, 5-HT) also plays several roles in the immune system and the expression of a number of its receptor subtypes in the immune cells has also been reported (Lima & Urbina, 2002; Fajardo *et al.*, 2003; Gordon *et al.*, 2003). Stefulj *et al.* (2000) used RT-PCR methods to examine the mRNA expression of 5-HT receptors in the cells of lymphoid tissues of the rat. 13 rat 5-HT receptor genes were cloned and examined in isolated spleen, thymus, and peripheral blood lymphocytes, as well as in mitogen-stimulated spleen cells. Positive signals were obtained for a number of 5-HT receptor mRNAs in all three compartments. Mitogen (ConA and PWM) stimulated cells additionally expressed mRNA corresponding to the 5HT-3 receptor. Also, lymphocytes have been reported to carry active transport systems for serotonin. Faraj *et al.* (1994) showed that lymphocytes isolated from the blood of normal human subjects contained a high-affinity uptake system for [^{3}H]5-HT. The uptake of [^{3}H]5-HT was

potently inhibited by the antidepressants clomipramine, imipramine, fluoxetine and fluvoxamine, which are specific for the 5-HT transporter.

1.4 – Ligand-gated ion channels

Ligand-gated ion channels (LGIC), or ionotropic receptors, are receptor proteins that are also ion channels (or are directly linked to an ion channel). Binding of the transmitter to the receptor changes the channel associated with it from the open (conducting) to the closed (non-conducting) conformation. Vertebrate LGICs include **γ-aminobutyric acid type A ($GABA_A$)** and **type C ($GABA_C$)**, **glycine**, **nicotinic acetylcholine (nACh)**, **serotonin type 3 ($5\text{-}HT_3$)**, some invertebrate anionic **glutamate** receptors and P2X receptors.

1.4.1 – Structure of ligand-gated ion channels

Ligand-gated ion channel receptors are members of a superfamily of hetero pentameric glycoprotein receptors that span the membrane to form an ion channel (Macdonald & Twyman, 1991; Vernallis *et al.*, 1993). The five subunits can be homomeric or heteromeric. The receptors consist of a large extracellular N-terminus (containing a signal peptide, a cysteine bridge and glycosylation sites) and a short C-terminus (Figure 4A). There are also 4 hydrophobic transmembrane domains, M1-M4, where the polypeptides coil into alpha helices and span the membrane (Figure 4B), although there have been some reports to suggest that the polypeptides form a β-sheet in the M2 region. Between M3 and M4 is a large intracellular loop, which is the most variable region between subunits (Moss and Smart, 2001). This region may contain protein kinase A (PKA), protein kinase C (PKC), and tyrosine kinase phosphorylation sites. M2 is crucial for receptor gating and selectivity, as this region lines the channel pore and constitutes the most conserved part of the receptor. Binding of one or more molecules of the transmitter to the receptor protein induces it to shift its 3D shape (or conformation) slightly, altering the structure of the ion channel in a way that opens it. Once the transmitter unbinds or diffuses away (or is broken down), the receptor shifts back to its resting conformation.

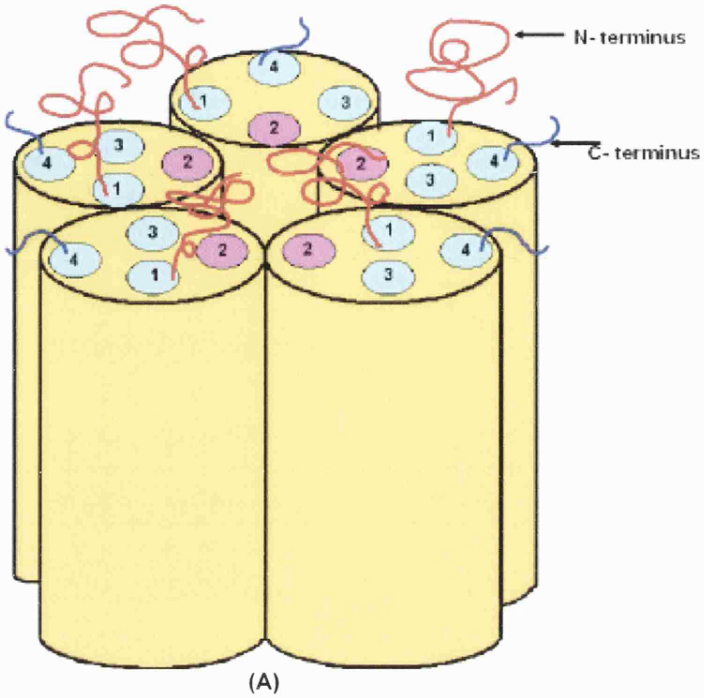

(A)

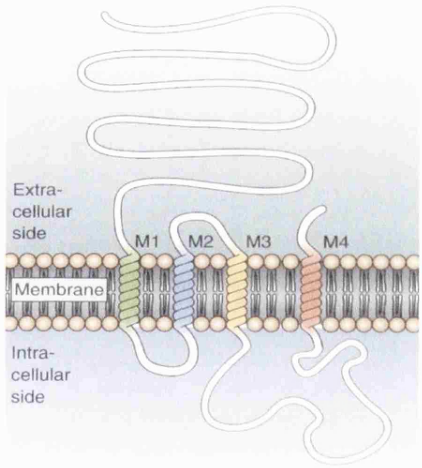

(B)

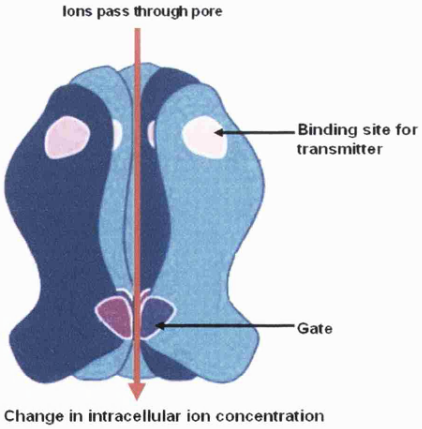

(C)

Fig 4: (A) Model of the structure of a ligand gated ion channel. This is a pentameric structure, composed of 5 subunits. Each subunit has 4 transmembrane domains named M1-M4 which is also depicted in (B) (Adapted from Bear *et al*, 1996). M2 lines the channel pore and is thought to be ion selective and a large intracellular loop is present between M3 and M4. Figures (A) and (B) also show each subunit contains a large extracellular N-terminus and a short C-terminus. Figure (C) shows a cross-section of the five assembled subunits of a ligand gated ion channel. When the transmitter binds to its receptor, the channel pore opens allowing ions to flow through into the cytoplasm of the cell. (Adapted from Bate *et al.*, 1996)

Synaptic targeting and clustering of ligand gated ion channel receptors are mediated by the interaction of the intracellular domains of these receptor subunits with the cytoskeleton (Moss and Smart, 2001). The intracellular domains of individual receptor subunits can interact with a range of diverse proteins including cytoskeletal elements, microtubule-binding proteins, neurotransmitter transporters, protein kinases and other signalling molecules.

1.4.2 – $GABA_A$ Receptors

In the central nervous system GABA is a major inhibitory transmitter. GABA is synthesised from glutamic acid, the major excitatory neurotransmitter, by one of two forms of glutamic acid decarboxylase (GAD) (Erlander and Tobin 1991). It is released from GABAergic neurons and binds to its three receptors: the ligand gated $GABA_A$ and $GABA_C$ receptors and the G – protein coupled $GABA_B$ receptor (Olsen and Tobin, 1990; Macdonald and Olsen, 1994; Chebib and Johnston, 1999).

Functional $GABA_A$ receptors are a complex of five subunits that form an intrinsic chloride ion selective channel. GABA binds to $GABA_A$ receptors allowing a passive flow of negatively charged chloride ions through the ion channel pore (as shown in Figure 4C), which usually results in hyperpolarisation of the cell membrane. However, in some neurons the activation of $GABA_A$ receptors has been shown to lead to an efflux of chloride ions and a depolarisation of the cell membrane due to higher $[Cl^-]_{int}$ than $[Cl^-]_{ext}$ (Bormann, 1988; Macdonald and Olsen, 1994; Sieghart, 1995; Wagner *et al.*, 1997).

In mammals, $GABA_A$ receptor subunits are highly heterogenous. Nineteen subunits encoded by different genes have been cloned to date and form seven families, many with multiple isoforms: α (6 isoforms), β (3 isoforms), γ (3 isoforms), ρ (3 isoforms) and one each of δ, ε, π and θ (Davies *et al.*, 1997; Hedblom *et .al.*, 1997; Bonnert *et al.*, 1999; Cherubini & Conti, 2001). The ρ subunits, identified in the retina and also present in other brain structures, are thought to co-assemble into homomeric channels that are highly sensitive to GABA

and insensitive to the $GABA_A$ receptor antagonist bicuculline, forming a distinct receptor class, called $GABA_C$ receptors (Bormann *et al.,* 1995; Bormann *et al.,* 2000). However, ρ subunits can co-assemble with other subunits to form heteromeric $GABA_A$ receptors (Qian & Ripps, 1999). The isoforms of each subunit (e.g. α1 – α6) typically exhibit amino acid sequence identities of 70 – 80%, whereas 30 – 40 % identities are found between different subunits of $GABA_A$ receptors (Lüscher, 2002). The relationship between the amino acid sequences of rat $GABA_A$ receptor subunits are depicted by the phylogenetic tree in Figure 5. The length of each branch is proportional to the inferred evolutionary distance between receptor subpopulations.

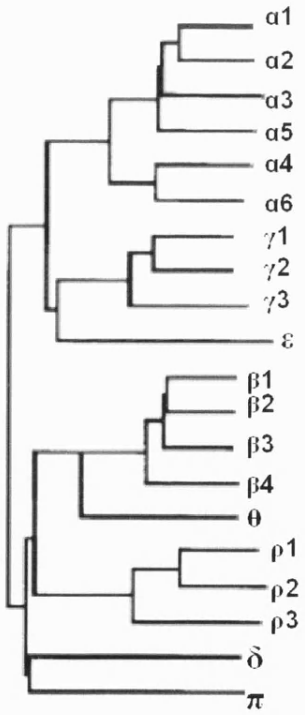

Figure 5: Phylogenetic tree of the deduced amino acid sequences of rat $GABA_A$ receptor subunits (Adapted from Cherubini & Conti, 2001). The length of each branch of the tree correlates with evolutionary distance between the different polypeptides.

The molecular masses of the subunits vary between 48,000 kDa (γ2) and 64,000 kDa (α4), and the most common native receptor stoichiometry is 2α, 2β and 1γ/δ/ε subunits (Farrar *et al.* 1999). The recently identified subunit θ, cloned from rat striatum, can also coassemble with α2, β1, γ1 (Whiting, 1999). Also, alternative splicing generates further increases in diversity. For example, the γ2 subunit gene generates two splice variants, γ2L and γ2S, that exert different functions (Cherubini & Conti, 2001).

The proximity of $GABA_A$ receptor genes on individual chromosomes may be related to their coordinate temporal and spatial regulation (Tyndale *et al.*, 1995). The chromosomal locations may therefore provide insight into the regulation of the genes, and possibly provide assistance in understanding which receptor subunits combine together *in vivo* to form functional channels. For example, the major isoform of the $GABA_A$ receptor in the brain consists of α1, β2, and γ2 subunits (Laurie *et al.*, 1992; Benke *et al.*, 1994; Macdonald & Olsen, 1994; Rabow *et al.*, 1995; McKernan & Whiting, 1996) and they have been found to colocalise in specific brain regions (Persohn *et al.*, 1992; Wisden *et al.*, 1992). Most of the subunit genes are clustered on different chromosomes, indicating gene duplication as well as cluster duplication. The α1/β2/γ2/α6 cluster is located on human chromosome 5, α5/β3/γ3 on chromosome 15, α2/β1/γ1/α4 on chromosome 4, α3/ε/θ on chromosome X, and ρ1 and ρ2 on chromosome 6. The π subunit gene is on chromosome 5 but is not clustered with the other four, and the δ subunit is alone on chromosome 1 (Tyndale *et al.*, 1995).

1.4.3 – Glycine Receptors

Glycine was first identified as an inhibitory neurotransmitter by Aprison and Werman (1965), and Davidoff *et al.* (1967), who described in detail the distribution of glycine throughout the central nervous system. Glycine has been found to be the main inhibitory transmitter in hindbrain areas (Aprison *et al.*, 1978), and its effect is

mediated through the activation of high affinity receptors localized on neurones of the spinal cord, medulla and pons (Young *et al.*, 1973). Functional studies have shown that glycine hyperpolarises postsynaptic motor neurons by increasing chloride conductance (Werman *et al.*, 1967; Curtis *et al.*, 1968a; Curtis *et al.*, 1968b).

The glycine receptor molecule was first purified as strychnine binding sites in synaptic membrane fractions of adult rat spinal cord (Pfeiffer & Betz, 1981; Pfeiffer *et al.*, 1982). It was found to compose of three distinct polypeptides: two glycoproteins of 48 kDa and 58 kDa, termed the α and β subunits respectively, and a 93 kDa cytoplasmic protein termed gephyrin (Pfeiffer & Betz, 1981; Pfeiffer *et al.*, 1982). Three different α subunit isoforms have been identified in the rat: the originally purified 48 kDa α1 subunit, a 49 kDa α2 subunit (Becker *et al.*, 1988; Kuhse *et al.*, 1990a; Akagi *et al.*, 1991) and a 50 kDa α3 subunit (Kuhse *et al.*, 1990b). Most glycine receptors in the CNS are probably composed of α and β subunits with an invariant subunit ratio of 3α:2β (Betz *et al.*, 1999; Langosch *et al.*, 1988). However, *in vitro*, homomeric α subunits can also produce functional ion channels (Grenningloh *et al.*, 1987; Betz *et al.*, 1999). Whilst homomeric glycine receptors can assemble from α-subunits, either in early development *in vivo* or from recombinant techniques to form glycine receptors with a similar pharmacology to adult spinal cord α/β heteromeric glycine receptors, they do so with low efficiency. Co-expression of recombinant α and β subunits substantially increases the efficiency of expression (Grenningloh *et al.*, 1990a; Handford *et al.*, 1996) and produces glycine receptors with an invariant stoichiometry, like that of adult spinal cord glycine receptors (Langosch *et al.*, 1988; Kuhse *et al.*, 1993). However, β subunits alone do not readily form glycine receptors, indicating that their ability to promote receptor expression and govern subunit stoichiometry arises through interactions with α subunits (Rajendra *et al.*, 1997).

A high degree of homology exists between the deduced amino acid sequences of α subunits (82 %), whereas the identity between the α1 and β subunits is 47 %

(Grenningloh, 1990b, Becker, 1992). The evolutionary distances between the glycine receptor subunits is shown by the phylogenetic tree in Figure 6.

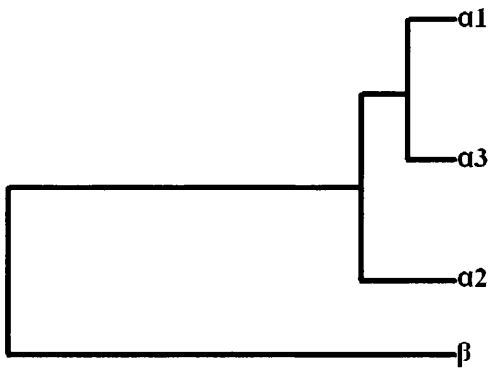

Figure 6: Phylogenetic tree of the deduced amino acid sequences of rat glycine receptor subunits (Feng & DooLittle, 1990). The length of each branch of the tree correlates with the evolutionary distance between the different polypeptides.

1.4.4 – $GABA_A$ and glycine receptor pharmacology

$GABA_A$ receptors are the sites of action of a large number of clinically useful neuroactive drugs (Olsen *et al.*, 1991a; Ticku, 1991; Sieghart, 2000). By definiton, $GABA_A$ receptors are linked to chloride channels, and are activated by isoguvacine, allosterically modulated by barbiturates and benzodiazepines, and antagonised by bicuculline (Burt & Kamatchi, 1991; Macdonald & Twyman, 1991; Olsen *et al.*, 1991b; DeLorey & Olsen, 1992). Benzodiazepines (e.g. valium and librium) modulate the actions of GABA, acting at a site different from the agonist recognition site or the barbiturate site. Functionally they enhance $GABA_A$-receptor-mediated inhibition by altering the rate of chloride channel opening that follows activation of the receptor. The benzodiazepine mode of action permitted the purification of the $GABA_A$ receptors by benzodiazepine affinity chromatography, and it has also been shown that both the affinity and efficacy of benzodiazepines is determined by the α and β subunit present in the receptor (Hadingham *et al.*, 1993; Sieghart. 1995; Hadingham *et al.*, 1996; Whiting, 1999).

Confirmatory evidence for a specific benzodiazepine site comes from molecular biology, where the α, β, and γ subunits of the receptor have been assembled in various cell lines (Olsen & Tobin, 1990). Studies have shown that benzodiazepines bind with high affinity to the $GABA_A$ receptor at an allosteric modulatory site situated on the α and γ subunit interface (Stephenson, 1995; Barnard *et al.*, 1998; Moss and Smart, 2001).

Many pharmacological agents act on the $GABA_A$ receptor including, general anesthetics and convulsants such as bicuculline, penicillin G, and β–carbolines, and GABA analogues such as muscimol (Barnard *et al.*, 1987; Burt and Kamatchi, 1991; Ticku, 1991). Other allosteric modulators of $GABA_A$ receptors include the barbiturate drugs, non-competitive chloride channel blocking agents (including picrotoxin, t-butylbicyclophosphorothionate (TBPS), certain neurosteroids, the avermectin anthelminthic agents Zn^{2+}, ethanol and the anti-convulsant drug, loreclezole (Cherubini *et al.*, 1991; Macdonald & Twyman, 1991; Smart *et al.*, 1991; Whiting *et al.*, 1997; Schmid *et al.*, 1999, Hosie *et al.*, 2003). The different $GABA_A$ receptor subunits have different sensitivities to GABA and to modulatory drugs, which bind to distinct sites within the receptor complex (Stephenson, 1995, Whiting *et al.*, 1999), which has allowed dissection by site-directed mutagenesis, leading to identification of amino acid residues involved in channel formation, subunit interactions, phosphorylation susbstrates, and ligand-binding site domains.

Unlike the $GABA_A$ receptor, the known agonist profile of the glycine receptor is limited to only a few ligands. At least two separate regions in the N-terminal extracellular domain contribute to the binding site for glycinergic agonists and strychnine (Rajendra *et al.*, 1997). A number of amino acids have been shown to mimic the action of glycine in depressing spinal cord neuron firing rates including beta-alanine, taurine, L- and D-alpha-alanine, L-serine and D-serine (Curtis and Watkins, 1960; Werman *et al.*, 1968). Also, these inhibitory efficacies parallel the ability of these amino acids to displace the high-affinity antagonist [^{3}H]strychnine from the receptor, indicating a largely competitive interaction between glycinergic agonists and strychnine (Young and Snyder, 1973).

Channel activation by glycine is competitively antagonised by strychnine albeit in a noncooperative way (Schmieden *et al.*, 1989; Sontheimer *et al.*, 1989; Aprison, 1990). Besides strychnine and its derivatives, there are only a few ligands binding to the glycine receptor with affinities in the low nanomolar range; these include the steroid RU 5135 (3α-hydroxy-16-imino-5β-17-aza-androstan-11-one) and 1,5-diphenyl-3,7-diazaadamantan-9-ol. Picrotoxin and picrotoxinin are noncompetitive inhibitors and therefore thought to interact with the anion pore of the glycine receptor. Different affinities for this alkaloid (in the micromolar range) have been reported for glycine responses recorded from a variety of CNS regions at different developmental stages (Davidoff and Aprison, 1969; Evans, 1978; Barker *et al.*, 1983) pointing to the heterogeneity of the respective glycine receptors.

1.5 – Extraneuronal functions of GABA and glycine

$GABA_A$ mediated responses are not found exclusively in the central nervous system, and several reviews have focussed on the possible role of GABA outside the mammalian nervous system (Tanaka, 1985; Erdo and Wolff, 1990; Erdo and Wekerle, 1990). GABA and its synthesising enzyme GAD, have been detected in well-defined structures of the gastrointestinal system (Hills *et al.*, 1987, Hills *et al.*, 1988), and autoradiographic studies have shown GABA-accumulating cells to be present in the duodenum (Gilon *et al.*, 1987). $GABA_A$ receptors serve to reduce hormone secretion in components of the endocrine system, including glucagon- and somatostatin-secreting cells of pancreatic islets (Michalik and Erecinska, 1992), catecholamine-secreting chromaffin cells of the adrenal medulla (Bormann & Clapham, 1985) and in several types of anterior pituitary cells (Valerio *et al.*, 1992).

Biochemical and autoradiographic studies carried out by Erdo *et al.* (1989) revealed the presence of binding sites specific for GABA and muscimol in the rat stomach. Specific binding sites for [^{3}H]GABA and [^{3}H]muscimol showing the characteristics of $GABA_A$ receptors, were demonstrated on gastric membranes. Specific muscimol binding sites were found in all regions of the stomach and were present in both the

mucosal layer and the remaining tissue of the stomach. Oral pretreatment of the rats with GABA, selective $GABA_A$ receptor agonists, or inhibitors of GABA degradation protected the gastric mucosa against the ulcers induced by acidified ethanol, in both intact and vagotomized rats. These findings suggested $GABA_A$ receptors in the rat stomach may mediate mucoprotective effects. $GABA_A$ receptors have also been described in rat and rabbit uterus (Erdo, 1984) and in the guinea pig ileum (Ong & Kerr, 1982; Ong and Kerr, 1984). Also light and electron microscopy studies have revealed GABA immunoreactivity in the rat kidney (Parducz *et al.*, 1992). Another site for GABA and $GABA_A$ receptors is in the reproductive system, particularly in the ovary, fallopian tube and uterus (Laszlo *et al.*, 1989; Erdo *et al.,* 1990; Majewska and Vaupel, 1991). In female reproductive organs $GABA_A$ receptors have been found to include a benzodiazepine-barbiturate-chloride-ionophore complex, similar to that of $GABA_A$ receptors in the central nervous system (Erdo and Maksay, 1988; Erdo and Wolff, 1990). Benzodiazepines acting at this receptor complex were shown to interfere with ciliogenesis in the oviduct. Also, Erdo and Wekerle (1990) studied the specific binding of [^{3}H]GABA to seminal membranes of swines and rams, which showed pharmacological characteristics corresponding to $GABA_A$ type receptors, suggesting that GABA may have a direct effect on spermatozoa. Hu *et al.* (2002) found that GABA can trigger mammalian sperm acrosome reaction and they presented evidence to show that rat spermatozoa contain $GABA_A$ receptors, composed of $\alpha5$, $\beta1$ and $\beta3$ subunits. GABA and GAD have been shown to be present in rodent thymus gland (Cavallotti *et al.*, 1999), and the levels of GABA have been shown to increase following an immune response (Hall *et al.*, 1985) indicating that GABA may play a role in modulation of immune responses.

Outside the nervous system glycine receptors have been reported to be present in the liver (Kupffer cells) (Ikejima *et al.,* 1997; Wheeler, 1999a; Froh *et al.*, 2002) and in neutrophils (Wheeler *et al.*, 2000) and macrophages (Wheeler and Thurman, 1999; Froh *et al.*, 2002). All these studies suggested that glycine serves to inhibit cell responses to inflammation. Studies conducted by Yamashina *et al.* (2001) demonstrated the presence of glycine-gated chloride channels in bovine endothelial cells. Glycine was shown to inhibit endothelial cell proliferation in a dose-dependent manner, and growth factor-induced migration was also significantly

blunted. Also, as glycine was shown to inhibit agonist (vascular endothelial growth factor) induced increases in $[Ca^{2+}]_i$ in endothelial cells, it was suggested that glycine may inhibit endothelial cell proliferation via inhibition of Ca^{2+} signalling. Other studies have shown that liver, lung and kidney cells exposed to endotoxin shock have increased survival rates upon application of glycine (Miller *et al.*, 1994; Ikejima *et al.*, 1996; Zhong *et al.*, 1999; Wheeler *et al.*, 2000)

1.6 – Presence of GABA and glycine receptors on mammalian immune cells

A few studies have indicated that GABA and also glycine may play a role in immunomodulation. The possible role that glycine receptors may play in rat neutrophils was demonstrated by Wheeler *et al.* (2000), where glycine was shown to inhibit agonist-induced increases in intracellular free calcium. Wheeler *et al.*, (2000) have shown some evidence that rat neutrophils may contain functional glycine-gated chloride ion channels. It was hypothesized that when glycine enters the cell, membrane hyperpolarisation occurs leading to an inactivation of voltage-gated calcium channels, and inhibits $[Ca^{2+}]_i$ release from intracellular stores. They demonstrated this by showing that upon administration of glycine to rat neutrophils, fMLP and LPS induced Ca^{2+} release was inhibited. Also, these responses were inhibited upon the application of strychnine, the competitive glycine receptor antagonist.

Bergeret *et al.* (1998) and Froh *et al.* (2002), have shown molecular evidence for the presence of a number of $GABA_A$ and glycine receptor subunits respectively. RNase protection assays, RT-PCR and western blotting experiments conducted by Froh *et al.* (2002) provided evidence for the presence of glycine receptor $\alpha 1$, $\alpha 2$ and β subunits in rat splenic and alveolar macrophages and neutrophils. Other studies have shown that application of glycine to rat alveolar macrophages and lipopolysaccharide (LPS) treated monocytes leads to decreased levels of superoxide and TNF-α production and increased levels of IL-10 expression (Wheeler and

Thurman, 1999; Spittler *et al.* 1999). The presence of $GABA_A$ receptors on immune cells was determined by Bergeret *et al.* (1998) on P815 (mouse mastocytoma mast cell line) and H9 cells (human T cell line), where the $GABA_A$ $\alpha 1$, $\alpha 2$, $\alpha 4$ and $\beta 1$ subunits were detected in RT-PCR and immunoblotting studies. Bergeret *et al.* (1998) investigated a possible contribution of GABA to the physiology of immune competent cells, and reported that GABA modulates T cell-mediated cytotoxicity, probably through $GABA_A$ receptors. Also the results showed a decreased cytotoxicity of T cells when added to GABA-treated targets indicating that GABA may also protect GABA responsive cells. Also, Tian *et al.* (1999) described the possible presence of functional $GABA_A$ receptors on mouse T cells, where the application of GABA led to inhibition of anti-CD3 and antigen-specific T cell proliferation in a dose dependent manner. These responses were also obtained upon application of the $GABA_A$ receptor agonist, muscimol, were enhanced by pentobarbital and were blocked by picrotoxin and bicuculline. These studies suggest that both $GABA_A$ and glycine receptors could be present on immune cells, where they can mediate inhibition of immune responses, and that these receptors can be modulated in a similar way to their neuronal counterparts.

AIM

There are recent reports providing pharmacological evidence for the presence of inhibitory receptors related to the $GABA_A$ and glycine ligand gated ion channel receptor families, on several different immune cell types, including T cells and neutrophils (Bergeret *et al.,* 1998; Tian *et al.*, 1999; Wheeler *et al.*, 2000). These reports included data suggesting a potential role for these receptor types in the downregulation of immune cell activation, leading to the inhibition of inflammatory immune responses. Such receptors may therefore be important targets for the development of drugs for the treatment of respiratory and inflammatory disorders. To date, however, there are no reports of the molecular isolation of functional LGICs from immune cells. The aim of my project therefore was to screen for the presence of inhibitory LGICs, in particular $GABA_A$ and glycine receptors, on human leukocytes.

RT-PCR and real-time quantitative TaqMan RT-PCR were used to screen for $GABA_A$ and glycine receptor subunit mRNAs in human leukocytes. Immunoblotting and immunofluorescence experiments were carried out to confirm the presence of $GABA_A$ $\alpha 1$ receptor subunit protein in human PBMCs and neutrophils as well as in the human T cell leukaemia cell line Jurkat J6 and in HL-60 cells, a human promyelocytic cell line. Finally, the effects of GABA and glycine on the increase in intracellular $[Ca^{2+}]$ in response to 1nM fMLP or 1mg/ml LPS was studied in rat and human PBMC and neutrophils, as an attempt to determine whether or not their receptors had any functional role in immune cells.

Chapter 2

Methods and Materials

General Materials

2.1 – Jurkat J6 and HL-60 cells

Jurkat J6 cells were kindly provided by Dr Stephen Ward, Department of Pharmacy and Pharmacology, University of Bath.

HL-60 cells were obtained from the European Collection of Cell Cultures (ECACC number 98070106, deposited by Dr. Chris Bunce, Dept. of Medicine, University of Birmingham, UK).

2.2 – Culture media and conditions

1 X RPMI 1640 medium (with L-glutamine and 25 mM HEPES) was purchased from GIBCOBRL. The medium was supplemented with 10% (v/v) fetal bovine serum (SIGMA) and 10,000 units/ml penicillin / 10mg/ml streptomycin (SIGMA).

2.3 – Freezing media

The medium used to freeze Jurkat J-6 cells consisted of 50% (v/v) FBS, 20% (v/v) DMSO, 30% (v/v) 1 X RPMI 1640 medium (with L-glutamine and 25 mM HEPES).

The medium used to freeze HL-60 cells consisted of 90% (v/v) FBS, 10 % (v/v) glycerol.

2.4 – Buffers

Table 1: Recipes for common buffers

Buffer	Composition
10 x TBE	0.89 M Tris-HCl; 0.89 M boric acid; 20 mM EDTA, pH 8.0
TE	10 mM Tris-HCl, pH 8.0; 0.1 mM EDTA
PBS	137 mM NaCl; 2.7 mM KCl; 10 mM Na_2HPO_4; 2 mM KH_2PO_4, pH 7.4
LB	10 g tryptone; 5 g yeast extract; 10 g NaCl in 1L dd H_2O
SOC	20 g tryptone; 5 g yeast extract; 0.5g NaCl; 20 mM glucose in 1L dd H_2O

Methods

2.5 – Isolation of human PBMC

Whole blood was collected into vacutainer bottles containing 15% (w/v) EDTA (Beckton Dickenson). To ensure maximum viability, cells were processed immediately. If storage was required the tubes were kept at 4° C for less than 12 hours.

To isolate peripheral blood mononuclear cells, HISTOPAQUE® 1077 (SIGMA) was used as the density gradient (polysucrose, 57 g/L, sodium diatrizoate, 90 g/L). 15 ml of HISTOPAQUE® 1077 was warmed to room temperature and added to a 50 ml LeucoSep® tube (Greiner) containing a porous filter disc. This was centrifuged at 200 x g for 5 min to spin the HISTOPAQUE® 1077 to the bottom. 25 – 30 ml of freshly anticoagulated blood was then poured into the tube and centrifuged at 800 x g for 15 min at room temperature. Once centrifuged the sequence of tube contents from top to bottom was as shown in Figure 7.

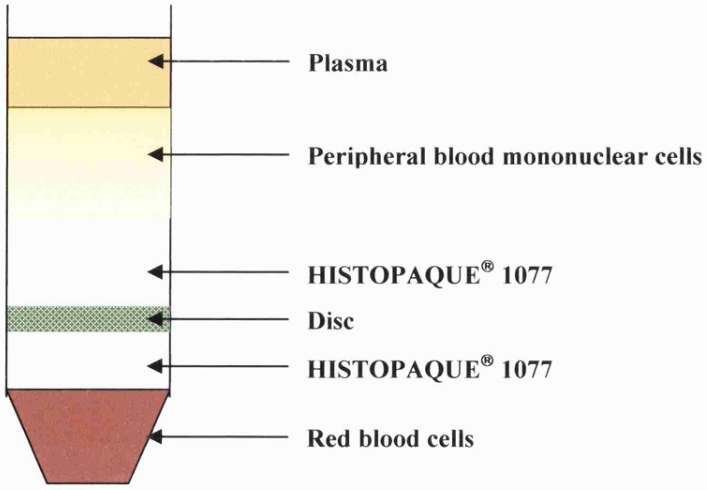

Figure 7: Sequence of tube contents in PBMC cell isolation fraction

The plasma layer was aspirated off and PBMCs were harvested and washed 3 times in 10 ml ice cold PBS/1mM EDTA and centrifuged at 300 x g for 10 min at 4° C. The purified PBMCs were then resuspended in 5 ml 1 x PBS.

2.6 – Isolation of human neutrophils

Whole blood was collected into tubes containing 15% (w/v) EDTA (Beckton Dickenson). To isolate neutrophils 17 ml of Polymorphprep (Invitrogen) at 20 °C was placed into 50 ml tubes. 25 ml of whole blood was carefully layered on to this and spun for 30 min at 500 x g. The sequence of tube contents was as shown in Figure 8. Plasma and lymphocyte layers were aspirated off and the granulocyte layer was then transferred to a fresh 50 ml tube. PBS containing 0.2% (w/v) glucose was then added to 50 ml, and the cells spun at 300 x g for 10 min. The supernatant was poured off and the cell pellet resuspended in 7.5 ml ice-cold 0.2% (w/v) NaCl. Cells were mixed for 1 min and then 7.5 ml ice-cold 1.6% (w/v) NaCl was added. PBS (with 0.2% (w/v) glucose) was added to 50 ml and cells spun at 200 x g for 10 min. This was repeated twice, and the cell pellet resuspended in 1 X PBS or the required assay buffer (see Table 10).

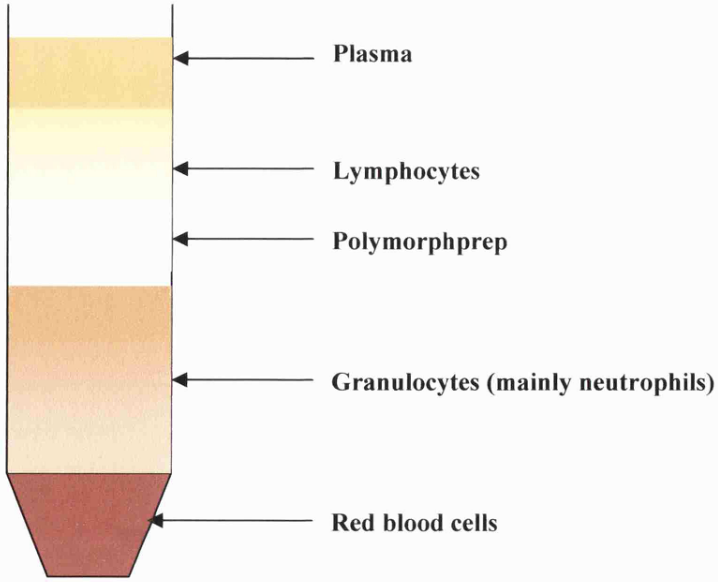

Figure 8: Sequence of tube contents during isolation of human neutrophils

2.7 – Isolation of rat neutrophils

Whole blood was collected into tubes containing 15 % EDTA (Beckton Dickenson). To isolate rat neutrophils, HISTOPAQUE® 1077 (SIGMA) (polysucrose, 57 g/L, sodium diatrizoate, 90 g/L), and HISTOPAQUE® 1119 (polysucrose, 60 g/L, sodium diatrizoate, 167 g/L) were used as the density gradients. Both were warmed to room temperature prior to use.

12ml of HISTOPAQUE® 1119 was added to a 50 ml centrifuge tube, and 12 ml of HISTOPAQUE® 1077 was gently layered onto this. 24 ml of freshly anticoagulated whole blood was then carefully layered onto the upper gradient, and the tubes were centrifuged at 700 x g for 30 min at room temperature. Once centrifuged, two distinct opaque layers could be observed. The sequence of tube contents from top to bottom was as shown in Figure 9.

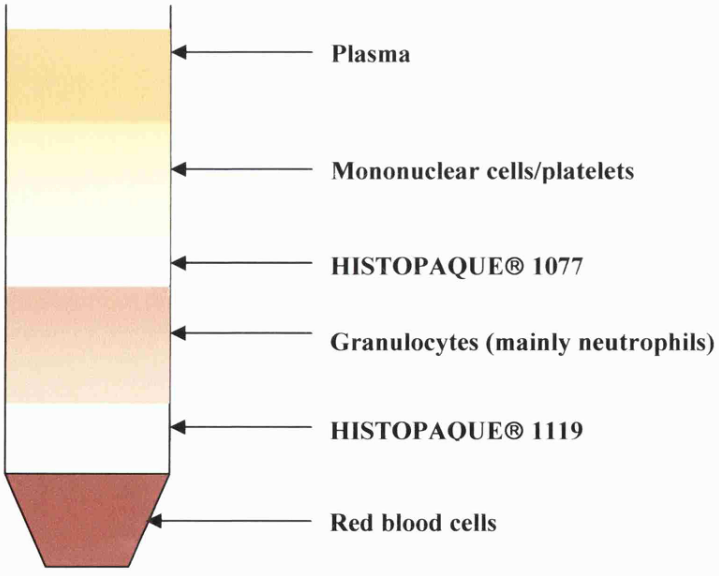

Figure 9: Sequence of tube contents during isolation of rat neutrophils

All layers to within 0.5 cm of the granulocyte layer were aspirated off, and granulocytes were then transferred to a fresh 50 ml tube. PBS containing 0.2 % (w/v) glucose was then added to 50 ml, and the cells spun at 300 x g for 10 min. The supernatant was removed and the cell pellet resuspended in 7.5 ml ice-cold 0.2 % (w/v) NaCl. After mixing for 1 min, 7.5 ml ice-cold 1.6 % (w/v) NaCl was added. PBS (with 0.2 % (w/v) glucose) was added to 50 ml and cells spun at 200 x g for 10 min. This was repeated twice, and the cell pellet resuspended in 1X PBS (with 0.2 % (w/v) glucose) or the required assay buffer (see Table10).

2.8 – Wool column purification of human T cells

PBMC were prepared as described in section 2.2.1. The final PBMC pellet was resuspended in 2 ml RPMI-1640 medium (SIGMA) with 2 mM glutamine (SIGMA) and 5 % (v/v) human AB serum (SIGMA).

2.8.1 – Preparation of wool column

Columns were prepared by placing 6 g of teased out nylon wool (Robbins Scientific, Cheshire, UK) into a 10 ml syringe and autoclaving the whole column. Prior to use the wool column was soaked in 10 ml of RPMI-1640 medium with 5 % (v/v) human AB serum. After allowing the medium to flow through, and ensuring the wool was thoroughly soaked, the bottom of the column was stoppered, and then placed in an incubator at 37 °C for 5 min in order to pre-warm the column.

2.8.2 – Isolation of T-cells

Freshly prepared PBMCs were added to the column after the stopper was removed. Once the PBMC fraction had flowed through the nylon wool matrix, the stopper was replaced and the column incubated for 1 hr at 37 °C in an incubator. The

bottom stopper was removed and 20 ml of RPMI-1640 medium was added dropwise to the column and the effluent containing purified T cells were collected into a 50 ml centrifuge tube. The cells were then counted on a Coulter counter, spun down and resuspended in RPMI-1640 medium (without serum) at 5 x 10^5 cells/ml.

2.9 – Jurkat J6 and HL-60 cells

2.9.1 - Routine cell culture

Cells were maintained in 1 X RPMI 1640 (with L-glutamine and 25 mM HEPES) (GIBCOBRL), 10 % (v/v) fetal bovine serum (SIGMA) and 1 % (v/v) penicillin /streptomycin (SIGMA). The cells were incubated at 37° C in a humid atmosphere containing 5% CO_2. A cell stock was preserved at all times in 10 ml of medium in a 25 cm^3 flask. Fresh aliquots from frozen stocks of Jurkat J6 and HL-60 cells were routinely thawed at 4-week intervals, to avoid any decline in function with time.

2.9.2 - Freezing and thawing cells

0.9 ml of cells at ~ 40% confluency were aliquoted into cryotubes. The tubes were kept on ice for 15 min, after which 0.9 ml freezing medium (see section 2.1.3) was placed into each cryotube. The tubes were then kept at – 80 °C for 3 days, after which they were stored in liquid N_2 (-120 °C to -130 °C).

2.9.3 - Cell passaging

Cells were passaged every 2 – 3 days by resuspending in warm (37° C) medium, at 1:10 –1:40 dilutions. Cells in stock flask were always kept at ~ 50% confluency.

2.10 – Isolation of total RNA from immune cells

Total RNA was isolated using PURESCRIPT® RNA isolation kit (GENTRA).

Table 2: List of reagents used to isolate RNA

REAGENTS	COMPONENTS
Cell Lysis Solution	Citric acid, EDTA, SDS (proprietary formulation)
Protein-DNA-Precipitation Solution	Citric acid, sodium chloride (proprietary formulation)
Diethylpyrocarbonate (DEPC) treated water	1 ml DEPC added to 1 L double distilled water. Solution mixed in a fume hood and then autoclaved.

3 ml of isolated PBMCs or cultured cells were added to an Oak Ridge centrifuge tube and centrifuged at 15,000 x g for 1 min. The supernatant was removed leaving behind a visible white cell pellet and 100 – 200 µl of residual liquid. The tube was vortexed vigorously to resuspend the cells, which greatly facilitates cell lysis. 3 ml Cell Lysis Solution was then added to the tube and pipetted up and down 3 times to lyse the cells.

1 ml Protein-DNA Precipitation Solution was added to the cell lysate, and the tube inverted gently 10 times and placed on an ice bath for 10 min. This was then centrifuged at 15, 000 x g for 5 min. The precipitated proteins and DNA formed an irregular brown pellet.

The supernatant containing the RNA was pipetted off and transferred into a clean Oak Ridge centrifuge tube containing 3 ml 100% isopropanol (BDH). The sample was mixed by inverting gently 50 times and centrifuged at 15, 000 x g for 5 min.

At this point the RNA became visible as a small translucent pellet. The supernatant was poured off and the tube was inverted and drained on clean absorbent paper.

3 ml of 70% (v/v) ethanol was added and the tube inverted several times to wash the RNA pellet. This was then centrifuged at 15,000 X g for 2 min and the ethanol poured off. The tube was inverted and drained on clean absorbent paper and air dried for 15 min.

To hydrate the RNA pellet, 100 µl of DEPC-treated water was added. The RNA was allowed to rehydrate on ice for at least 30 min, and then vortexed vigorously for 5 seconds, pulse spun and carefully transferred to a 1.5 ml microcentrifuge tube. The sample was stored at – 70° C to – 80° C until use.

Before use the sample was vortexed vigorously for 5 seconds and pulse spun. The sample was pipetted up and down several times to ensure adequate mixing. From this isolated procedure approximately 2-7 µg/ml of RNA from whole blood was obtained.

2.11 – Measurement of RNA concentrations

The concentration and purity of total RNA isolated was determined by measuring the absorbance at 260 nm (A260) and 280 nm (A280) in a spectrophotometer. Absorbance readings at 260 nm measure RNA concentration and should be greater than 0.15 to ensure significance.

The concentration was calculated using the equation:

$$\textbf{[RNA] µg/ml} = \textbf{Absorbance}_{260} \textbf{ x 40 x dilution factor}$$

where '40' corresponds to 40 µg/ml of RNA per 1 unit of absorbance at 260 nm.

This relationship is valid for measurements in water. Therefore to measure RNA concentrations spectrophotometrically, the samples were diluted in DEPC-treated water.

2.12– Assessment of RNA Purity

The ratio between the readings taken at 260 nm and 280 nm (A260 / A280) provided an estimate of the purity of RNA. The A260 / A280 ratio is influenced by pH. As water is unbuffered, the same RNA sample may show different A260/A280 ratio in different types of water, ranging from 1.5–1.9. Also, the addition of the RNA itself influences the pH of the water. Therefore, in order to determine the A260 / A280 ratios samples were diluted in 10 mM Tris-Cl, pH 7.5. Pure RNA has an A260 / A280 ratio of 1.8–2.1 in 10 mM Tris-Cl, pH 7.5. All samples used in these experiments had an A260/A280 ratio of at least 1.8.

2.13 – Agarose gel electrophoresis of RNA

The integrity of the isolated total RNA was checked by non-denaturing agarose gel electrophoresis. A 0.8 % (w/v) agarose gel with ethidium bromide (0.7 μg/ml) was prepared in RNAase free 1 X TAE buffer. The gel cast, comb and tank were treated overnight with 1 % (v/v) H_2O_2 prepared in DEPC-treated water, and washed with DEPC-treated water. The RNA sample was prepared in Promega 6 X dye used only for RNA. The gel was run at 80 V for 2 hours and visualised under ultraviolet illumination.

2.14 – Purification of mRNA

Poly $(A)^+$ RNA was isolated using Dynabeads® oligo $(dT)^{25}$ magnetic beads (DYNAL), 2.8 μm in diameter, with a 25 nucleotide long chain of deoxythymidylate attached covalently to the bead surface via a 5′ linker group. Beads were stored in PBS containing 0.02 % (v/v) NaN_3. 0.2 ml (1 mg) of bead suspension was pipetted into a 1.5 ml microcentrifuge tube, which was placed into a Dynal MPC®-E magnetic particle concentrator, and the supernatant removed. The beads were washed by the addition and removal of 100 μl 2X binding buffer (20 mM Tris-Cl, pH 7.5; 1 M LiCl; 2 mM EDTA). 100 μg total RNA was resuspended in 10 mM Tris-HCl (pH 7.5) and heated for 2 min at 65°C to disrupt the secondary structures. This was then added to the washed beads and mixed thoroughly by placing on a rotating platform for 3 – 5 min at room temperature. This allows the mRNA to anneal to the beads. The tube was then placed on the magnet to allow removal of the supernatant. The beads were washed twice with 200 μl of washing buffer (10 mM Tris-HCl, pH 7.5, 0.15 M LiCl, 1 mM EDTA) and resuspended in 10 μl 10 mM Tris-HCl before heating at 65°C for 2 min. This was then placed on the magnet again so eluted poly $(A)^+$ RNA could be transferred to a new RNase-free tube.

2.15 – cDNA Synthesis

Poly $(A)^+$ RNA was reverse transcribed into cDNA using SUPERSCRIPT™ II RNase H^- Reverse Transcriptase enzyme, a recombinant reverse transcriptase from Moloney Murine Leukaemia Virus (M-MLV) lacking RNaseH activity (Gibco-Life Technologies).

Table 3: List of reagents used to synthesise first strand cDNA

REAGENTS	COMPONENTS
5X First Strand Buffer	250 mM Tris-HCl, pH 8.3; 375mM KCl, 15mM $MgCl_2$
DTT	100 mM
dNTPs	10 mM (10 mM each dATP, dGTP, dTTP, dCTP neutral pH)
Superscript™ II RNase H⁻ Reverse Transcriptase buffer	20 mM Tris-HCl (pH 7.5); 100 mM NaCl; 0.1 mM EDTA; 1mM DTT; 0.01% (v/v) NP-40; 50% (v/v) glycerol
Superscript™	200 units/µl
RNaseOUT™ Recombinant Ribonuclease Inhibitor buffer	20 mM Tris-HCl (pH 8.0); 50 mM KCl; 0.5 mM EDTA; 8 mM DTT; 50% (v/v) glycerol
(RNaseOUT™)	40 units/µl
E.coli RNase H	2 units/µl

To 10 µl of eluted mRNA, 1µl of oligo dT, 1 µl of 10 mM dNTPs, and 1 µl of RNA free water were added, the mixture heated to 65°C for 5 min and quick chilled on ice. 4 µl of 5X First Strand Buffer, 2 µl of DTT and 1 µl RNaseOUT™ Recombinant Ribonuclease Inhibitor were added to the previous mix and the tube incubated at 42°C for 2 min. 1 µl of Superscript™ was then added and mixed by pipetting gently up and down and the reverse transcription was allowed to proceed at 42°C for 50 min in a thermocycler. The reaction was inactivated by heating at 70°C for 15 min. Any remaining RNA was removed by adding 1 µl of *E.Coli* RNase H and incubating at 37°C for 20 min. The final product was stored at – 20°C before being used for PCR.

2.16 – Reverse Transcription-Polymerase Chain Reaction

The Expand High Fidelity PCR system from Roche was used to amplify cDNA from human brain, human PBMC and Jurkat J6 cells. This is composed of an enzyme mix containing thermostable Taq DNA polymerase and a proofreading polymerase. For a single reaction the following components were added to a thin-walled PCR tube:

Table 4: List of reagents used per tube in RT-PCR

Reagents	Components	Volume (µl)
Sterile dd H_2O	-	34.60
Expand High Fidelity Buffer	10X, with 15 mM $MgCl_2$	5
dNTP mix	2 mM (2 mM each dATP, dGTP, dTTP, dCTP at neutral pH)	7.5
cDNA	5 – 10 ng/ml	1
Forward primer	20 µM	0.75
Reverse primer	20 µM	0.75
Expand High Fidelity PCR system, Enzyme mix	20 mM Tris-HCl, pH 7.5, 100 mM KCl, 1mM DTT, 0.1 mM EDTA, 0.5% Tween-20 (v/v), 0.5% Nonidet P40 (v/v), 50% glycerol (v/v). Taq DNA polymerase, proofreading polymerase (3.5×10^3 units/ml)	0.40

2.17 – Sensitivity and specificity of TaqMan assay

To confirm the PCR results quantitatively, real-time TaqMan RT-PCR was performed on a range of human tissues in which 18 S RNA was used as an endogenous control. By using an endogenous control as an active reference, quantitation of an mRNA target can be normalised for differences in the amount of total RNA added to each reaction. However, as 18S RNA is a ribosomal RNA species it may not always represent the overall cellular mRNA population. Despite this, it is one of the most commonly used normalisers and was therefore used as the active reference in the TaqMan experiments.

Serial dilutions (10 fold) of control RNA (brain, placenta, testis mix) from 1/10 to $1/10^7$ were performed to test the sensitivity of the assay. 18S rRNA was used as an internal standard in the real-time quantification of mRNA levels in the samples studied. The fluorochrome dye VIC was used to label the probe used for 18S, which is preferred for use with FAM (the reporter dye), as FAM and VIC have the largest difference in emission maximum (Dorak, 2000; Grove, 1999).

The 18S rRNA primer/probe set effectively amplified all cDNAs as expected (Figure 10). This showed that all samples in the wells contained a sufficient amount of RNA to be detected by the sequence detector. Human brain cDNA was amplified between cycles 9 – 10 indicating high levels of amplification. The no template control showed amplification of products very late at cycle 36, which indicates the absence of amplification (Figure 10A).

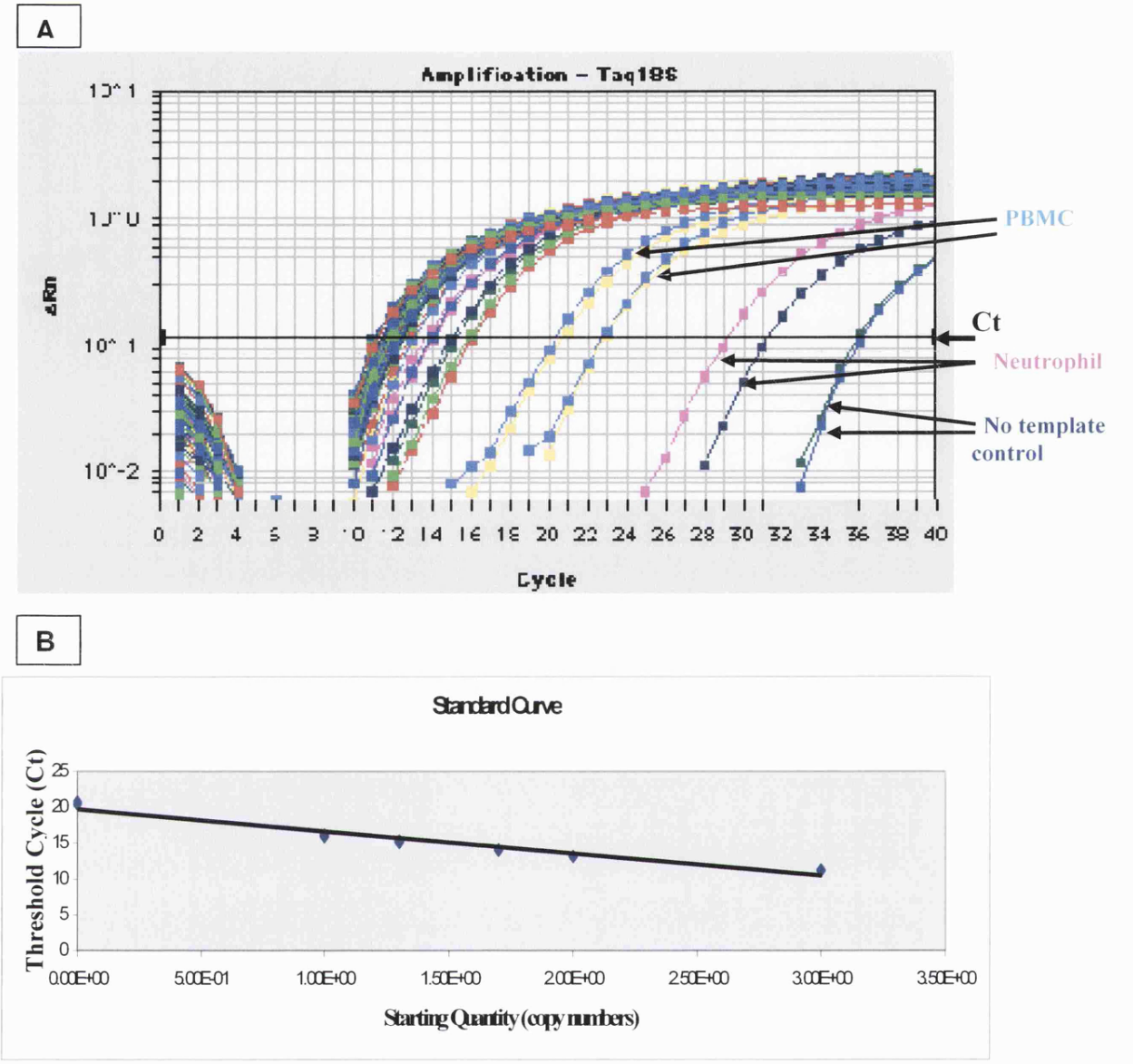

Figure 10: Amplification plot (A) and standard curve (B) from TaqMan RT-PCR using the 18S rRNA probe and primer set. In A, the normalised reporter dye emission (ΔRn) is plotted against the cycle number. Samples shown to amplify between cycles 10-12 were cDNA obtained from a variety of human tissues, including human brain and a range of human immune cells. All samples were present as duplicates in the 96-well plate, the amplification plots of which are represented as pairs of colours. Only samples of interest have been labelled. Samples shown to amplify between cycles 14-18 are cDNA from two separate sets of human PBMC (yellow and sky blue plots), while samples showing amplification between cycles 24-29 are cDNA obtained from human neutrophils (blue and pink). The no template control (blue and green) shows amplification signals between cycles 33-34. In B, the standard curve (cDNA obtained from a mix of human brain, placenta and testis) shows the Ct values from each of the plots in A plotted against the relative rRNA copy numbers.

2.18 – Primers designed for RT-PCR

Table 5: Primers designed for the amplification of $GABA_A$ receptor subunit mRNAs. Nucleotide positions of primers within the cDNA sequence are shown. The 'internal' primers are nested within the 'external' primers. This is because the PCR product obtained using the 'external' primers was used as a template for the PCR reaction using the 'internal' primers. All primers were purchased from MWG-BIOTECH.

$GABA_A$ Receptor subunit	External Forward Primer (5' - 3')	External Reverse Primer (5'- 3')	Internal Forward Primer (5'- 3')	Internal Reverse Primer (5'- 3')
α1	[1235]GGTTATGCAT GGGATGGC[1252]	[1476]CGGTCAATTTT GCTGACACT[1457]	[1319]GCTCCAACAGC AACCAGC[1337]	[1414]GACCTCTTTAG GTTCTATGG[1396]
α2	[1232]AGGATGGACT TGGGATGG[1245]	[1439]TTCTTTGCTTC AGCTGGC[1420]	[1312]TTATGCAGTGGC TGTTGC[1329]	[1392]CGTGGTTGCAC TCTTGGA[1375]
α3	[1181]AGTTGGGCTT GGGAAGGC[1198]	[1428]AGGTCTTGGTC TCAGTCG[1410]	[1262]GCACTACCTTCA ACATCG[1280]	[1378]TGATTGTTGGG GTTGAGG[1350]
α4	[1072]GAAAGACATC AAAGCCCC[1089]	[1559]TGTGCCAGATC CAGAAGG[1542]	[1200]TCTGAATCTGAT GTTGGC[1217]	[1454]AGCAGATCCA ACTGAAGC[1395]
α5	[1334]CTTTACCAAG AGAGGCTG[1351]	[1550]GCTTTCAGAAG TCTTCTC[1532]	[1371]GCCTTGGAAGC AGCCAAG[1389]	[1505]TGTATTCGACG TCCCTGC[1484]
α6	[1013]TCTTCAGACA CAGAAGGC[1030]	[1282]TGGTCTATTTT ACTGGTGC[1264]	[1078]CTACTGAACCTT TGGAAGC[1099]	[1228]GGTGTTGATTG TAAGATGGG[1209]
β1	[1050]GAGCTAGCAA ACAAGACC[1067]	[1371]TTCACATCAGT CAAGTCG[1354]	[1138]CAGCACCCTGG AAATCCG[1146]	[1250]GCTTGCGGTAC TGGATGC[1233]
β2	[1244]TGAGAAGGCT GCCAGTGC[1262]	[1558]TTCACATCAGT CAAGTCA[1539]	[1315]TCTTACTGAGCA CTCTCG[1323]	[1484]CACATGTCGTT CCAGAGC[1466]
β3	[1097]CAAGGCAAAG AATGACCG[1100]	[1388]CACATCGGTTA GATCAGG[1370]	[1170]CGCTGGAAGTT CACAATG[1193]	[1280]CGAGGCATGCT CTGTTTC[1262]
γ2	[1307]AGCAACCGGA AACCAAGC[1324]	[1551]TCCATTTTGGC AATGCGG[1534]	[1372]CGCCCAAGATC AGCAACC[1390]	[1509]GCTCCTGTTCG ACAATCTTC[1489]
γ3	[1046]CTACTATTCC AGCTGTAG[1063]	[1346]GATGTCTATGT GAATACGC[1328]	[1114]CAAGATGGATT CCTGAGC[1131]	[1296]CATAGCAGCA GAAGAAGC[1279]
δ	[1031]AGGTCAAGGT CTCCAGGC[1048]	[1283]TCAATGGTGTC TGCGTCG[1266]	[1082]CCTCTTCTCCCT CTCTGC[1102]	[1210]CCTTCTTCGTC TCCCCTG[1196]
ε	[1153]CCATGCTTCTC CTAAACTCC[1180]	[1486]GTTATCCAGGC GGTAGAC[1468]	[1256]GTGTGCCAGATT GTCACC[1274]	[1395]GCTTGCACCAC TCACAGC[1377]
θ	[1108]ACCGCTACCA GCAAGTGG[1126]	[1775]CGAAGGAGAA CCCTTCAG[1757]	[1159]GTGGAAGACGG AGTCAGC[1177]	[1630]GCTCCTTAATG GCAAGGC[1613]

Table 6: Primers designed for the amplification of glycine receptor subunit mRNAs.

Glycine Receptor subunit	External Forward Primer (5'- 3')	External Reverse Primer (5'- 3')	Internal Forward Primer (5'-3')	Internal Reverse Primer (5'- 3')
α1	^{1308}GGCAACATAAGGAGCTGC^{1321}	^{1543}CGATCTTCTTGGCCCTCT^{1528}	^{1368}GGATGAAGCTGGAGAAGGC^{1376}	^{1468}GGTGGTGTTACTGTTGTTGG^{1450}
α2	^{1411}TCCAGGCAACACAAGGAG^{1428}	^{1628}CGGTCCACAAACTTCTTC^{1610}	^{1466}AGGAAGAAGACGTTACTCG^{1485}	^{1585}TTGTGGGAGTGGGTTGGC^{1567}
α3	^{1458}ACTTCTGAGATTTCGACG^{1475}	^{1665}GGTATCAATCTTCTTGGC^{1648}	^{1503}AGGGAAAGCCGATTCAGC^{1521}	^{1631}TTCCTCATTTCATCAGGAC^{1613}
β	^{1173}GAATTGCTAAGGCTGAGC^{1191}	^{1457}GGGGAGGCTTCTTGTTGT^{1439}	^{1234}GAATGGAACAGGGACTCC^{1216}	^{1392}CCATAGCAGTCATAATTGGA^{1374}

2.19 – Primers and probes designed for TaqMan RT- PCR

All primers and probes for TaqMan RT-PCR were purchased from Applied Biosystems, Perkin-Elmer.

Table 7: Primers and probes designed for $GABA_A$ and glycine receptor subunit mRNAs. The forward and reverse primers were designed as ciose as possibie to the probe without overiapping the probe. Nucleotide positions are shown on either side of the sequences.

Receptor subunit	Forward Primer (5'- 3')	Reverse Primer (5'- 3')	TaqMan Probe (5' (FAM)- (Methyl Red) 3')
$GABA_A$ α1	1358GGCGACCCGGGCTTAG1374	1431GGTTTTGTTTCGGGCTTGAC1411	1375CACCATTGCTAAAAGTGCAACCATAGAACCTAAAGA1411
$GABA_A$ α3	1284GGACCACCTATCCCATCAACCT1306	1425TTGGTCTCAGTCGGGCTGTC1405	1347CTCCCAGTGCCTCCTCAACCCCAA1371
$GABA_A$ β2	1476CGACATGTGGCGCAAAAG1494	1545AGTCAGGGATGGTGATTTTCAGTT1521	1502TCGCCTGAGGAGACGCGCCT1521
$GABA_A$ β3	673AGCTCCCGCAGTTCTCCAT692	738CACCTGTGGCGAAGACAACAT717	694TGGAGCACCGTCTGGTCTCGAGG717
$GABA_A$ δ	666CACGGAGCTGATGAACTTCAAG688	776ACGGAGGGCATGTAGGATTG756	733AGGAACCGCGGCGTGTACATCATC756
$GABA_A$ ε	1421CCCGATTGTGAGGGCAGTAC1441	1547AAACAAGCCAGTAGAGCACATTGA1523	1442TGGCAGCAGGGCCGCCGCCTC1462
Glycine α1	381GCTCGCTCCGCAACCA396	448CCGGAGGTTCTCCCCATTA429	399CCTATGTCACCCTCGGATTTCCTGGATAAG429
Glycine α2	1205GGGTTTCCTTTTGGATAAATATGGAT1230	1306ATGCCCTGGAGCCTGAACT1287	1258ATCACCACAGTCTTAACGATGACCACCCA1287
Glycine α3	1233CTGGGTTTCGTTCTGGATCAA1253	1312TAGTCATCGTTAGCACGGTGGTTAT1287	1259ATGCAGCACCGGCCAGGGTAGC1281
Glycine β	1104CCCTGGTGGAGTATGCAGTTG1125	1252AGGAGTCCCTGTTCCATTCACA1230	1126CCAGGTGATGCTGAACAACCCCAAAAG1153

2.20 – Agarose gel electrophoresis

Agarose gels for DNA analysis were made by the addition of 1.5 – 2% (w/v) agarose to 1 x TBE buffer. Heating in a microwave oven at 40 % power dissolved the agarose. Visualisation of DNA was achieved by the addition of 5 μg/ml ethidium bromide to this solution. Gels were poured in a gel cast with a comb and allowed to set before running in a 1X TBE buffer, in a horizontal gel apparatus at 100 V. DNA samples were loaded with 6X loading dye (26 % (v/v) H_2O; 50 % (v/v) glycerol; 21 % (v/v) 0.05 M EDTA; 0.1 % (w/v) bromophenol blue; 0.1 % (w/v) xylene cyanol). To determine the size of bands 100 bp (NEB) and 1 Kb (Promega) molecular weight markers were used.

2.21 – Purification of DNA from agarose gels

The QIAquick Gel Extraction Kit (QIAGEN) was used to purify DNA from agarose gels. This allows the extraction and purification of DNA from 100 bp to 10 Kb out of agarose gels in TBE buffer. In high salt conditions the silica-membrane contained on spin-columns absorbs the DNA, while contaminants pass through the column. All the centrifugation steps were performed at 13000 X g.

The DNA band was excised and weighed in a 1.5 ml microcentrifuge tube. 3 volumes of buffer QG were added to the tube, and incubated at 50 °C for 10 min (or until the gel slice had completely dissolved). 1 gel volume of isopropanol was then added to the sample, mixed and applied to a QIAquick column and centrifuged for 1 min. The flow-through was discarded, and the column replaced in the same collection tube. To remove all traces of agarose, a further 0.5ml of Buffer QG was added to the column, spun for 1 min and the flow-through discarded. To wash, 0.75 ml of Buffer PE was added to the column, left to stand for 2 – 5 min and then spun for 1 min. The flow-through was discarded and the column centrifuged for an additional minute. The QIAquick column was then placed into a clean 1.5 ml

microcentrifuge tube. To elute the DNA 30 µl of Buffer EB was added directly to the centre of the QIAquick membrane, left to stand for 1 min and then centrifuged for 1 min. The eluted DNA was stored at – 20°C.

2.22 – Cloning of PCR products

PCR products were cloned into the vector pCR®- Blunt II vector using the Zero Blunt™ PCR cloning kit (Invitrogen). The TOPO® vector was supplied linearised. The ligation mix consisted of 1 µl of the vector, ~ 4 µg/µl PCR product, 1µl salt solution (1.2 M NaCl, 0.06 M $MgCl_2$) and 0.5 µl sterile water. This was incubated for 5 minutes at room temperature. 50µl (one vial) of cells was used per transformation. After the vial containing the One Shot™ TOP10 competent cells was thawed on ice, 2µl of the recombinant plasmids were added. This was gently mixed and incubated on ice for 5 – 30 min. Cells were then heat shocked for 30 sec in a 42° C water bath followed by immediate transfer to ice for 2 min. 250µl of SOC medium (at room temperature) was added to the cells before placing the tubes in a horizontal shaker for 1 hour at 37° C. 50, 100 and 150µl of the transformation mix were spread on to prewarmed LB agar plates containing 50µg/ml kanamycin and these were incubated at 37° C overnight. Colonies were picked and grown for 12 – 16 hours in LB medium containing 50 µg/ml kanamycin and plasmid DNA was purified from the bacteria using the CONCERT™ Rapid Plasmid Purification System (Life Technologies, Gibco BRL®). This DNA was analysed initially by restriction digestion and then sequencing.

2.23 – Small scale preparation of plasmid DNA

The alkaline lysis method from the CONCERT™ Rapid Plasmid Purification System (Life Technologies, Gibco BRL®) was used to isolate plasmid DNA from bacterial cultures. 3 ml of an overnight culture was centrifuged at 12000 x g for 2 min and all medium removed. The resulting pellet was resuspended in 210 µl of

buffer G1 (containing RNase A) to form a homogenous solution. 210 µl of solution G2 was added and mixed by inversion before incubation at room temperature for 5 min to produce a clear solution. 280 µl of G3 buffer was added and the solution mixed by inversion before centrifugation of samples at 12,000 x g for 10 min. The resulting supernatant was placed into a spin cartridge, containing silica-based membranes where the plasmid DNA is selectively adsorbed, which was contained in a 2 ml wash tube. Following removal of the flow-through the column was washed with 500 µl of buffer GX followed by a wash with 700 µl of buffer G4 (containing 95 – 100 % ethanol) at 12000 x g for 1 min. DNA was eluted by the addition of 75 µl of TE buffer, incubation for 1 min at room temperature and then final centrifugation at 12000 x g for 2 min.

Table 8: List of reagents used for preparing plasmid DNA

REAGENTS	COMPONENTS
Cell suspension Buffer (G1)	50 mM Tris-HCl, pH 8.0; 10 mM EDTA
RNaseA	20 mg/ml in water
Cell Lysis solution (G2)	200 mM NaOH, 1 % (w/v) SDS
Neutralisation Buffer (M3)	Acetate and guanidine hydrochloride, (proprietary formulation)
Wash Buffer (GX)	Acetate, guanidine hydrochloride, EDTA, ethanol (proprietary formulation)
Wash Buffer (G4)	NaCl, EDTA and Tris-HCl, pH 8.0 (proprietary formulation)
TE Buffer (TE)	10 mM Tris-HCl, pH 8.0; 0.1 mM EDTA

2.24 – Endonuclease restriction of DNA

DNA samples of 1 – 5 μg were digested with one or two restriction enzymes (10-20 units) in the reaction buffer (4 μl) recommended by the manufacturer. Sterile water was added to a volume of 40 μl and the reaction incubated at 37°C for 1 – 4 hours.

2.25 – Sequencing of clones and sequence analysis

Approximately 250 ng of DNA preparation was mixed with 10 pmol of primer in 6 μl of double distilled water and sent for sequencing at the University of Bath DNA Autosequencing Service. The primers used for sequencing the cloned products in pCR®-Blunt vector were the M13 forward and M13 reverse from Invitrogen. Sequence analysis was carried out on the GCG (Genetic Computer Group, Wisconsin, USA) suite of programs, accessible via the gnome and elf workstations, for analysis and comparison with existing sequences in the database.

2.26 – Preparation of rat brain membranes

Sprague-Dawley rat brains were rapidly removed and homogenised in 20 ml/g original weight of ice-cold 10 % (w/v) 0.32M sucrose, pH 7.4 (containing 1mM EDTA, 0.1 mM PMSF and 0.01 % (w/v) NaN_3). The whole homogenate was centrifuged at 1000 x g for 10 min. Supernatant (S1) was decanted and retained on ice, while pellet (P1) was resuspended in 5 ml/g original weight in ice cold 0.32 M sucrose and centrifuged at 1000 x g for 10 min. Supernatant (S2) was then combined with S1 and centrifuged at 12,000 x g for 30 min. The pellet (P2) was resuspended in 2.5 ml/g original weight in ice-cold 50mM phosphate buffer (80 mM K_2PO_4, 20 mM KH_2PO_4, pH 7.4), containing 1 mM EDTA, 1 mM PMSF and 0.1 % (w/v) NaN_3. This was washed 2 times by centrifugation at 12,000 x g for 30 min. The washed pellet was then resuspended in 2.5 ml/g original weight in ice-

cold 50 mM phosphate buffer containing 1 mM EDTA, 1 mM PMSF and 0.1 % (w/v) NaN_3. The suspension was divided into 5 ml aliquots and stored at – 20°C for up to 3 months.

2.27 – Preparation of PBMC, Jurkat J6 and HL-60 and HEK-293 cell membranes

Jurkat J6, HL-60 cells and HEK-293 cells were grown to 50 % confluency and harvested at 500 x g for 5 min. The cell pellets were resuspended and washed three times in ice-cold PBS with 1 mM EDTA and protease inhibitor. Isolated human PBMC were harvested at 300 x g for 5 min.

The pellets were resuspended in 10 ml ice-cold 1X PBS with 1 mM EDTA and protease inhibitor and 0.1 % (w/v) sodium azide. The cells were homogenised using a sonicator (3 x 15 s pulses) and then transferred to a 10 ml Oak Ridge ultracentrifuge tube. Samples were centrifuged at 12,000 x g for 30 min at 4°C. The pellet was resuspended and centrifuged for a further 20 min at 12,000 x g at 4°C. The supernatant was discarded and the cell pellet resuspended in 1 – 2 ml ice-cold 1X PBS with 1 mM EDTA, 1 mM PMSF and 0.1 % (w/v) sodium azide. Samples were stored at – 20°C.

2.28 – Preparation of cell lysates

Isolated human T-cells, human neutrophils and BaF13 cells were harvested at 300 x g for 5 min. The cell pellet was resuspended in 5 ml ice-cold 1 X PBS with 1 mM EDTA, 1 mM PMSF and 0.1 % (w/v) sodium azide. The cells were homogenized with a sonicator (3 x 15 s pulses). Samples were stored at – 20°C.

2.29 – Protein Quantitation

The Coomassie® Plus Protein Assay Reagent Kit (PIERCE) was used for total protein quantitation. The method of protein detection is based on the Bradford method (Bradford, 1976). The reagent contains: Coomassie dye, methanol, phosphoric acid and solubilizing agents in water. Microwell plates were used and 15 µl of sample or standard (BSA provided with the kit) were added per well plus 300 µl of Coomassie® reagent. Plates were mixed on a shaker for 30 sec and the absorbance was measured at 595 nm. A standard curve was prepared by plotting the average blank corrected 595 nm reading for each BSA standard, versus its concentration in µg/ml. This curve was used to determine the protein concentration of each unknown sample.

2.30 – SDS-Polyacrylamide gel electrophoresis (SDS-PAGE)

Table 9: List of reagents used for SDS-PAGE

REAGENTS	COMPONENTS
30 % Acrylamide mix	30 % (w/v) acrylamide, 0.8 % (w/v) bis acrylamide
1X Tris-HCl, pH 8.8	1.5 M Tris-HCl (stored at 4°C)
1X Tris-HCl, pH 6.8	0.5 M Tris-HCl (stored at 4°C)
SDS	10% (w/v) sodium dodecyl sulphate
APS	10% (w/v) ammonium persulphate in dd H_2O
6X SDS Loading Buffer	0.35 M Tris-HCl, pH 6.8; 10.28 % (w/v) SDS; 36 % (v/v) glycerol; 5 % (v/v) β-mercaptoethanol; 0.012 % (w/v) bromophenol blue (stored at - 20°C)
5X Running Buffer	3 g Tris-base, 14.4 g glycine and 0.5 g SDS in 100 ml of dd H_2O
Coomasie Blue Solution	50 % (v/v) methanol, 0.05 % (w.v) Coomasie Brilliant Blue R, 10 % (v/v) acetic acid in dd H_2O (Coomasie Brilliant Blue R was dissolved in methanol before adding acetic acid and water)
Destaining Solution	5 % methanol (v/v), 7 % (v/v) acetic acid in ddH_2O

For the preparation of two 8 % (w/v) separating gels, 2.7 ml 30 % acrylamide mix (SIGMA) were combined with 4.6 ml dd H_2O, 2.5 ml 1.5 M Tris-HCl (pH 8.8), 100 µl 10 % (w/v) SDS (SIGMA), 100 µl 10 % (w/v) APS (Life Technologies) and 6 µl of TEMED (SIGMA). Using a 5 ml pipette the solution was transferred to Atto™ mini-gel rigs, overlaid with isopropanol and allowed to polymerise at room temperature. When the gels were ready the solvent was removed and the gel interface rinsed with distilled H_2O. A 5 % (w/v) stacking gel was prepared by mixing 0.83 ml of 30 % acrylamide mix, 3.4 ml of dd H_2O, 0.63 ml of I M Tris-Cl, 50 µl 10 % (w/v) SDS, 50 µl 10 % (w/v) APS and 5 µl TEMED. The solution was pipetted over the separating gels and the combs inserted while the gel was allowed to set.

Gels were placed into an electrophoretic chamber and 1X running buffer was added. Combs were removed and wells washed out with buffer. Samples were prepared by resuspension in 6X SDS loading buffer and denatured by incubation in a boiling water bath for 5 min and spun down at 12000 x g for 3 min immediately prior to loading onto the gel.

Gels were run at 100 V until the dye front reached the bottom of the gel. Gels were stained by soaking and rotating in Coomasie Blue solution for 10 minutes and destained with 3 washes in destaining solution until background staining was removed.

2.31 – Western Blotting

2.31.1 – Semi-dry blotting

Two gel sized sets of 2 sheets of extra thick filter paper (Bio-Rad) were soaked for 30 min in transfer buffer (25 mM Tris-HCl pH 8.3, 150 mM glycine, 0.037 % (w/v) SDS and 20 % (v/v) ethanol added (immediately before use). The first set was aligned on the graphite transfer plate of a NovaBlot blotter (Pharmacia)

followed by a nitrocellulose membrane (Amersham), previously rinsed in dd H_2O and in transfer buffer. The SDS-PAGE gel was rinsed in water and in transfer buffer and rolled out on top of the membrane. The stack was overlaid with the second set of soaked filter papers and any air bubbles between layers, were removed by rolling a glass pasteur pipette over the top of the sandwich. The upper graphite plate was put on the top and the rig connected to the power supply set at 0.8 mA/cm^2 of gel for 1 hour.

2.31.2 – Wet blotting

Two gel sized (9 cm x 6 cm) sheets of extra thick filter paper (Bio Rad) were soaked for 15 min in transfer buffer (25 mM Tris-HCl pH 8.3, 192 mM glycine, 20 % methanol). A mini trans-blot cell and module (Bio Rad) was used for the transfer of proteins from the gel matrix onto nitrocellulose membrane (Life Sciences). A presoaked fiber pad was aligned onto one of the two plates of the gel holder cassette. A piece of pre-soaked filter paper was then placed upon this, upon which first the gel and then the membrane were aligned. A second piece of pre-soaked filter paper was placed on top and a 1 ml glass pipette was rolled over the top to removed any air bubbles. To complete the sandwich, a second pre-soaked fiber pad was placed on top and the cassette was firmly clamped. The cassette was placed inside the transfer cell, with the gel side facing the negative electrode, and this was then placed inside the tank. In order to regulate temperature a Bio-ice cooling unit was also placed inside the tank. The apparatus was then set up to run at a constant current of 30 mA at 4 °C overnight, or at 100 mA at 18 °C for 2 hours.

2.32 – Chromogenic substrate detection

The nitrocellulose membrane was incubated overnight at 4 °C in blocking solution (2 % (w/v) glycine, 5 % (w/v) Marvel™ non-fat milk powder in PBS with 0.1 % (v/v) Tween). The blot was washed in PBS/Tween 2 times and incubated for 2 – 3

hours at room temperature in primary antibody diluted 1:1000 in PBS/Tween.. To remove unbound antibody, the membrane was washed in PBS/Tween for 5 min, 10 min and 15 min on a rotating table. The VECTASTAIN® ABC kit (Vector Laboratories) was used to detect immunoreactivity in the blot. Upon removal of primary antibody, the membrane was incubated for 1 hr at room temperature in the biotinylated secondary antibody diluted 1:1000 in PBS/Tween. At the same time Avidin DH and biotinylated horseradish peroxidase were each diluted 1:500 in PBS/Tween (ABC reagent), and mixed on a rotating table for 1 hour at room temperature. Unbound secondary antibody was removed by washing in PBS/Tween 2 times, and the blot was then incubated in the ABC reagent for 1 hour at room temperature. This was then washed in PBS/Tween 2 times and in 1X PBS 2 times before applying the chromogenic substrate (2 ml 4-chloro-1-napthol, 10 ml PBS (1X) and 5 µl 30 % H_2O_2. 1 ml added per lane). To stop the reaction, the blot was washed in 1X PBS 2 times and then with copious amounts of dd H_2O) to remove the peroxidase. The membrane was then dried between two pieces of Grade 1 filter paper (Whatman).

2.33 – Preparation of coverslips and fixation of cells

Coverslips were treated with 1 % (w/v) PEI solution to allow cells to stick to the surface. A 10 % (w/v) stock solution of PEI was prepared by adding 1 g of PEI to 9 ml dd H_2O and dissolved for 2 hours at 37° C. In the fume hood this was then sterilised with a 0.22 µm filter. For experiments, 100 µl of the PEI stock solution was dissolved in 10 ml, 100 mM borax buffer (pH 8.3). 0.5 – 2 ml was used on the coverslip and left for 3 hours – overnight at 37 °C. To remove excess PEI the coverslips were then washed 3 times with 3 ml PBS.

Jurkat cells (50 – 70 % confluency) were transferred to 50 ml falcon tubes and centrifuged at 400 x g, 15 °C for 5 min. The medium was aspirated and cells resuspended in 30 ml PBS. 0.5 – 2 ml of the cell suspension was pipetted over the treated coverslips and incubated at room temperature for 20 – 30 min. Excess cell

suspension was removed by aspiration and the coverslips washed 3 times in 2 – 3 ml 1X PBS.

To fix cells 2 ml 4% PFA/PBS was added to the coverslips and left at room temperature for 20 min, Alternatively, ice-cold methanol was added to the coverslips and incubated at – 20 °C for 5 min. The coverslips were then washed 3 times in 2 – 3 ml 1X PBS. To minimise non-specific adsorption of antibody to the cells, 1 % BSA/PBS or 1 % FBS/PBS was used as blocking buffer. Coverslips were covered with 35 – 50 µl blocking buffer for 10 – 15 min at room temperature.

2.34 – Antibody staining

The primary antibody was diluted (1 in 100) in either the medium or the blocking buffer. Once excess blocking buffer was aspirated off, the coverslips were inverted onto 70 – 80 µl of primary antibody mix for 1 hr or more at room temperature. The mix consisted of a 1:100 dilution of a CD marker mouse anti-human antibody IgG (Serotec) and a 1:100 dilution of $GABA_A$ α1 rabbit anti-bovine antibody (a gift from Prof. Anne Stephenson, London School of Pharmacy). Unbound antibody was removed with two 5 min washes in blocking buffer and then two 5 min washes in PBS.

To bind secondary antibody, coverslips were inverted onto 70 µl of the secondary antibody mix (a 1:100 dilution of FITC conjugated anti-rabbit IgG secondary serum (SIGMA) and a 1:100 dilution of Texas Red conjugated anti-mouse IgG secondary serum (SIGMA). This was left for 20 min at room temperature in the dark and then, keeping the dish covered, washed twice, 5 min each with blocking buffer. Coverslips were then washed another 2 times, 5 min each with PBS.

The coverslips were mounted onto microscope slides using 15 – 20 µl of Mowiol, placed in the dark and allowed to dry overnight. The slides were examined under a Zeiss LSM 510 confocal fitted to an inverted Axiovert 100 M microscope, using a

helium neon laser and FITC and rhodamine filter set. Negative controls for immunostaining were set up in parallel in the presence of secondary antibody only.

2.35 – Loading immune cells with FLUO-3AM, a fluorescent Ca^{2+} indicator

Jurkat and HL-60 cells in RPMI 1640 medium, or isolated PBMCs or neutrophils in 1X PBS (with 0.2 % (w/v) glucose), were centrifuged at 300 x g at room temperature for 5 min. The supernatant was aspirated and cells resuspended in 10 – 15 ml mHBSS assay buffer (Table 10). After being centrifuged again at 300 x g at room temperature for 5 min, the cells were resuspended in 5 ml mHBSS buffer. To load the cells, 5 μM FLUO-3AM was added to the cell suspension, which was then left on a roller at room temperature for 90 min.

FLUO-3AM loaded cells were centrifuged at 300 x g for 5 min, the supernatant discarded, and the cells resuspended in assay buffer to a concentration of 4 x 10^6 cells/ml (for studies using the FLIPR) or 1x 10^6 cells/ml (for studies using the FACS).

Table 10: Components of assay buffer (pH 7.4) used to investigate $[Ca^{2+}]_i$

Compound	Concentration
NaCl	110 mM
KCl	5 mM
Na_2HPO_4	0.3 mM
KH_2PO_4	0.4 mM
Glucose	5.6 mM
$MgSO_4.7H_2O$	0.8 mM
$CaCl_2$	1.26 mM
$NaHCO_3$	4 mM
HEPES	15 mM
Serum (rat or human)	0.1%

2.36 – Investigating $[Ca^{2+}]_i$ in human neutrophils using the Fluorescent Imaging Plate Reader (FLIPR)

2.36.1 – Estimation of fMLP and LPS working concentrations

In order to determine which concentration of agonists would give the maximal response, fMLP and LPS were exposed to loaded human neutrophils at eleven different concentrations. fMLP was investigated at concentrations ranging from 1 μM to 0.1 nM , and LPS from 1 mg/ml to 1 ng/ml.

2.36.2 – Addition of agonists and GABA or glycine to neutrophils

The assay was performed in 96-well Poly-D-Lysine coated black plates (Becton Dickinson). To each well, 50 μl of cells was added to give 200,000 cells/well. 50 μl of test compound or vehicle was added to the wells at 2X final concentration. The plates were then centrifuged at approximately 200 x g for 5 min and then incubated at room temperature for 30 min. Calcium transients in response to agonists and antagonists were measured using a FLIPR. Fluorescence readings were taken every 2 seconds for a total run time of 2 min. Cells were excited at 488 nm, and emission readings taken at 525 nm. 50 μl of agonist at 3X final concentration was added after 10 seconds. The assay plate conditions are summarised below:

A 96-well plate was prepared containing 200,000 cells/well and 50 μl of vehicle (buffer) or test compound. A baseline fluorescence determination was made, and 50 μl of 1 nM fMLP or 1 mg/ml LPS was added after 10 seconds. Fluorescence data were collected over 2 min. GABA or glycine were then added at 2X final concentration, in 0.5 log dilutions, with the highest final concentration for GABA and glycine at 3 mM. Fluorescence data were once again collected over 2 min.

Responses to agonists and treatment with GABA or glycine were measured as arbitrary fluorescence units and were calculated by taking the difference between the maximum response and the minimum.

2.37 – Investigating $[Ca^{2+}]_i$ in immune cells using flow cytometry (FACScan)

2.37.1 – Trypan blue exclusion

A trypan blue exclusion was carried out to determine the approximate number of viable cells before and after agonist and antagonist addition. Trypan blue was diluted 1/10 in PBS from stock solution (SIGMA). 10 µl trypan blue was added to 10 µl cells. Viable cells were counted using a haemocytometer.

2.37.2 – Addition of agonists and GABA, muscimol or glycine to cells

For each experiment carried out on the FACS, 1 ml of the loaded cell suspension was added to a clear FACS tube (BD Trucount™ absolute counting tube, BD Biosciences). Recordings were taken at 50,000 events per sample on the FL1 channel (as this channel is best suited for the filter sets used for FLUO-3AM) and forward and side scatter were used to selectively gate the cell population. For kinetic analysis of $[Ca^{2+}]_i$ changes, events were continuously acquired with CellQuest Pro software (BD Biosciences) and the mean fluorescence of events acquired at 1 – 2 s intervals was calculated. Excitation was from an argon laser at 506 nm, while emission at 526 nm was measured on a linear scale. Autofluorescence of non-loaded cells was used to set lower gating levels and voltage and gain settings were then adjusted in order to obtain a baseline fluorescence using unstimulated cells loaded with FLUO-3AM.

1 mM GABA, 1 mM glycine or 100 μM muscimol, was added to a tube of 1 ml cell suspension, and incubated for 5s – 5 min. Agonists (1 nM fMLP, 1 mg/ml LPS) was then added to the cell suspension, and the fluorescence reading taken immediately. As a positive control, 1 μM ionomycin was added to the cell suspension in order to induce maximal Ca^{2+} release. Responses to agonists and antagonists were measured as arbitrary fluorescence units and were calculated by taking the median cellular fluorescence value.

Chapter 3

Detection of $GABA_A$ and glycine receptor subunit mRNAs in immune cells.

3 – RT- PCR detection of $GABA_A$ and glycine receptor subunits

Functional nicotinic ACh receptors have been reported to be present on mammalian immune cells (Fujii *et al.*, 1999; Kawashima and Fujii, 2000; Wang *et al.*, 2002) where they have been shown to modulate cell response to inflammation. A few reports have also suggested the presence of a few $GABA_A$ and glycine receptor subunit mRNAs in mouse (Bergeret *et al.*, 1998) and rat (Froh *et al*, 2002) primary immune cells (see section 1.6). However, to date the presence of functional inhibitory ligand-gated ion channels in human immune cells has not been clearly shown. The initial aim of this project was to determine if receptor subunit mRNAs could be detected in Jurkat J6 cells and human PBMC by using qualitative reverse transcriptase polymerase chain reactions (RT-PCR).

Primers were designed to regions corresponding to the intracellular loops between transmembrane domains M3 and M4, as this is the least conserved region between subunits, thereby increasing primer specificity. Also, a variation of the standard RT-PCR, termed 'nested' RT-PCRs were carried out in order to screen for each subunit. This was because it was assumed that any $GABA_A$ and glycine receptor subunits present would be expressed at low levels in immune cells. Although standard RT-PCR is a sensitive technique, its sensitivity can be further increased by performing nested RT-PCR. This involves taking an aliquot of the product from the primary RT-PCR, and using it as a template for a secondary round of PCR amplification. To avoid further amplification of primer-dimer artifacts or nonspecific products generated in the primary PCR, a different set of primers were used in the second PCR reaction. These nested primers were internal to the primers used in the primary PCR (therefore termed 'internal primers'), yielding a shorter PCR product.

3.2 – Results

Poly A^+ RNA isolated from whole brain (CLONTECH), was used as a positive control to test the specificity of the PCR conditions. The ratio of absorption (260:280 nm) of all RNA preparations was in the range 1.8 – 2.0, indicating that protein contamination had not occurred.

3.2.1 – Amplification of $GABA_A$ and glycine receptor subunit cDNAs

The PCR reaction performed on cDNA synthesised from the mRNA using specific up- and downstream primers gave amplification products of appropriate base pair lengths for each subunit analysed (Table 11 and 12). All experiments were repeated at least three times, using separate cDNA preparations each time in order to ensure that the results were consistent. Also, all RT-PCR products were confirmed by sequencing (see section 2.25). Figures 11 and 12 show representative ethidium bromide stained agarose gel electrophoresis of $GABA_A$ and glycine receptor subunit RT-PCR products.

The primers for the $GABA_A$ and glycine receptor subunits were designed according to published sequences and were optimised with regards to a standardised melting temperature (55 – 60° C) and primer dimer formation. Control experiments, where a PCR reaction was performed on RNA without including the reverse transcription step, did not produce any bands, thus confirming that total RNA was free from genomic DNA. A no template PCR was also performed as a negative control, to ensure that all components of the PCR reaction were free from contamination.

Table 11: $GABA_A$ receptor subunit cDNAs amplified from: B = human brain cDNA; J = Jurkat cell cDNA; P = human PBMC cDNA. '+' indicates the presence of the most intensely stained PCR bands, '±' indicates the presence of faint bands and '–' indicates absence of bands.

$GABA_A$ receptor subunit	Product size (bp) External/Internal	T_m °C External/Internal	Present in : (Using external primers)			Present in : (Using internal primers)		
			B	J	P	B	J	P
α1	241/95	55/55	+	+	+	+	+	+
α2	207/90	55/55	+	-	-	+	-	-
α3	247/116	55/56	+	+	+	+	+	+
α4	487/254	56/53	+	+	+	+	+	+
α5	216/134	53/57	+	-	-	+	-	-
α6	269/150	52/54	+	±	-	+	+	-
β1	321/112	53/57	+	+	-	+	+	-
β2	314/169	55/55	+	+	-	+	+	+
β3	319/110	53/54	+	+	±	+	+	+
δ	252/128	57/56	+	-	+	+	-	+
ε	315/139	55/55	+	+	+	+	+	+
γ2	244/137	56/56	+	+	-	+	+	±
γ3	300/182	52/54	+	-	-	+	-	-
θ	667/471	57/57	±	±	-	±	±	-

Figure 11: Representative ethidium bromide stained agarose gel electrophoresis of the RT-PCR products obtained using $GABA_A$ receptor subunit specific external and internal primers. Figures 11 A(i) to 11 N(i) show PCR products obtained from external primers. Figures 11 A(ii) to 11 N(ii) show PCR products obtained from internal primers.

1 2 3 4

Fig 11 A: (i) $GABA_A$ α1. Lane 1: PBMC; Lane 2: Jurkat; Lane 3: Brain; Lane 4: 100 bp ladder

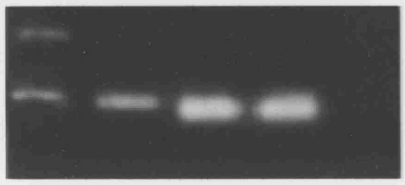

1 2 3 4

(ii) $GABA_A$ α1. Lane 1: 100 bp ladder; Lane 2: PBMC; Lane 3: Jurkat; Lane 4:Brain

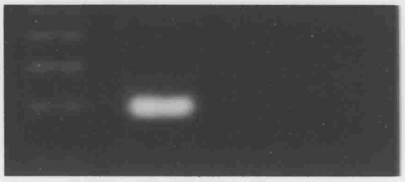

1 2 3 4

Fig 11 B: (i) $GABA_A$ α2. Lane 1: 100 bp ladder Lane 2: Brain ; Lane 3: Jurkat; Lane 4: PBMC

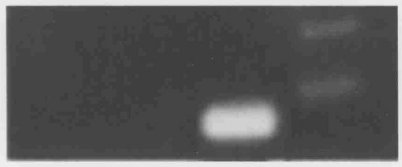

1 2 3 4

(ii) $GABA_A$ α2.. Lane 1: PBMC; Lane 2: Jurkat; Lane 3: Brain; Lane 4:100 bp ladder

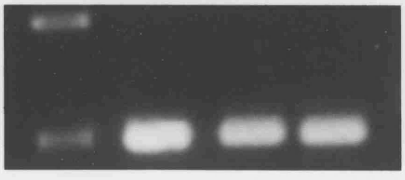

1 2 3 4

Fig 11 C: (i) $GABA_A$ α3. Lane 1: 1000 bp ladder Lane 2: Brain ; Lane 3: Jurkat; Lane 4: PBMC

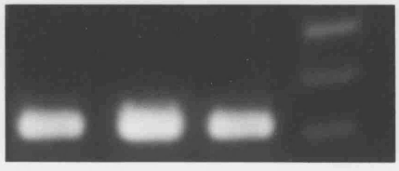

1 2 3 4

(ii) $GABA_A$ α3.. Lane 1: PBMC; Lane 2: Jurkat; Lane 3: Brain; Lane 4: 100 bp ladder

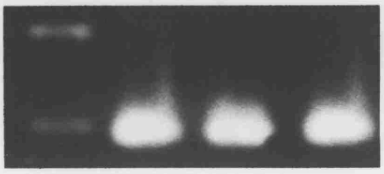

1 2 3 4

Fig 11 D: (i) $GABA_A$ α4. Lane 1: 1000 bp ladder
Lane 2: Brain ; Lane 3: Jurkat; Lane 4: PBMC

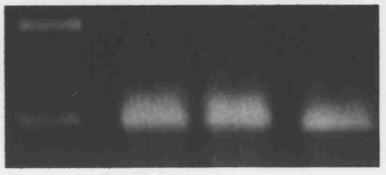

1 2 3 4

(ii) $GABA_A$ α4. Lane 1: 1000 bp ladder;
Lane 2: Brain; Lane 3: Jurkat; Lane 4: PBMC

1 2 3 4

Fig 11 E: (i) $GABA_A$ α5. Lane 1: PBMC
Lane 2: Jurkat ; Lane 3: Brain ;Lane 4: 100 bp ladder

1 2 3 4

(ii) $GABA_A$ α5. Lane 1: PBMC; Lane 2:
Jurkat; Lane 3: Brain; Lane 4: 100 bp ladder

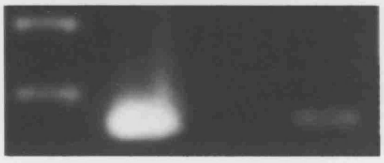

1 2 3 4

Fig 11 F: (i) $GABA_A$ α6. Lane 1: 100 bp ladder
Lane 2: Brain ; Lane 3: PBMC; Lane 4: Jurkat

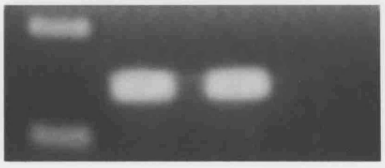

1 2 3 4

(ii) $GABA_A$ α6. Lane 1: 100 bp ladder;
Lane 2: Brain; Lane 3: Jurkat; Lane 4: PBMC

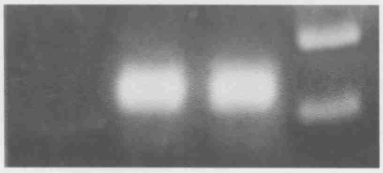

1 2 3 4

Fig 11 G: (i) $GABA_A$ β1. Lane 1: PBMC
Lane 2: Brain ; Lane 3: Jurkat; Lane 4:100 bp ladder

1 2 3 4

(ii) $GABA_A$ β1. Lane 1: 100 bp ladder;
Lane 2: Brain; Lane 3: PBMC; Lane 4: Jurkat

1 2 3 4

Fig 11 H: (i) $GABA_A$ β2. Lane 1: 1000 bp ladder Lane 2: Brain ; Lane 3: Jurkat; Lane 4: PBMC

1 2 3 4

(ii) $GABA_A$ β2. Lane 1: PBMC; Lane 2: Jurkat; Lane 3: Brain; Lane 4: 100 bp ladder Lane 2:

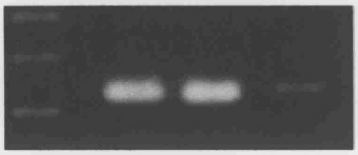

1 2 3 4

Fig 11 I: (i) $GABA_A$ β3. Lane 1: 1000 bp ladder 2: Brain ; Lane 3: Jurkat; Lane 4: PBMC

1 2 3 4

(ii) $GABA_A$ β3. Lane 1: PBMC; Lane 2: Jurkat; Lane 3: Brain; Lane 4: 100 bp ladder Lane

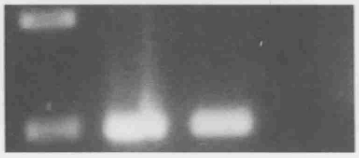

1 2 3 4

Fig 11 J: (i) $GABA_A$ δ.. Lane 1: 1000 bp ladder Lane 2: Brain ; Lane 3: PBMC; Lane 4: Jurkat

1 2 3 4

(ii) $GABA_A$ δ. Lane 1: 100 bp ladder; Lane 2: Jurkat; Lane 3: Brain; Lane 4: PBMC

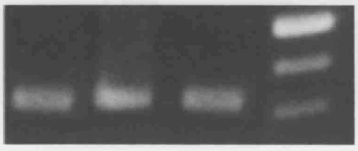

1 2 3 4

Fig 11 K: (i) $GABA_A$ ε. Lane 1: Jurkat Lane 2: PBMC ; Lane 3: Brain; Lane 4: 100 bp ladder

1 2 3 4

(ii) $GABA_A$ ε. Lane 1: 100 bp ladder; Lane 2:Brain; Lane 3: Jurkat; Lane 4: PBMC

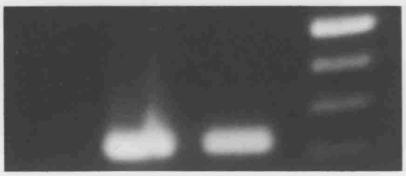

1 2 3 4

Fig 11 L: (i) $GABA_A$ γ2. Lane 1: PBMC
2: Jurkat; Lane 3: Brain; Lane 4:100 bp ladder

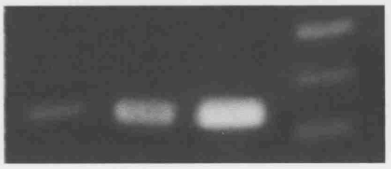

1 2 3 4

(ii) $GABA_A$ γ2. Lane 1: PBMC; Lane 2: Lane
Jurkat; Lane 3: Brain; Lane 4: 100 bp ladder

1 2 3 4

Fig 11 M: (i) $GABA_A$ γ3. Lane 1: 1000 bp ladder
Lane 2: Brain; Lane 3: Jurkat; Lane 4: PBMC

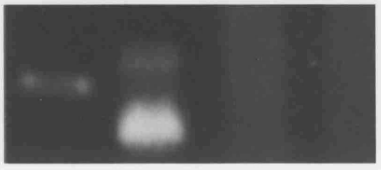

1 2 3 4

(ii) $GABA_A$ γ3. Lane 1: 100 bp ladder; Lane
2: Brain; Lane 3: Jurkat; Lane 4: PBMC

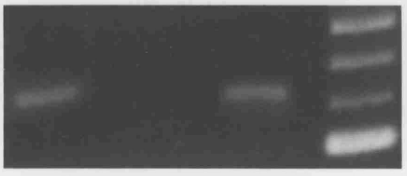

1 2 3 4

Fig 11 N: (i) $GABA_A$ θ. Lane 1: Brain
Lane 2: PBMC; Lane 3: Jurkat; Lane 4:100 bp ladder

1 2 3 4

(ii) $GABA_A$ θ. Lane 1: PBMC; Lane 2:
Jurkat; Lane 3: Brain; Lane 4: 100 bp ladder

Profiles of $GABA_A$ receptor subunit expression in human brain, Jurkat cells and human PBMC cDNAs are shown in Figure 11. As can be seen from Table 11 and Figure 11, all the $GABA_A$ receptor subunits tested were expressed in the brain. Differences in levels of expression of the same subunit were also noticeable in different mRNAs. For example, strong bands (at 319 bp) corresponding to the $GABA_A$ $\beta 3$ subunit amplified by external primers were present in brain and Jurkat cDNAs, while only a faint band was detected in PBMC (Figure 11 Ii and Iii).

The $GABA_A$ receptor $\alpha 1$ subunit was detected in brain, Jurkat and PBMC cDNA although the signal in the latter was weak in comparison to brain and Jurkat expression. However, it was detected by using both external and internal primers at the expected sizes of 241 and 95 bp respectively (Figures 11 Ai and Aii). While the $\alpha 2$ and $\alpha 5$ subunits were only detected in brain cDNA (Figures 11 B and 11 E), strong signals were detected for the $\alpha 3$ subunit cDNA in brain, PBMC and Jurkat cDNAs using both external and internal primers at 247 and 116 bp respectively (Figures 11 Ci and Cii). The $GABA_A$ receptor $\alpha 4$ subunit was also detected in brain, Jurkat and PBMC using both external and internal primers at 487 and 254 bp respectively, although interestingly, the product signal was weaker in the nested PCR reaction (Figure 11 Dii). The $\alpha 6$ and $\beta 1$ subunits were only detected in brain and Jurkat cDNAs (Figures 11 F and 11G), and the $\beta 2$ subunit was only detected in PBMC using internal primers. However, strong signals were detected in brain and Jurkat cDNAs using both external and internal primers (Figures 11 H). The $\beta 3$ subunit was detected at low levels in PBMC using internal primers (Figure 11 Ii), while a strong signal corresponding to the subunit was obtained using external primers (Figure 11 Iii). Bands (252 and 128 bp) corresponding to the δ subunit were detected in human brain and PBMC cDNAs, but was absent in Jurkat cDNA (Figure 11J), while strong signals for the ε subunit (315 and 139 bp) were detected in all three cDNA samples (Figure 11K). The γ_3 subunit cDNA was detected only in human brain (Figure 11M), and strong signals for the γ_2 subunit was detected in human brain and Jurkat cDNAs, and a weak signal was detected in human PBMC (Figure 11L). Faint signals corresponding to the $GABA_A$ θ subunit was detected in

human brain and PBMC, but not in Jurkat cells at 667 and 471 bp (Figure 11 Ni and Nii).

Profiles of glycine receptor subunit expression in human brain, Jurkat cells and human PBMC cDNAs are summarised in Table 12 and shown in Figure 12.

Table 12: Glycine receptor subunit cDNAs amplified from: B = human brain cDNA; J = Jurkat cDNA; P = PBMC cDNA. * indicates sample was amplified using Touchdown PCR (see below for conditions). '+' indicates the presence of the most intensely stained PCR bands, '±' indicates the presence of faint bands and '–' indicates absence of bands.

Glycine Receptor subunit	Product size (bp) External/Internal	T_m °C External/Internal	Present in : (Using external primers) B J P	Present in : (Using internal primers) B J P
α1	235/100	56*/60	+ - -	+ - -
α2	217/119	55/56	+ - -	+ - -
α3	207/128	53/55	+ - -	+ - -
β	284/158	55/55	+ + -	+ + -

Figure 12: Representative ethidium bromide stained agarose gel electrophoresis of the RT-PCR products obtained using glycine receptor subunit specific external and internal primers. Figures 12 A(i) to 12 D(i) show PCR products obtained from external primers. Figures 12 A(ii) to 12 D(ii) show PCR products obtained from internal primers.

1 2 3 4

Fig 12 A: (i) Glycine α1. Lane 1: 100 bp ladder Lane 2: Brain; Lane 3: Jurkat; Lane 4: PBMC

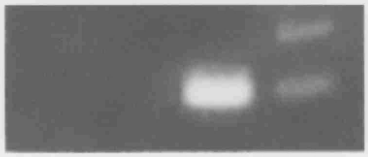

1 2 3 4

(ii) Glycine α1. Lane 1: 100 bp ladder; Lane 2: Brain; Lane 3: Jurkat; Lane 4: PBMC

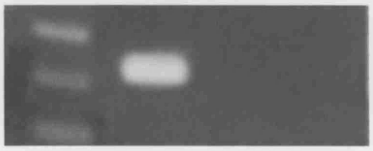

1 2 3 4

Fig 12 B: (i) Glycine α2. Lane 1: 100 bp ladder Lane 2: Brain; Lane 3: Jurkat; Lane 4: PBMC

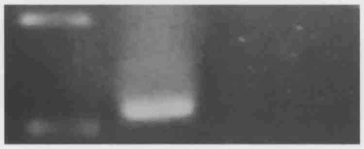

1 2 3 4

(ii) Glycine α2. Lane 1: 100 bp ladder; Lane 2: Brain; Lane 3: Jurkat; Lane 4: PBMC

1 2 3 4

Fig 12 C: (i) Glycine α3. Lane 1: 100 bp ladder Lane 2: Brain; Lane 3: Jurkat; Lane 4: PBMC

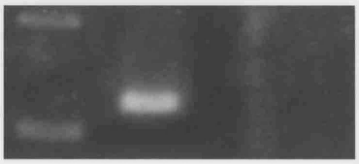

1 2 3 4

(ii) Glycine α3. Lane 1: 100 bp ladder; Lane 2: Brain; Lane 3: Jurkat; Lane 4: PBMC

1 2 3 4

Fig 12 D: (i) Glycine β. Lane 1: 100 bp ladder Lane 2: Brain; Lane 3: Jurkat; Lane 4: PBMC

1 2 3 4

(ii) Glycine β. Lane 1: 100 bp ladder; Lane 2: PBMC; Lane 3: Brain; Lane 4: Jurkat

The glycine receptor α1, α2 and α3 subunits were only detected in human brain cDNA (Figures 12A – 12C). For the expression of glycine α1 subunit in brain, a specialised form of RT-PCR, termed 'touchdown PCR' was used. Touchdown PCR is a method for increasing specificity of PCR reactions by using a cycling program where the annealing temperature is gradually reduced by 1 – 2 °C every second cycle. The initial annealing temperature is usually set several degrees above the estimated T_m of the primers. Annealing temperature is then gradually decreased until it reaches the calculated annealing temperature of the primers or some degrees below. Amplification is then continued using this annealing temperature. The idea is that any differences in T_m between correct and incorrect annealing gives approximately a 2-fold difference in product amount per cycle (4-fold °C).

In order to amplify the glycine α1 subunit, touchdown PCR was performed using the external primers. The reaction was performed at 56, 54, 52, 50, and 48° C for 1 min and 46° C for 2 min, for 35 cycles. The PCR product was then used as a template for a standard PCR reaction (at 55° C) using the internal primers. The expected 100 bp product derived from internal primers was observed from brain cDNA only (Figures 12 Ai and Aii). A no template control was performed in parallel, and did not give rise to any bands, thereby ruling out the possibility of contamination. Touchdown PCR was also attempted to detect the α subunits in Jurkat and PBMC cDNA, but the subunits could not be detected. However, standard RT-PCR produced bands corresponding to the glycine β subunit in brain and Jurkat cell cDNAs using external and internal primers. The PCR products were of the expected sizes at 284 and 158 bp (Figure 12D).

3.3 – Quantitative RT- PCR

The data obtained through RT-PCR indicated that several ligand-gated chloride channel subunit mRNAs were present in human immune cells. However, in order

to gain a better idea of the possible biological significance of this, quantitative measurements needed to be performed. Although RT-PCR is mainly used for qualitative studies, several modifications of this method have been developed that allow quantitative analysis. One such method is real-time RT-PCR which is a system based on the detection and quantitation of a fluorescent reporter, usually FAM (6-carboxyfluorescein) or SYBR Green. For the purposes of this project TaqMan RT-PCR was used for the quantitative detection of $GABA_A$ and glycine receptor subunit mRNAs. The fluorescent probes in this system use the fluorogenic 5' exonuclease activity of Taq DNA polymerase to measure the amount of target sequences in cDNA samples. The TaqMan probes used in this study contained the reporter fluorescent dye FAM on the 5' base, and the energy-adsorbing quenching dye Methyl Red on the 3' base. Methyl Red was used as it is superior to other available quenchers, in that it has no fluorescent emission of its own that can be detected by the sequence detector (ABI PRISM 7700 Sequence Detector System).

TaqMan primer and probe design is crucial to the success of the PCR reaction. The required parameters for well-designed primers and probes includes having a T_m for the probe that is at least 10°C higher than the primers, G-C content in probe to be in the 30 – 80% range, primers to be designed as close as possible to the probe without overlapping and the primer T_m being set between 58°C and 60°C. All primers and probes were designed using Primer Express Version 1.0 (Applied Biosystems), which was also used to select the position of the primer within the subunit sequence. Unlike qualitative RT-PCR, primers and probes were not exclusively designed to sequences within the M3 – M4 loop.

When irradiated, the excited fluorescent dye transfers energy to the nearby quenching dye molecule rather than fluorescing. TaqMan probes were designed to anneal to an internal region of the PCR product. When the polymerase replicates a template on which a TaqMan probe is bound, its 5' exonuclease activity cleaves the probe (Heid *et.al.* 1996). This ends the activity of the quencher and the reporter dye starts to emit fluorescence which increases in each cycle proportional to the rate of probe cleavage. Accumulation of PCR products is therefore detected by monitoring the increase in fluorescence of the reporter dye (Wang and Brown,

1999). Because the cleavage occurs only if the probe hybridises to the target, the fluorescence detected originates from specific amplification. Also, the monitoring of the whole reaction rather than just the end product permits the quantitation to be based on the early, linear part of the reaction. This permits a threshold cycle (Ct) to be determined at which fluorescence above background is first detected. Ct values correspond to the cycle number at which the fluorescence due to enrichment of the PCR product reaches significant levels above the background fluorescence (threshold).

TaqMan RT-PCR is a very sensitive method of detecting the presence of the original RNA, but it cannot be quantified without some standard against which to measure the final number of amplified strands. Normalisation is necessary to correct for possible variations in the template input amount among the samples, and methods commonly used include normalisation to β-actin mRNA, to glyceraldehyde 3-phosphate dehydrogenase mRNA, to 18S rRNA, and to the total RNA concentration. For the purposes of this project 18S rRNA was used as a housekeeping gene. A standard curve of ribosomal 18S rRNA was obtained for each sample and the Ct value for the 18S rRNA was subtracted from the Ct value of the target gene in order to normalise the data. The cycle number at which amplification of the product starts, corresponds to the levels at which its mRNA is present in the sample, i.e. the amplification of product at an early cycle indicates the presence of high levels of target mRNA. Therefore, in a 40-cycle PCR reaction, any amplification of products occurring after a Ct number of 35 were ignored.

Due to the high specificity and sensitivity of TaqMan RT-PCR, it was used to determine the presence of a number of $GABA_A$ and glycine receptor subunits in a variety of human tissues and immune cells including monocytes, CD4+, CD8+, irradiated B-cells, PBMC and neutrophils. Receptor subunit mRNAs displaying the most intensely stained PCR products from human PBMC using standard RT-PCR were screened for. These included the α1, α3, β2 and β3 $GABA_A$ receptor subunits as well as the δ and ε subunits. Also, RT-PCR results showed that only the glycine β subunit mRNA was detected in Jurkat cells, and none of the subunits were present in PBMC. However, due to reports that functional glycine receptors may be present in rat neutrophils (Wheeler *et al.*, 2000), we used the TaqMan

method to see if the glycine receptor subunits could be detected in a number of immune cells.

The 96-well plates used for the experiments were all prepared at AstraZeneca (R&D Charnwood, Loughborough). These contained an array of human tissues and immune cell cDNAs. RNA from whole human brain, heart, lung, liver, trachea and placenta were supplied as total RNA from Clontech or Invitrogen. All the immune cells used were isolated by flow cytometry (e.g. immature and mature dendritic cells and monocytes), immunomagnetic separation with dynabeads (e.g. CD4+ T cells, CD8+ T cells and B cells) or by using density gradient solutions (neutrophils and T-helper cells) at AstraZeneca (Loughborough). Total RNA was prepared using TRIzol and glycogen (GIBCO BRL) and then reverse-transcribed into cDNA with random hexamer primers and Superscript II (GIBCO BRL). The cDNA was then loaded onto the 96-well plates, where each sample was added to two separate wells.

3.3.1 – Detection of $GABA_A$ receptor subunits

As expected, the highest amount of amplification of all $GABA_A$ receptor subunits was from whole brain (positive control), while amplification from other human tissues and immune cells was variable. The α_1 subunit cDNA was detected in small amounts from monocytes, CD8+ and irradiated B-cells and in slightly higher amounts in CD4+ cells. The subunit was detected at the highest amounts in

PBMCs (Figure 13). This was consistent with the amplification patterns of each sample. Figure 14 shows the amplification plot of the α_1 subunit cDNA from (A) human brain and in (B) human PBMC, CD4+, CD8+ and irradiated B-cells. The PCR reaction was allowed to run for 40 cycles, and as can be seen in Figure 14A, the α_1 subunit cDNA started to amplify from the brain cDNA at a Ct value of 19. In PBMC, amplification occurred at a Ct of 22, while CD4+, CD8+, irradiated B cells and monocytes show amplification of the product at Ct values of 27, 28, 30

and 30 respectively (Figure 14B). This indicates that the $GABA_A$ receptor $\alpha 1$ subunit is present at higher levels in PBMC cDNA in comparison to the other immune cells tested.

The $GABA_A$ receptor $\alpha 3$ subunit cDNA was expressed at low levels in CD4+ and irradiated B cells, although it was not detected in human PBMC or neutrophils. The $GABA_A$ receptor $\beta 2$ subunit cDNA was amplified in variable amounts from a number of tissues (Figure 15), especially lung and liver tissue. It was also detected in small amounts in monocytes, CD4+, CD8+, PBMC and neutrophils, although at these low levels, the presence of functional $\beta 2$ subunit polypeptides is somewhat questionable. Irradiated B cells showed the highest levels of detection compared to all the other immune cells tested. Low levels of the $\alpha 1$ and $\beta 2$ subunits were also detected in a mixed population of lymphocytes stimulated with the proinflammatory cytokine, tumor necrosis factor-α (TNF-α) for 6 hours. In contrast, the $\beta 3$ subunit cDNA was expressed at negligible levels in non-neuronal human tissues and immune cells.

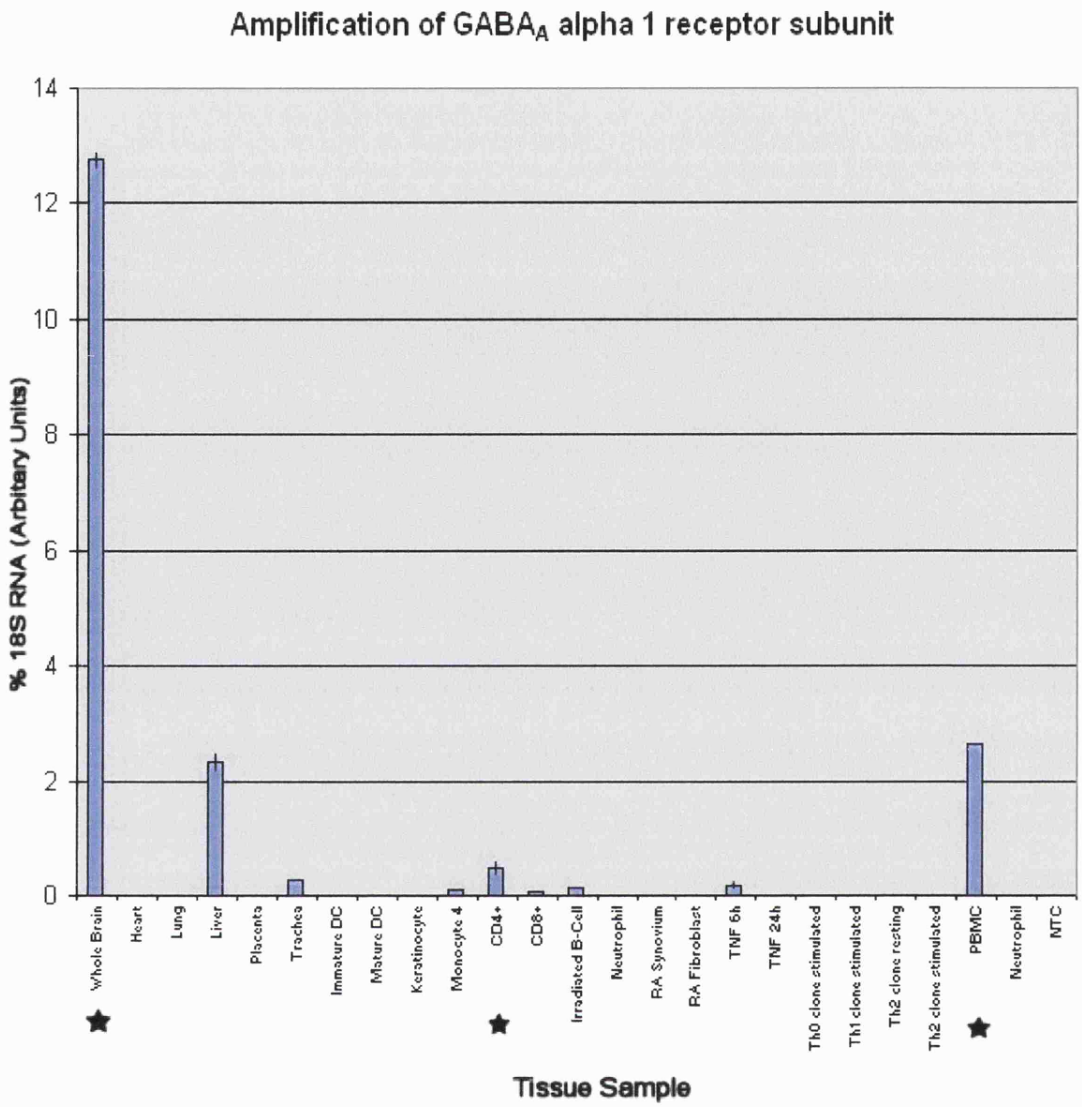

Figure 13: Distribution of GABA$_A$ receptor α1 subunit cDNA in human tissues. TaqMan Ct values were converted to arbitrary units, followed by 18S rRNA normalisation to correct for RNA quantity and integrity. Data are mean $\pm$ S.E. for duplicate reverse transcription reactions from each mRNA pool. The black stars indicate samples of interest.

(A) Amplification plot of $GABA_A$ α1 subunit from human brain cDNA

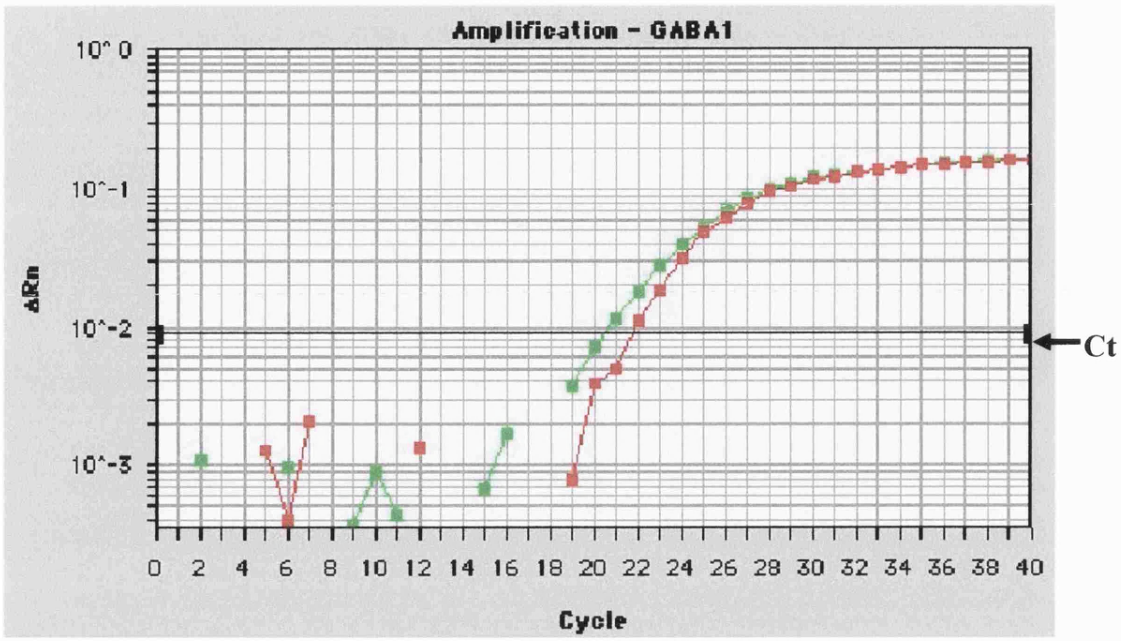

(B) Amplification plot of $GABA_A$ α1 subunit from human immune cell

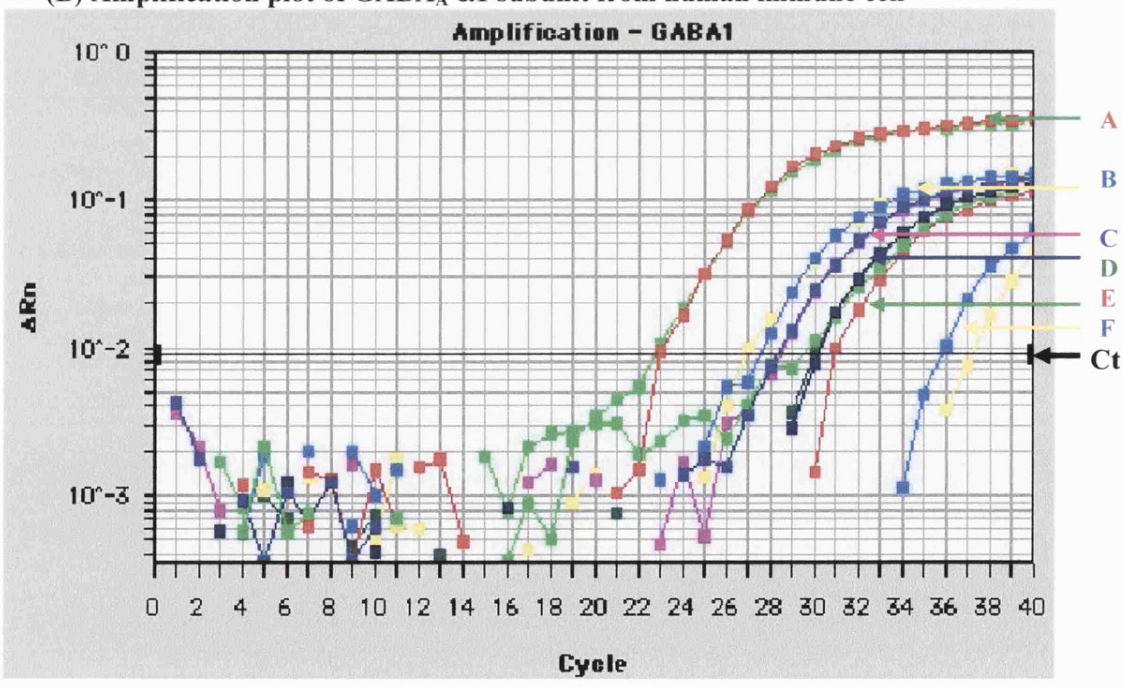

Figure 14: Amplification plot of the $GABA_A$ α1 subunit from (A) human brain cDNA (red and lime plots) and (B) from A – human PBMC (red and lime); B – CD4+ cells (sky blue and yellow); C – CD8+ cells (navy blue and pink); D – Irradiated B-cells (dark blue and green); E – Monocytes (red and lime) and F – (sky blue and yellow) a no template control. Ct represents the cycle threshold, i.e. the PCR cycle number at which fluorescence is detected above an arbitrary baseline. All samples were loaded onto the plates as duplicates the plots of which represented as pairs of colours.

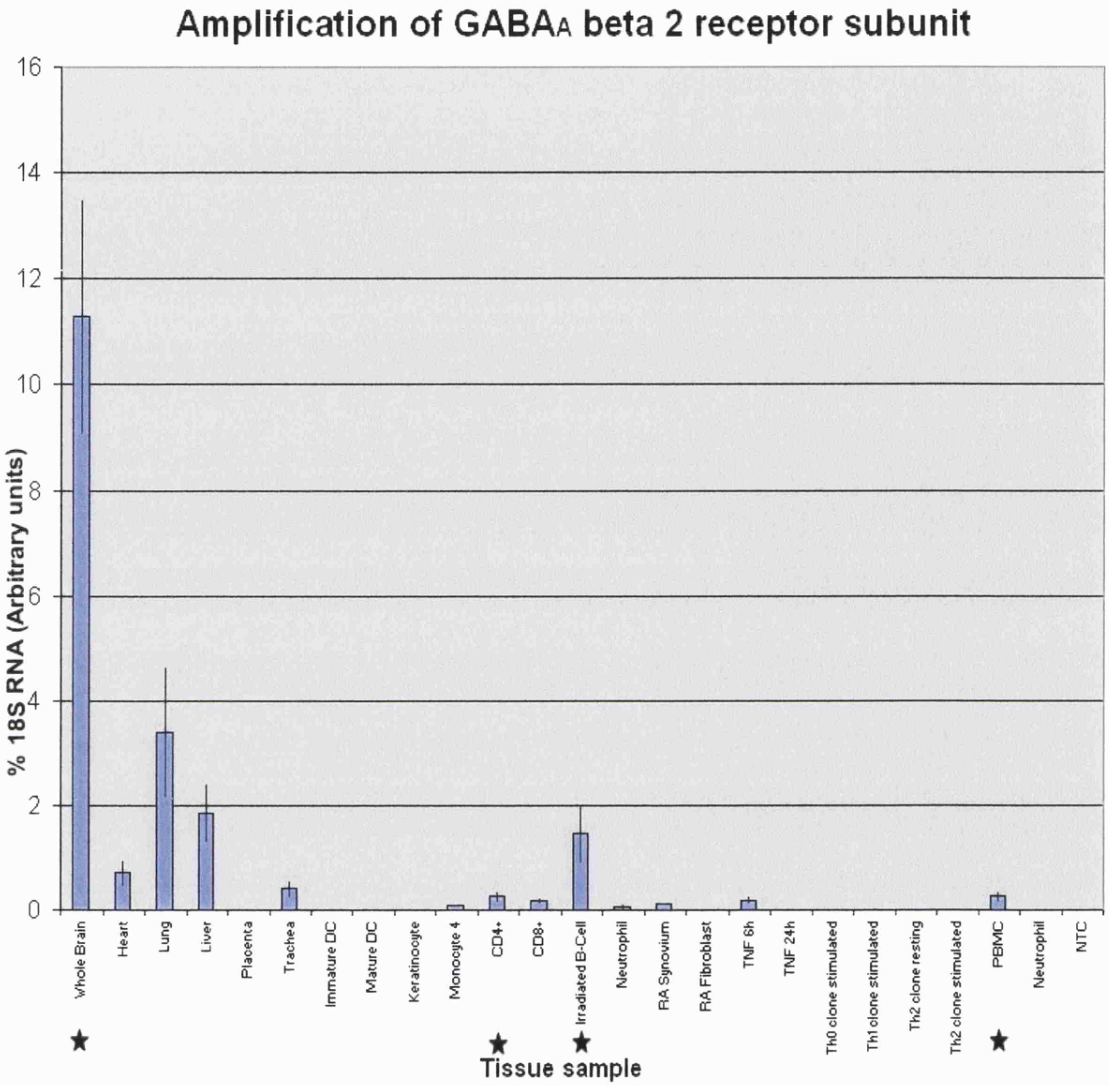

Figure 15: Distribution of $GABA_A$ β2 receptor subunit cDNA in human tissues. Data are expressed as arbitrary units normalised to 18 S RNA to correct for RNA quantity and integrity, and are mean ± S.E. for duplicate reverse transcription reactions from each mRNA pool. The black stars indicate samples of interest.

Table 13 shows a comparison of mean Ct values of the various $GABA_A$ receptor subunits amplified from a variety of human immune cells. The widest distribution of 'significant' (i.e. where amplification has occurred at a Ct number lower than 35) levels of subunit cDNA was observed for the $GABA_A$ $\alpha 1$ and $\beta 2$ subunits. The $GABA_A$ receptor δ and ε subunit mRNAs had also been screened for. However, no significant amplification of the subunit cDNAs were observed in any of the immune cells. This was probably due to poor primer and probe design, as amplification levels of both the δ and ε subunit in the brain cDNA was also low.

Table 13: Comparison of mean TaqMan Ct values of $GABA_A$ receptor subunit amplification from human brain and immune cells (n=2). Results are presented as arbitrary Ct values. Ct values lower than 35 are highlighted in blue.

Sample (source of RNA)	TaqMan Result (Ct) from $\alpha 1$	TaqMan Result (Ct) from $\alpha 3$	TaqMan Result (Ct) from $\beta 2$	TaqMan Result (Ct) from $\beta 3$
Whole Brain	20	21	18	22
Monocyte	29	36	34	38
CD4+	27	28	30	36
CD8+	28	35	33	37
Irradiated B cell	31	31	25	39
Neutrophil	38	39	34	40
TNF 6h	29	36	32	39
PBMC (own sample)	23	38	32	40
Neutrophil (own sample)	40	39	39	40

3.3.2 – Detection of glycine receptor subunits

For the initial TaqMan studies, the possible presence of glycine receptor subunits was screened for in the same human tissues and immune cells as above. Overall, compared to the $GABA_A$ receptor subunit cDNAs, the amount of glycine receptor subunit cDNAs showed a wider level of detected at the highest levels in human brain.

Of all the glycine receptor subunits, the α1 subunit showed the widest level of distribution in human immune cells (Figure 16, Table 14). The subunit was detected in CD4+ and mature dendritic cells at higher levels compared to monocytes, CD8+, irradiated B cells and immature dendritic cells (Figure 16). Low levels of the subunit were also detected in TNF-α stimulated lymphocytes (6 hours), and T-helper clone cells (Th0, Th1 and Th2). Highest levels of detection were present in TNF-α stimulated lymphocytes (24 hours) and PBMC cDNA. Figure 17A shows the amplification of the subunit in brain cDNA at cycle number 17 and in PBMC and neutrophil cDNA at a Ct of 24 and 26 respectively (Figure 17B).

The glycine α2 subunit mRNA also showed a wide level of distribution in the immune cells. Amplification occurred at high levels in CD4+ and PBMC cDNAs. Slightly lower levels were also detected in TNF-α stimulated lymphocytes (24 hours) and neutrophils (own sample), while low levels were detected in cDNAs from immature and mature dendritic cells, CD8+ cells, irradiated B cells, and in neutrophils (Astrazeneca). T helper clone cells (stimulated Th2 clone) and monocytes also showed low levels of amplification of the α2 subunit (Table 14).

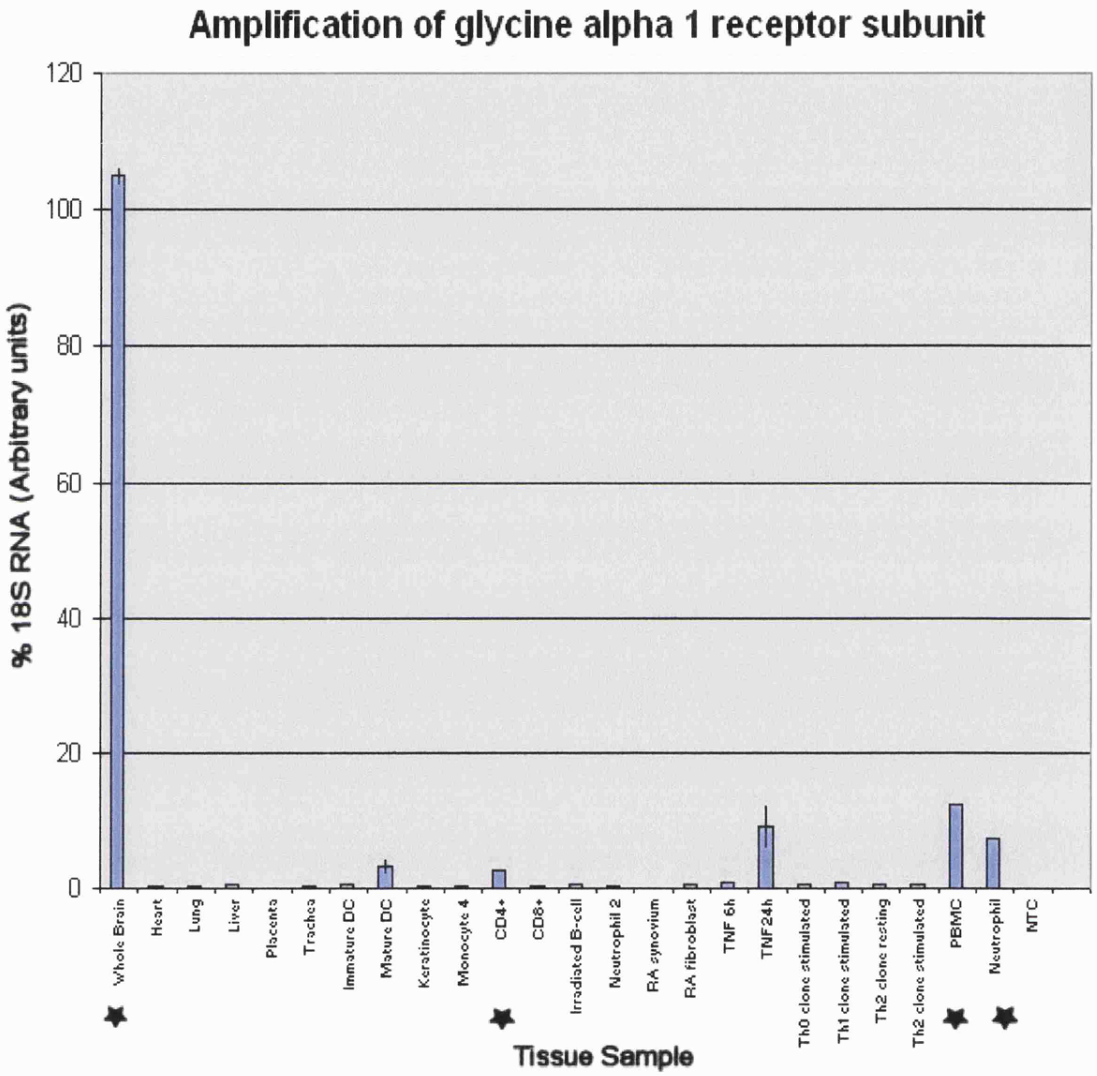

Figure 16: Distribution of glycine α1 receptor subunit cDNA in human tissues. Data are expressed as arbitrary units normalised to 18S RNA. Black stars are placed under samples of interest.

(A) Amplification plot for glycine α1 subunit from human brain cDNA

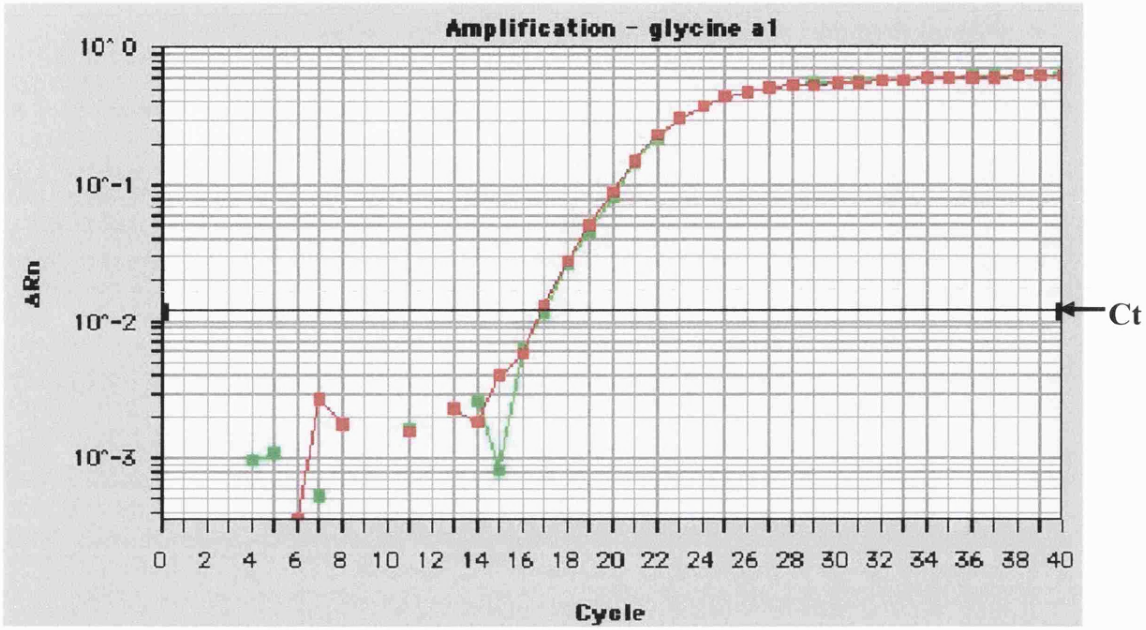

(B) Amplification plot for glycine α1 subunit from human neutrophil cDNA

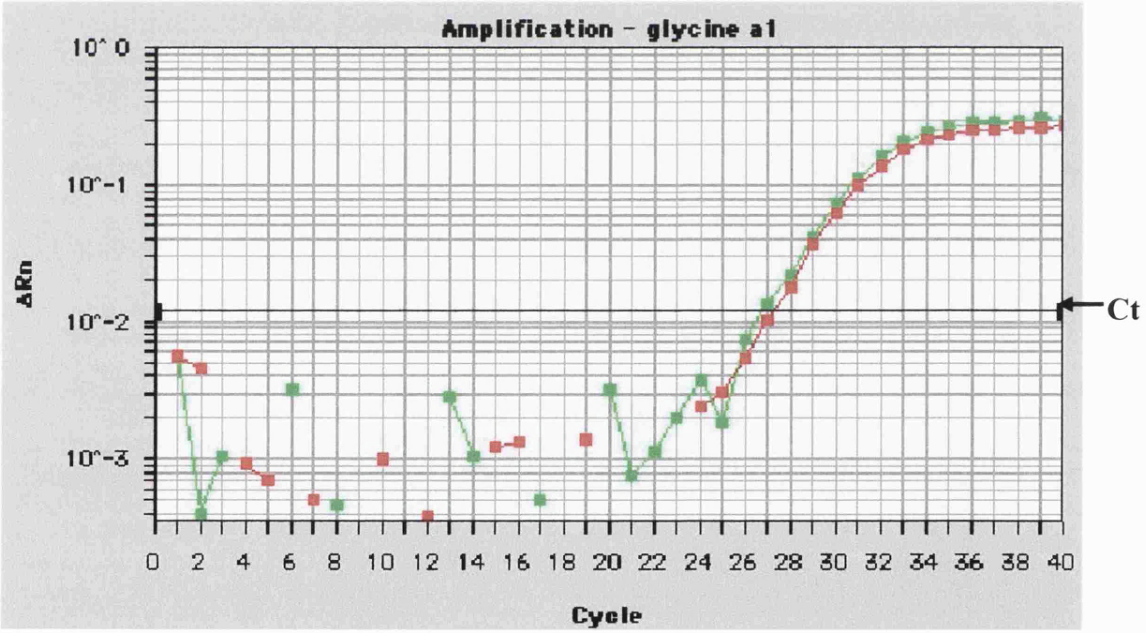

Figure 17: Amplification plot of the glycine α1 receptor subunit from (A) human brain and (B) human neutrophil cDNA. Samples were loaded onto the plates in duplicates (red and lime plots). Amplification of the product starts at cycle 14 in human brain. This takes place at a much later cycle number (cycle 25) in human neutrophils. Ct represents the cycle threshold, i.e. the PCR cycle number at which fluorescence is detected above an arbitrary baseline.

Compared to the glycine α1 and α2 subunits, the α3 subunit cDNA showed a slightly lower level of distribution in immune cells. It was detected in cDNAs from CD4+ cells and monocytes, but not from neutrophils or human PBMC (Table 14). Other immune cells expressing the α3 subunit mRNA included CD8+, irradiated B cells and the T helper clone cells (stimulated Th2 clone). Highest levels of the glycine β subunit were detected in cDNA from lymphocytes stimulated with TNF-α for 24 hours. High levels were also observed in cDNA from lymphocytes stimulated with TNF-α for 6 hours, and also in tissues taken from fibroblasts of patients with rheumatoid arthritis (RA). In comparison, slightly lower levels of the subunit were detected in cDNAs from tissues taken from the synovium of RA patients, PBMC and neutrophils (own sample). Figure 19 shows the amplification plots of cDNAs from neutrophils (Figure 19A), PBMC and brain (Figure 19B), which have Ct values of 23, 27 and 20 respectively.

Interestingly, the glycine α1, α2 and β subunits showed very different levels of detection in the two neutrophil samples. While in my own neutrophil cDNA sample it was observed at levels comparable to TNF-α stimulated lymphocyte cDNA (24 hours), in the cDNA sample prepared at AstraZeneca levels of the α1 subunit was barely detectable. Neutrophil isolation and cDNA synthesis from both samples had been prepared by using the same methods. The main variation was in the way the total RNA had been extracted, where I had used the method described in section 2.13, which being phenol and chloroform free, differs from the TRIzol and glycogen method. However, the TRIzol method is well established and is known to extract good quality RNA. A second difference in protocol was that I prepared total RNA from isolated neutrophils on the same day as the whole blood was collected (see section 2.6). This was to ensure minimal degradation of RNA. However, neutrophils isolated from whole blood at AstraZeneca was sometimes frozen at – 80 °C, and RNA was extracted at a later date. If the glycine α1, α2 and β subunits are present at low levels in human neutrophils, then it could become degraded upon freezing and thawing the cells prior to total RNA extraction.

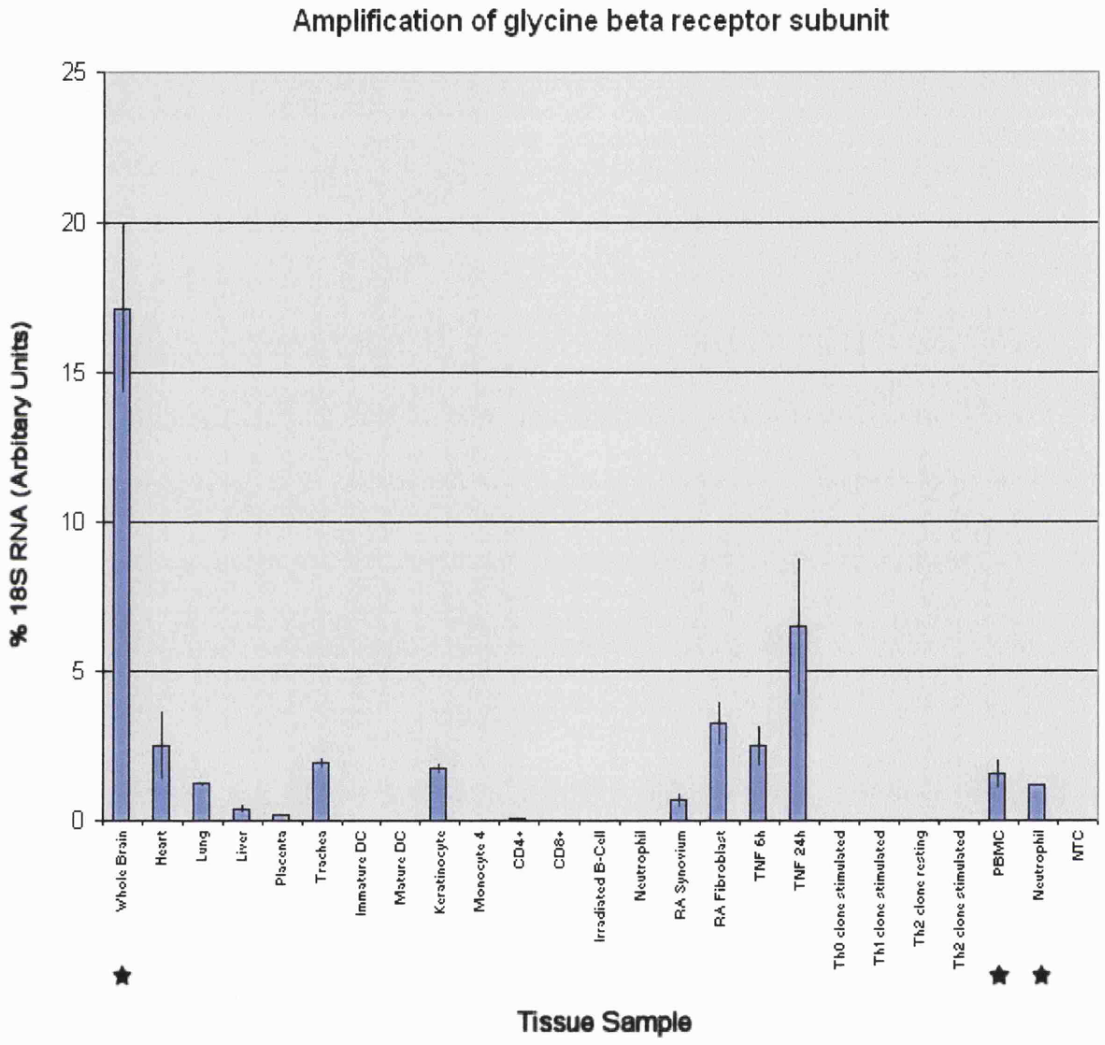

Figure 18: Distribution of glycine β receptor subunit cDNA in human tissues. Data are expressed as arbitrary units normalised to 18S RNA. Black stars are placed under samples of interest.

(A) Amplification plot of glycine β subunit from human neutrophils cDNA

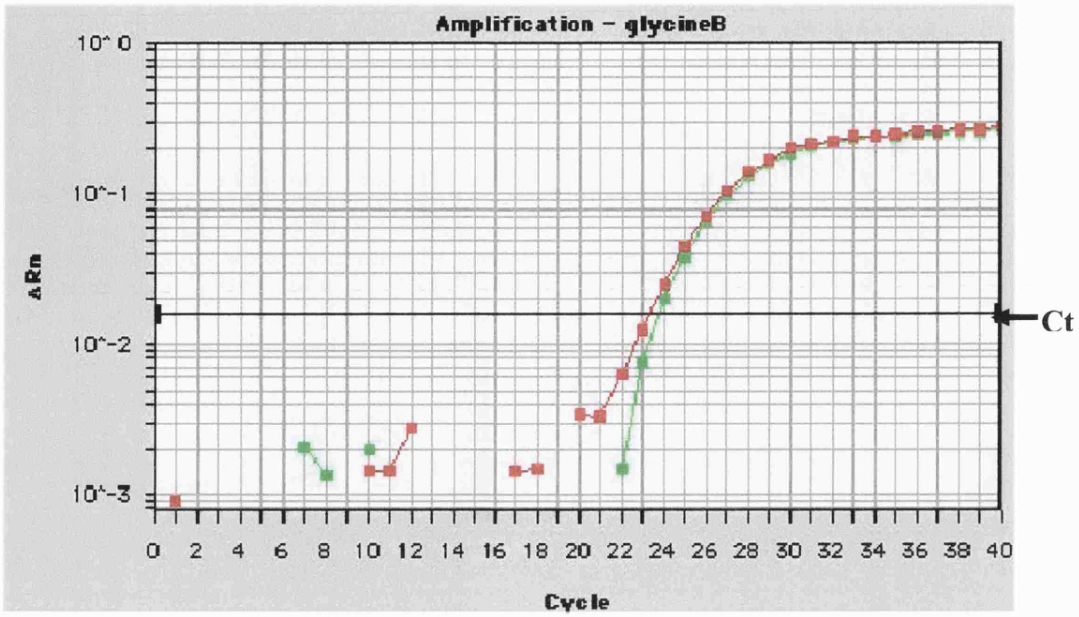

(B) Amplification plot of glycine β subunit from human brain and human PBMC cDNA

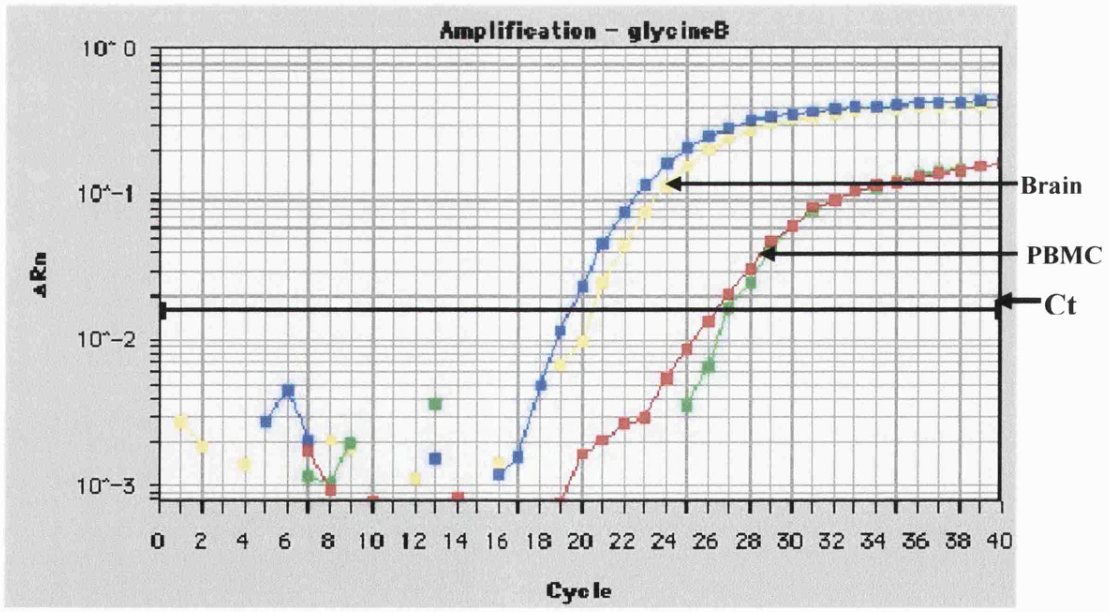

Figure 19: Amplification plot of the glycine β subunit from (A) human neutrophils (red and lime plots) and (B) human brain (sky blue and yellow) and human PBMC (red and lime) cDNAs. In human neutrophil cDNA, the product starts to amplify around cycle 22, while in human brain cDNA, amplification of product starts around cycle 19. In human PBMC cDNA amplification starts around cycle 25. Ct represents the cycle threshold, i.e. the PCR cycle number at which fluorescence is detected above an arbitrary baseline. All samples were loaded onto the plates as duplicates which are represented by pairs of colours.

Table 14: Comparison of mean TaqMan Ct values of glycine receptor subunit amplification from human brain and immune cells. Results are presented as arbitrary Ct values. Ct values lower than 35 are highlighted in blue.

Sample (source of RNA)	TaqMan Result (Ct) from α1	TaqMan Result (Ct) from α2	TaqMan Result (Ct) from α3	TaqMan Result (Ct) from β
Whole Brain	18	21	19	19
Immature DC	34	34	38	39
Mature DC	29	33	37	39
Monocyte	35	35	27	38
CD4+	30	29	29	35
CD8+	33	34	33	37
Irradiated B cell	34	32	31	38
Neutrophil	35	34	40	40
TNF 6h	32	34	35	27
TNF 24h	26	30	31	23
Th0 clone	34	35	36	39
Th1 clone	33	35	35	39
Th2 clone resting	35	37	35	40
Th2 clone stimulated	34	34	33	40
PBMC (own sample)	24	26	36	26
Neutrophil (own sample)	26	30	40	28

These results showed that a number of the $GABA_A$ and glycine subunits are detected in a number of human immune cells, and in cells involved in inflammatory reactions (e.g. TNF-α stimulated cells, and synovium and fibroblasts from RA patients). Table 15 shows a comparison of the detection levels of some of these subunits in the immune cells of interest. The main difference lies in the neutrophils, where in contrast to the glycine receptor subunits, the $GABA_A$ receptor subunits are clearly absent.

Table 15: A comparison of the levels of detection of $GABA_A$ and glycine receptor subunit cDNAs in a range of human immune cells. Levels are indicated with the '+' symbol (with +++ indicating high levels of expression, ++ as medium levels, + as low levels and - as no expression.

Receptor subunit	Monocyte	CD4+	CD8+	Irradiated B-cell	Neutrophils	Human PBMC
$GABA_A$ α_1	+	+ +	+	+	-	+ + +
$GABA_A$ α_3	-	+	-	+	-	-
$GABA_A$ β2	-	+	+	+ +	-	+
$GABA_A$ β3	-	-	-	-	-	-
Glycine α1	-	+	-	-	+ +	+ +
Glycine α2	+	+ +	+	+ +	+	+ +
Glycine α3	+	+ +	+	+	-	-
Glycine β	-	-	-	-	+ +	+ +

3.4 – Discussion

Analysis of $GABA_A$ and glycine receptor subunit expression in cDNA from total human brain (positive control), human PBMC and Jurkat J6 cells, was performed by reverse transcription polymerase chain reaction. The PCR analysis showed that receptor subunit cDNAs corresponding to a number of $GABA_A$ and glycine receptor subunits could clearly be detected (Figures 11 and 12). In the nervous system, the most common functional receptor subunit stoichiometry is $\alpha1\beta2\gamma2$, $\alpha2\beta1\gamma2$ (Backus *et al.*, 1993) and $\alpha2\beta2\gamma1$ (Chang *et.al.*, 1996; Tretter *et.al.*, 1997) and 75% of functional $GABA_A$ receptors contain a benzodiazepine binding site. However, the δ and ε subunits are reported to be able to replace the γ subunit to form a functional $GABA_A$ receptor (Sieghart *et al.*, 2000).

3.4.1 – Presence of $GABA_A$-receptor α and β subunits in immune cells

The RT-PCR results showed that the mRNAs for $\alpha1$, $\alpha3$ and $\alpha4$ and all three β subunits of the $GABA_A$ receptor were detected in Jurkat and PBMC cDNAs. The $\alpha6$ subunit was only detected in Jurkat cells, while the $\alpha5$ subunit was absent from both PBMC and Jurkat cells. Both α and β subunits are crucial for the formation of functional $GABA_A$ receptors, so these results show that due to the wide distribution of these two subunit types, and the presence of the δ and ε subunits in PBMC, it is reasonable to suggest there may be functional $GABA_A$ receptors present on immune cells.

Real-time quantitative RT-PCR showed that the cell and tissue distribution profile of the $GABA_A$ receptor subunits was variable (Table 13 and 15). Apart from the detection of the $\alpha1$ subunit in human PBMC (Figure 13, Figure 14B), none of the four subunits tested seemed to be expressed at high levels in PBMC or neutrophils. The $\alpha3$ and $\beta2$ subunits were expressed at lower levels in CD4+ and irradiated B cells, while the $\beta3$ subunit was not detected in any of the immune cells. This was

in contrast to the results obtained from qualitative RT-PCR, where the α3 and β3 subunit mRNAs were clearly present in PBMC. This was probably due to the differences in primer sequences used for the two methods. Taking the qualitative RT-PCR results into account, this probably suggests poor primer design.

3.4.2 – Absence of $GABA_A$ receptor γ subunits in immune cells

RT-PCRs carried out on cDNA's from human brain, PBMC and Jurkat cells, using the γ1 external and internal primers produced large smears on the gel. In an attempt to produce clear and specific bands corresponding to the subunit, the Mg^{2+} concentration in the buffer was varied, the primer pairs were redesigned, and touchdown RT-PCR was performed. However, despite changing all or some of these factors, the large smears were never removed. It could therefore not be determined from these studies if the γ1 subunit is present in immune cells.

One interesting point to note is that the γ3 subunit cDNA was not detected in Jurkat and PBMC (Figure 11 M). Also, only a faint band corresponding to the γ2 subunit was detected in PBMC using nested PCR (Figure 11 Lii). A similar result was found by Bergeret *et al.*, (1998), where neither the γ1 or γ2 were expressed in P815 (mouse mast cell) and H9 T cell-lines. To date, some of the best established $GABA_A$ receptor pharmacology is the sensitivity of the receptor to benzodiazepines. However, in order to confer benzodiazepine sensitivity, the α and β subunits must be co-expressed with a γ subunit (MacDonald & Olsen, 1994; Rabow *et al.* 1995), as the binding pocket for benzodiazepines is located in a subunit cleft between the γ and α subunits (Sigel, 2002). Therefore, the absence of the γ subunits suggests that any $GABA_A$ receptors in immunocompetent cells will not display benzodiazepine potentiation, unlike the $GABA_A$ receptors in the CNS.

3.4.3 – Detection of glycine subunits in immune cells

While the glycine receptor β subunit was detected in Jurkat cell cDNA, none of the α subunits were detected in either Jurkat or human PBMC. In order to have a functional glycine receptor, the presence of at least three α subunits is essential. Therefore, this absence of glycine receptor α subunit mRNAs made it unlikely that any functional glycine receptors are present in immune cells. To date, there is no published data to suggest otherwise, although in a study conducted by Froh *et al.* (2002), the α1, α2 and β subunit mRNAs were detected in rat peritoneal neutrophils.

Real-time quantitative RT-PCR showed that the expression levels of glycine subunit cDNAs (Tables 14 and 15) were higher than those of the $GABA_A$ receptor subunit cDNAs. This was in contrast to the results obtained in the qualitative RT-PCR, where none of the glycine receptor subunits were detected in PBMC cDNA. The reason for this disparity is unclear. It is possible that the subunits are present at low levels in the immune cells, which could not be detected by the less sensitive qualitative PCR.

Detection levels of the glycine α1, α2 and β receptor subunits were higher in PBMC and neutrophils in comparison to most other immune cells (Figure 16, Figure 17B, Table 14). In contrast, the α_3 subunit was barely detectable in PBMC and neutrophils, while high levels of the subunit was expressed in CD4+ cells and monocytes. The glycine β subunit had lower distribution levels in immune cells compared to the α subunit cDNAs, although moderately high levels were expressed in neutrophils and PBMC, indicating the presence of these subunits on these cell types. One main difference between $GABA_A$ receptor subunit and glycine receptor subunit expression was the high levels of glycine receptor subunit expression in mixed lymphocyte populations stimulated for 24 h with TNF-α, which showed amplification at a Ct of 26. TNF-α is a proinflammatory cytokine produced primarily by monocytes and macrophages, and it is known to activate T cells to lead

to increased inflammatory responses. Also the T-helper clone subsets (Th0, Th1 and Th2) cells showed expression of the glycine α1 subunit (Table 14). Th1 and Th2 cells in particular, are closely involved with cell mediated inflammatory reactions (through cytokine release and modulation of allergic responses), and studies have shown that the cluster differentiation antigen CD30, which is a member of the TNF receptor family, is expressed on Th2 cells (Roitt *et al.*, 1998). The presence of the glycine α1 subunit on these cells would therefore suggest that functional glycine receptors may be involved in the modulation of T cell responses.

Overall, the qualitative and quantitative RT-PCR data have shown that the mRNAs to a number of $GABA_A$ and glycine receptor subunits are clearly present in human immune cells. However, the data from the two RT-PCR techniques are not always in agreement, in particular with respect to the $GABA_A$ α3 subunit and glycine α1 – 3 subunit expressions. In general, real-time RT-PCR is regarded as being a more sensitive and reliable technique compared with standard RT-PCR. The low levels of $GABA_A$ α3 and β3 subunits detected by the TaqMan method does not necessarily negate the standard RT-PCR results. As the levels of expression of both subunits in all the immune cells (apart from α3 in CD4+ cells) was very low, it could be argued that the particular primer/probe combination used for these subunits were not ideal.

It can be assumed that any functional $GABA_A$ receptors on human PBMCs will contain α1and β2 subunits and may also include δ and ε subunits. On CD4+ and irradiated B-cells, functional receptors may contain α1, α3 and β2 subunits. The quantitative data also suggests that any functional glycine receptors present on human PBMC and neutrophils will contain α1, α2 and β subunits. It also suggests that any functional glycine receptors present on CD4+ and irradiated B cells will comprise of homomeric or heteromeric α2 and α3 receptor subunits. Therefore, these findings showed that our original hypothesis that functional $GABA_A$ and glycine receptors are present on human immune cells may be correct. The next step

in the project was to determine if the proteins corresponding to these receptor subunit mRNAs could be detected in human immune cells.

Chapter 4

Expression of the $GABA_A$ receptor α1 subunit polypeptide in human immune cells

4 – Expression of $GABA_A$ receptor α1 subunit

To date, there is no published data showing the presence of $GABA_A$ receptor and glycine receptor subunit proteins in human immune cells. Our results from both qualitative and quantitative RT-PCR clearly showed that a number of $GABA_A$ and glycine receptor subunit mRNAs was detected in Jurkat cells, human PBMC and CD4+ cells. We attempted to detect the $GABA_A$ receptor α1, α3, β2 and β3 subunits, and glycine α1 subunit in immune cells using immunoblotting and immunofluorescence. The glycine α1 antibody (abcam) used in these experiments was a polyclonal antibody raised against a KLH-conjugated synthetic peptide from the amino terminus of the human α1 glycine receptor subunit, which also cross-reacts with the human glycine receptor α2 subunit. Affinity-purified goat polyclonal $GABA_A$ receptor α3, β2 and β3 antibodies, raised against peptides mapping the $GABA_A$ receptor α3 (N-19), β2 (C-20) and β3 (C-20) of human origin (Santa Cruz Biotechnology) were used in the experiments. Unfortunately, these commercial antibodies resulted in high levels of non-specific staining.

An affinity-purified anti-$GABA_A$ receptor α_1 subunit antibody (a gift from Prof. Anne Stephenson, London School of Pharmacy) was used in all protein expression studies. This antibody was raised in Dutch-belted rabbits against a KLH-conjugated synthetic peptide (sequence **PEKPKKVKDPLIKKNNT**), and is directed against the intracellular loop (324-341) of the bovine $GABA_A$ receptor α1 subunit sequence (Duggan and Stephenson, 1990). The $GABA_A$ receptor has been well studied in the mammalian brain. Studies conducted in bovine cerebral cortex by Stephenson *et al.* (1988) showed that the $GABA_A$ receptor consists of alpha (53 kDa) and beta (57 kDa) subunits, and more refined protein chemistry revealed the existence of multiple α- and β-subunit isoforms (Buchstaller *et al.*, 1991a; Buchstaller *et al.*, 1991b). Studies using anti-peptide antibodies have shown that, at the protein level, the most abundant of the $GABA_A$ receptor α-subunit isoforms is the α1 subunit (Stephenson, 1988). In

whole rat brain it is reported to constitute 40% or more of detergent-solubilized receptor binding, and has a size of 50-51 kDa (McKernan *et al.*, 1991).

4.1 – Results

4.1.1 – $GABA_A$ α1 receptor subunit expression in rat brain and immune cells

Western blots were carried out on membrane preparations from rat brain, Jurkat J6 cells, HL-60 cells, HEK-293 cells and human PBMC. Whole cell lysate preparations from human T-cells, human neutrophils and BaF3 cells were also used in immunoblotting studies. BaF3 cells, a mouse pro-B cell line, were a gift from Dr. Melanie Wellham, Department of Pharmacy and Pharmacology, University of Bath and HEK-293 cells were a gift from Katherine Ralphs, Department of Biology and Biochemistry, University of Bath.

Proteins in the membrane preparations and cell lysate samples were separated by SDS-PAGE and then transferred onto nitrocellulose membranes, where they were exposed to the anti- $GABA_A$ α1 antibody. A band of the expected size at ~ 50 kDa was present in the preparations from rat brain, Jurkat J6 cells, HL-60 cells, BaF3 cells, isolated human PBMC and isolated human T-cells (Figure 20). The band was absent from isolated human neutrophils and HEK-293 cells (negative control). A strong band at ~ 37 kDa was also present in rat brain, Jurkat, HL-60, neutrophils, T-cells and BaF3 cells, but was absent in PBMC and HEK cells.

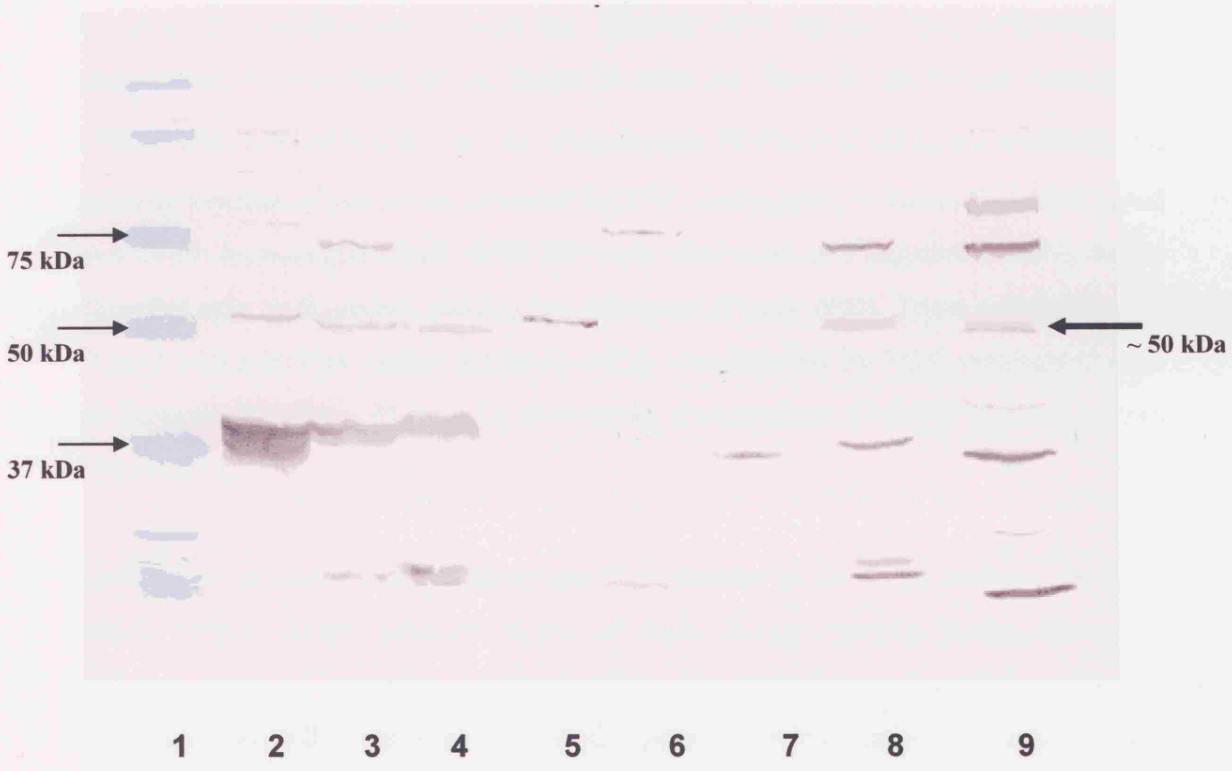

Figure 20: Western blot using affinity-purified anti-$GABA_A$ α_1 receptor subunit antibodies. Lane 1: BIORAD precision broad range protein standard (~ 15 μg). Lane 2: Membrane preparation from total rat brain (15 μg) (positive control). Lane 3: Membrane preparation from Jurkat J6 cells (30 μg). Lane 4: Membrane preparation from HL-60 cells (30 μg). Lane 5: Membrane preparation from human PBMC (30 μg). Lane 6: Membrane preparation from HEK-293 cells (30 μg) (negative control). Lane 7: Cell lysate obtained from isolated human neutrophils (40 μg). Lane 8: Cell lysate from isolated human T cells (40 μg). Lane 9: Cell lysate from BaF3 cells (40 μg).

4.1.2 – Immunofluorescent detection of the $GABA_A$ receptor $\alpha 1$ subunit

In order to confirm and extend the Western blot results, immunofluorescence experiments were carried out on Jurkat J6 cells, HL-60 cells and human neutrophils PBMC and HEK-293 cells. All cells were treated with anti-$GABA_A$ $\alpha 1$ antibody, the specific binding of which was detected by FITC-conjugated or Texas Red-conjugated anti-rabbit immunoglobulins. HEK-293 cells were used as a negative control, and as expected only background staining was observed (Figure 28B). These cells were also treated with anti-beta tubulin antibody which was detected by FITC-conjugated anti-rat immunoglobulins. These cells showed the characteristic β-tubulin staining pattern (Figure 28A).

Leukocytes express distinct assortments of molecules on their cell surfaces, many of which reflect either different stages of their lineage-specific differentiation or different states of activation or inactivation. One such assortment is the cluster of differentiation (CD) antigens which are present on the leukocyte cell surface. Therefore, a number of anti-CD antigen (CD3, CD4, CD14 and CD19) antibodies were also used alongside the $GABA_A$ $\alpha 1$ antibody to identify specific cell types in mixed populations such as PBMC.

CD3 is a complex of at least five membrane-bound polypeptides found in mature T-lymphocytes. The polypeptides are non-covalently associated with one another and with the T cell receptor (Koning *et al.*, 1990; Roitt *et al.*, 1998; Kastrup *et al.* 2002). The anti-CD3 antibody was used to treat isolated PBMCs and Jurkat J6 cells. Anti-CD4 antibody was also used to treat isolated PBMCs. CD4 is a 55-kD glycoprotein originally defined as differentiation antigens on T cells, but also found on other cells including monocytes and macrophages. On T cells they define the helper/inducer subset (Roitt *et al.*, 1998). CD14 are glycolipid-anchored membrane glycoproteins expressed on cells of the myelomonocyte lineage including monocytes, macrophages, and some granulocytes. They function as receptors for the complex of

lipopolysaccharide (LPS) and LPS-binding protein (Calvano *et al.*, 2003; Latz *et al.*, 2003). Flow cytometry and confocal microscopy studies have shown that intracellular CD14 is present in approximately 90% of human neutrophils (Rodeberg *et al.*, 1997). Anti-CD14 antibodies were used to treat HL-60 cells as well as isolated PBMCs and neutrophils. Finally, CD19 are differentiation antigens expressed on B cells and B cell precursors. They are involved in regulation of B cell proliferation (de Rie *et al.*, 1989; Callard *et al.*, 1992). The anti-CD19 antibody was used to treat B cells within the PBMC preparation.

In order to detect the $GABA_A$ receptor $\alpha 1$ subunit, cells were treated with the polyclonal anti- $\alpha 1$ antibody, which was detected with FITC-conjugated anti-rabbit immunoglobulins, and anti-CD antibodies were detected with Texas Red-conjugated anti-mouse immunoglobulins. In Jurkat cells $GABA_A$ $\alpha 1$ immunoreactivity was present in the cytoplasm and to a lesser extent associated with the plasma membrane (Figure 21A). As Jurkat cells are a T-cell line, these were also labelled with monoclonal antibodies to CD3. Immunofluorescence was detected mainly on or near the plasma membrane and some diffuse staining in the cytoplasm was also present (Figure 21B). The merged image (Figure 21C) shows a level of co-localisation around the plasma membrane of the cells. Negative controls were carried out for each experiment, where cells were labelled with secondary antibody only (Figure 21 D). HL-60 cells (Figure 22) showed a similar result with respect to $GABA_A$ $\alpha 1$ immunoreactivity (Figure 22 A). As these cells are a promyelocytic cell line, they were also labelled with the monocyte marker, CD-14. Anti-CD14 was localised to the cytoplasm (Figure 22 B), and the merged image (Figure 22 C) showed a high level of co-localisation of the two antigens.

Isolated PBMCs were labelled with a number of different CD antigens, as the preparation contained a mixed population of cells (mainly T-cells, B-cells and monocytes). As in Jurkat cells, anti-CD3 fluorescence was developed mainly around the plasma membrane with some staining of the cytoplasm occurring as well (Figure 23B). This pattern of staining was also observed with anti-CD4 antibodies (Figure 24C). PBMCs treated with anti-CD14 showed two different types of staining (Figure 25B). While most of the cells in the preparation labelled by the antibody showed

diffuse cytoplasmic immunofluorescence, about 10% of the cells showed strong staining around the plasma membrane. These cells also showed this type of immunoreactivity for $GABA_A$ $\alpha 1$. Anti-CD19 also showed strong staining around the plasma membrane, while diffuse staining in the cytoplasm was absent (Figure 26B). Figure 27A shows that the neutrophils used in this study, showed a similar pattern of immunoreactivity for CD14. However, the anti-$GABA_A$ $\alpha 1$ antibody showed non-specific staining in the cells (Figure 27B).

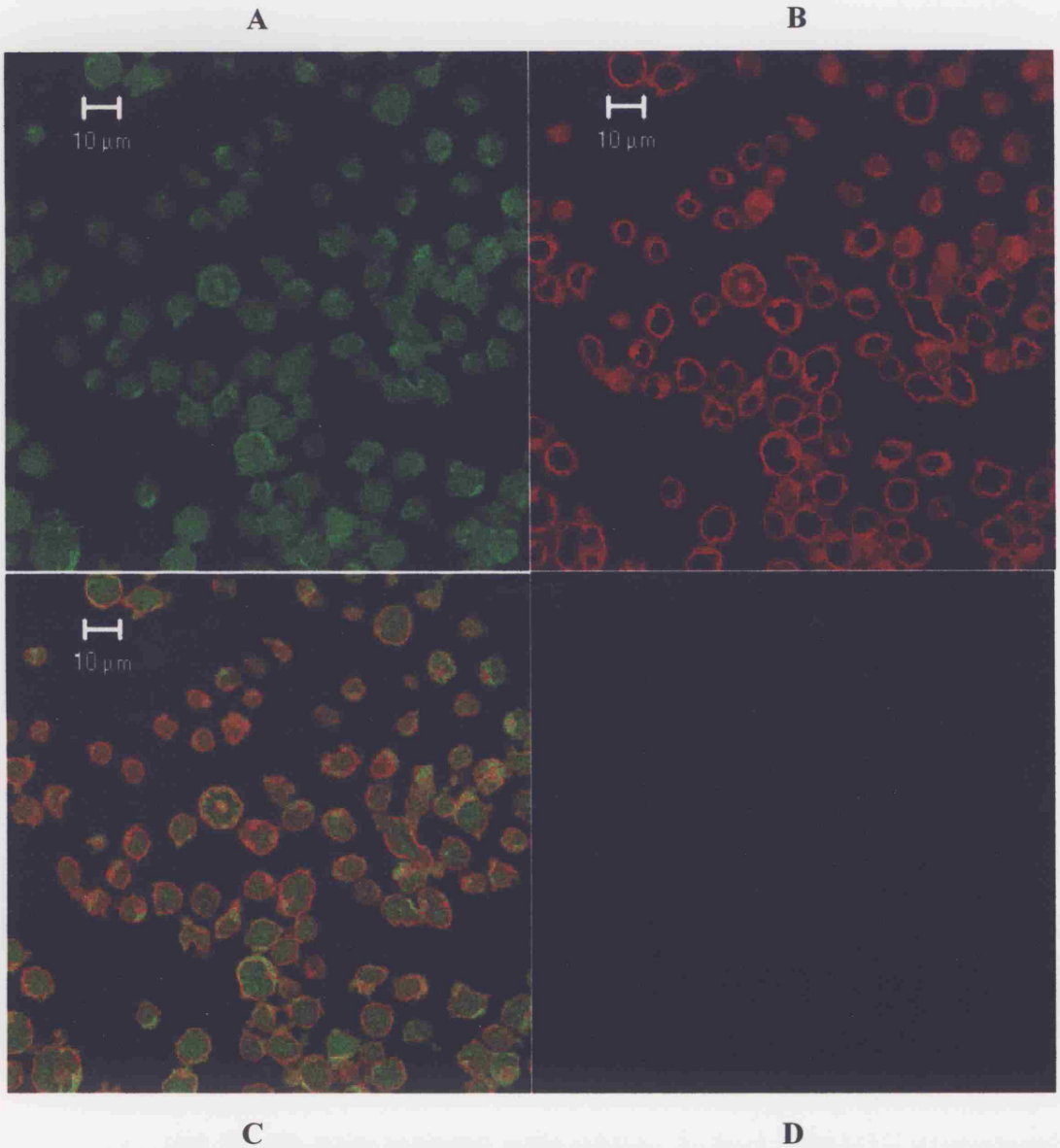

Figure 21: (A) Jurkat cells labelled with $GABA_A$ anti-α1 and FITC conjugated anti-rabbit IgG. (B) Jurkat cells labelled with anti-CD3 and Texas Red conjugated anti-mouse secondary antibody. (C) Merged image of panels A and B. (D) Negative control. Cells labelled with FITC conjugated anti-rabbit secondary antibody only. Calibration bar 10 µm.

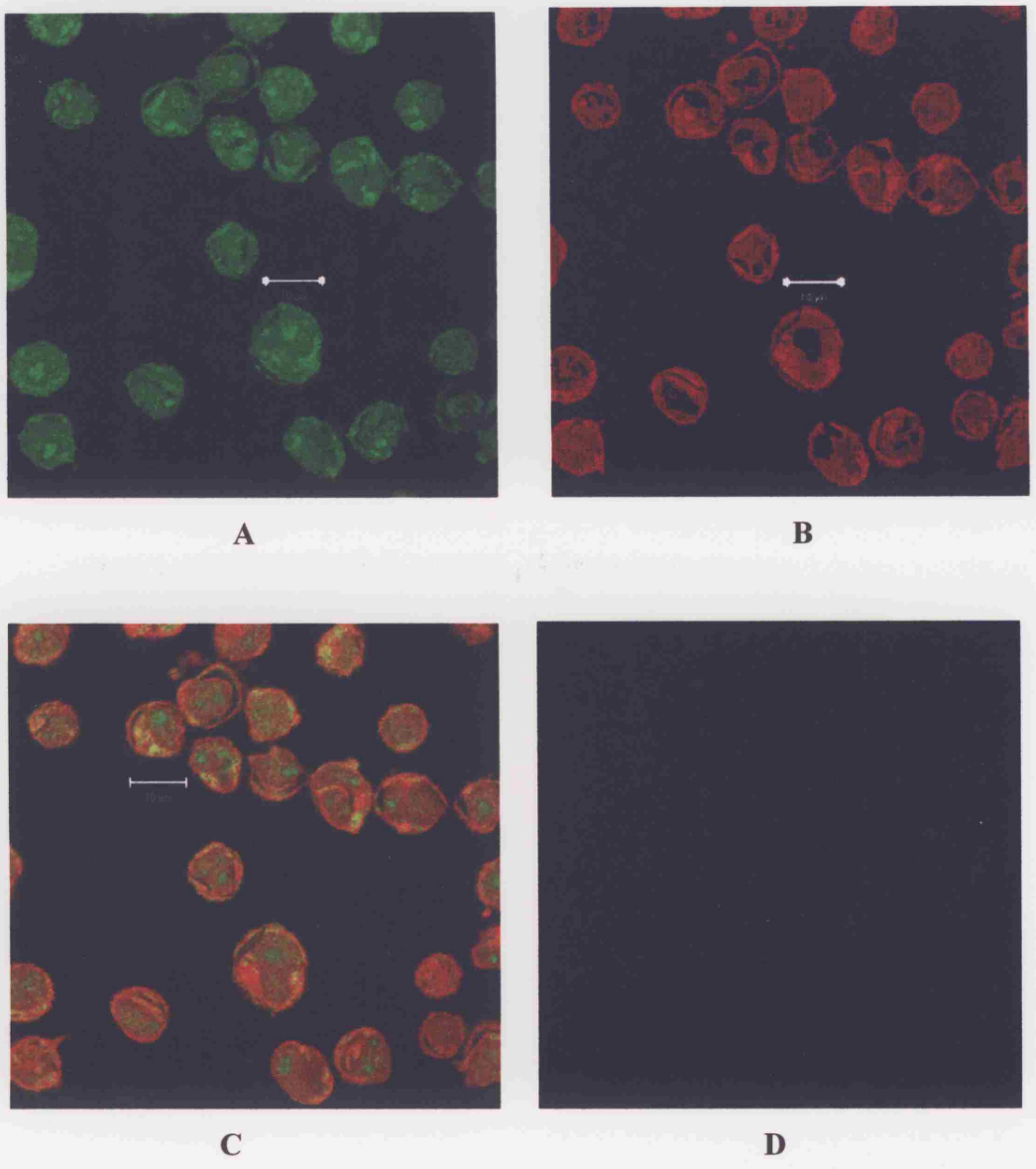

Figure 22: (A) HL-60 cells labelled with $GABA_A$ anti-α1 and FITC conjugated anti-rabbit IgG. (B) HL-60 cells labelled with anti-CD14 and Texas Red conjugated anti-mouse secondary antibody. (C) Merged image of panels A and B. (D) Negative control. Cells labelled with FITC conjugated anti-rabbit secondary antibody only. Calibration bar 10 μm.

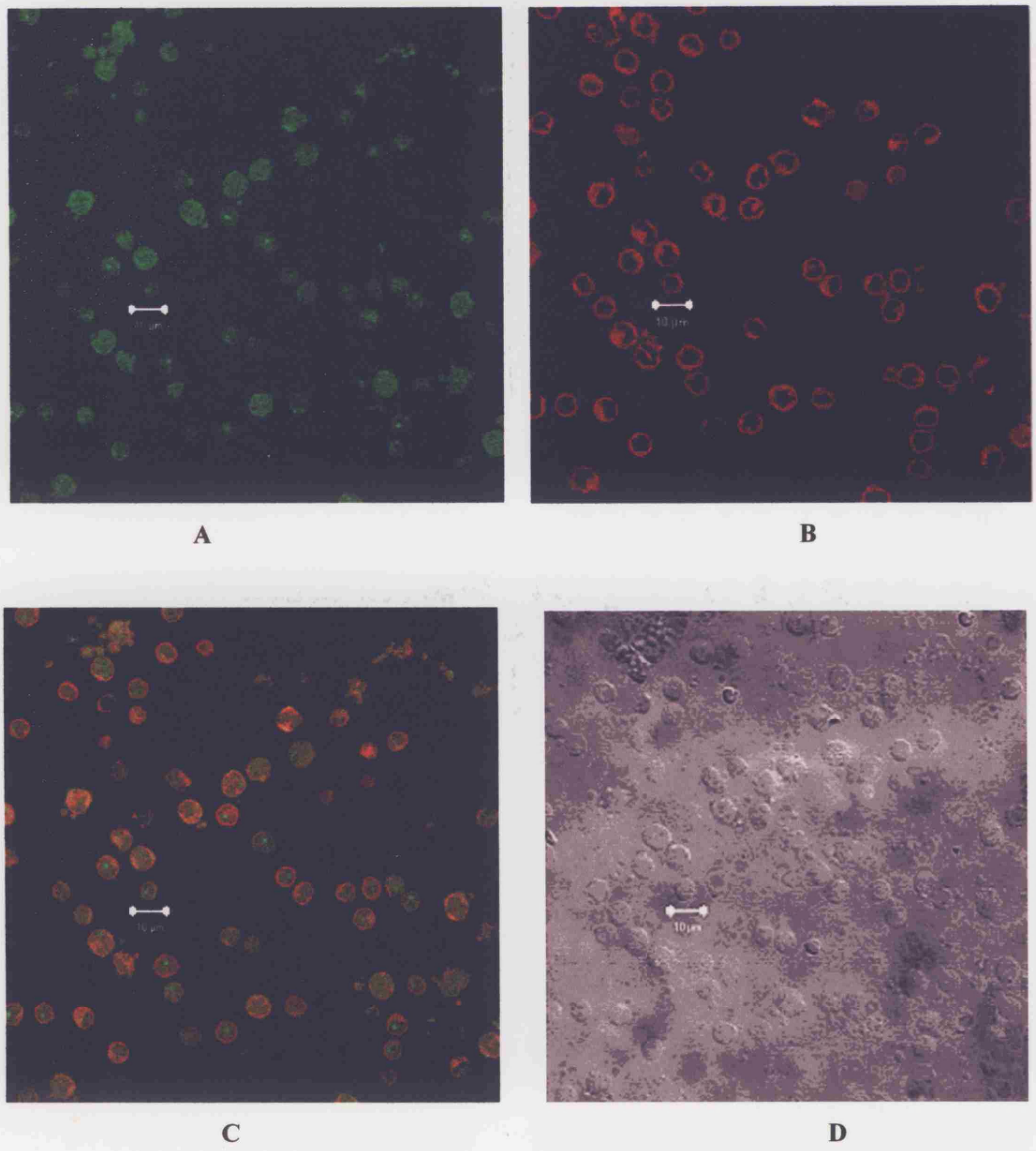

Figure 23: (A) Isolated human PBMCs labelled with $GABA_A$ anti-α1 and FITC conjugated anti-rabbit IgG. (B) PBMCs labelled with anti-CD3 and Texas Red conjugated anti-mouse IgG. (C) Merged image of panels A and B. (D) Cells viewed under transmitted light. Calibration bar 10 μm.

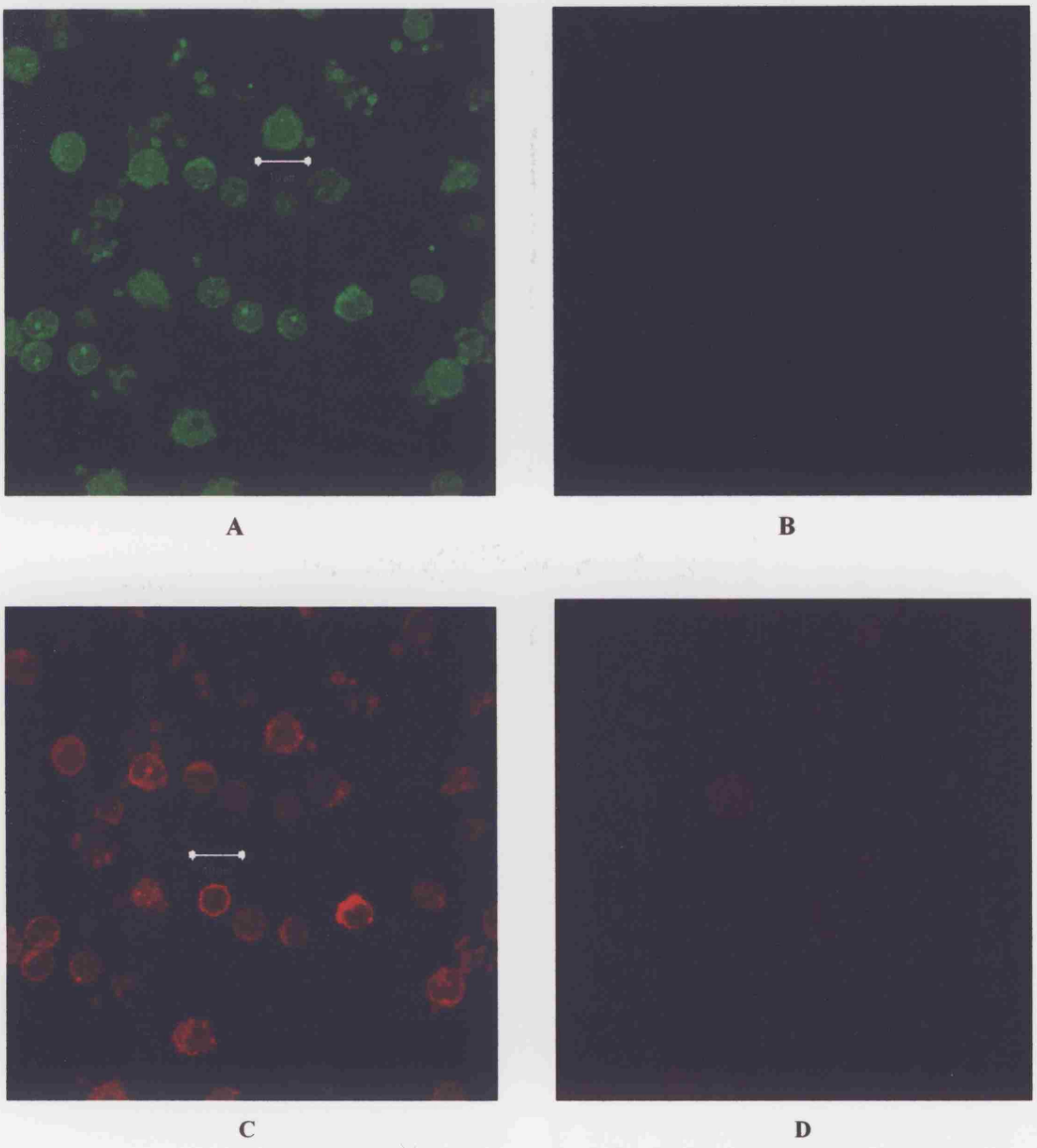

Figure 24: (A) Isolated human PBMCs labelled with $GABA_A$ anti-α_1 and FITC conjugated anti-rabbit IgG. (B) Negative control. Cells labelled with FITC conjugated anti-rabbit secondary antibody. (C) PBMC labelled with anti-CD4 and Texas Red conjugated anti-mouse IgG. (D) Negative control. Cells labelled with Texas Red conjugated anti-mouse secondary antibody . Calibration bar 10 μm.

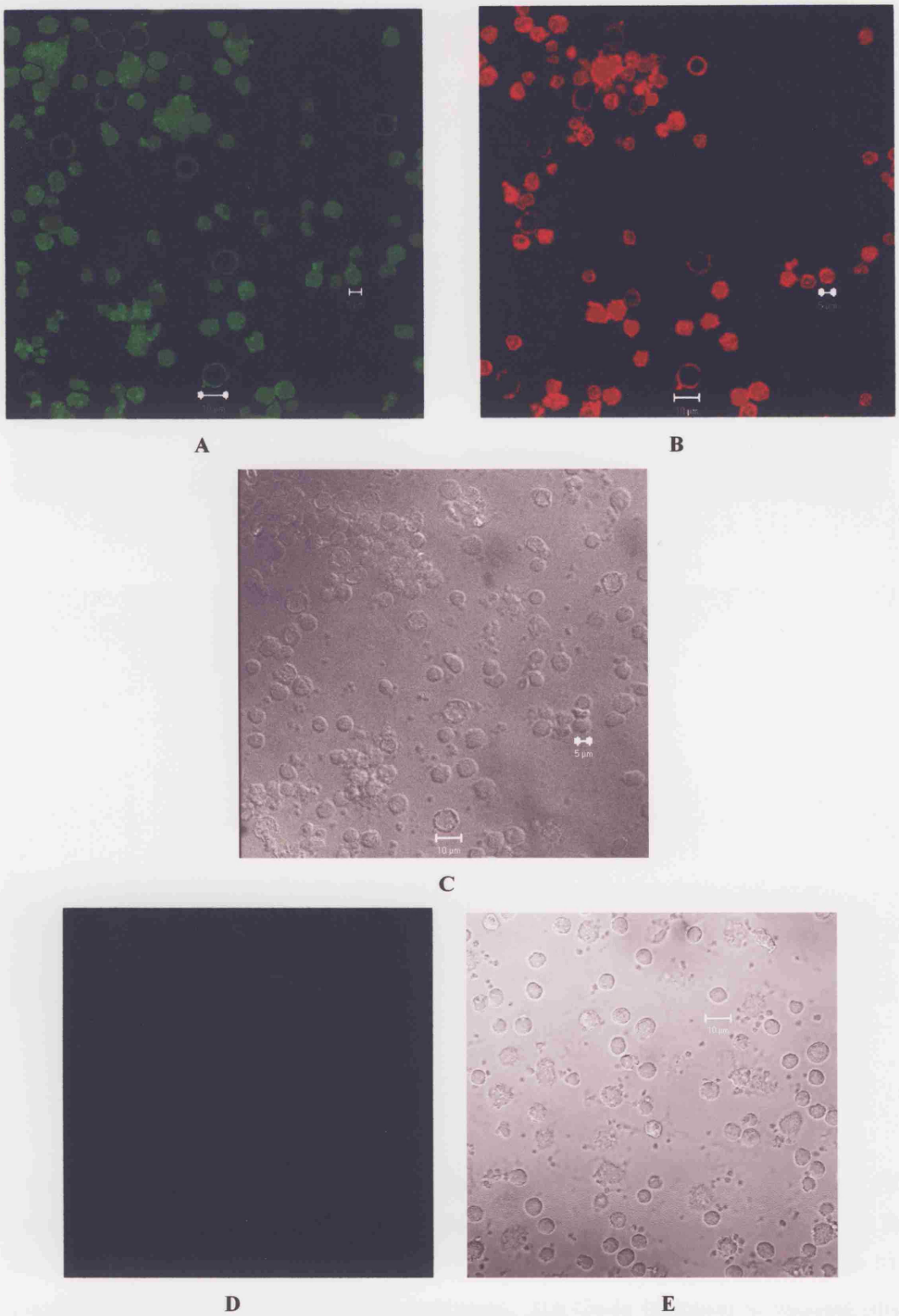

Figure 25: (A) Isolated human PBMC labelled with $GABA_A$ anti-α_1 and FITC conjugated anti-rabbit IgG. (B) PBMC labelled with anti-CD14 and Texas Red conjugated anti-mouse IgG. (C) Cells in panels A and B viewed under transmitted light. (D) Negative control. Cells labelled with FITC conjugated anti-rabbit secondary antibody. (E) Cells in panel D viewed under transmitted light. Calibration bar 5 μm and 10 μm.

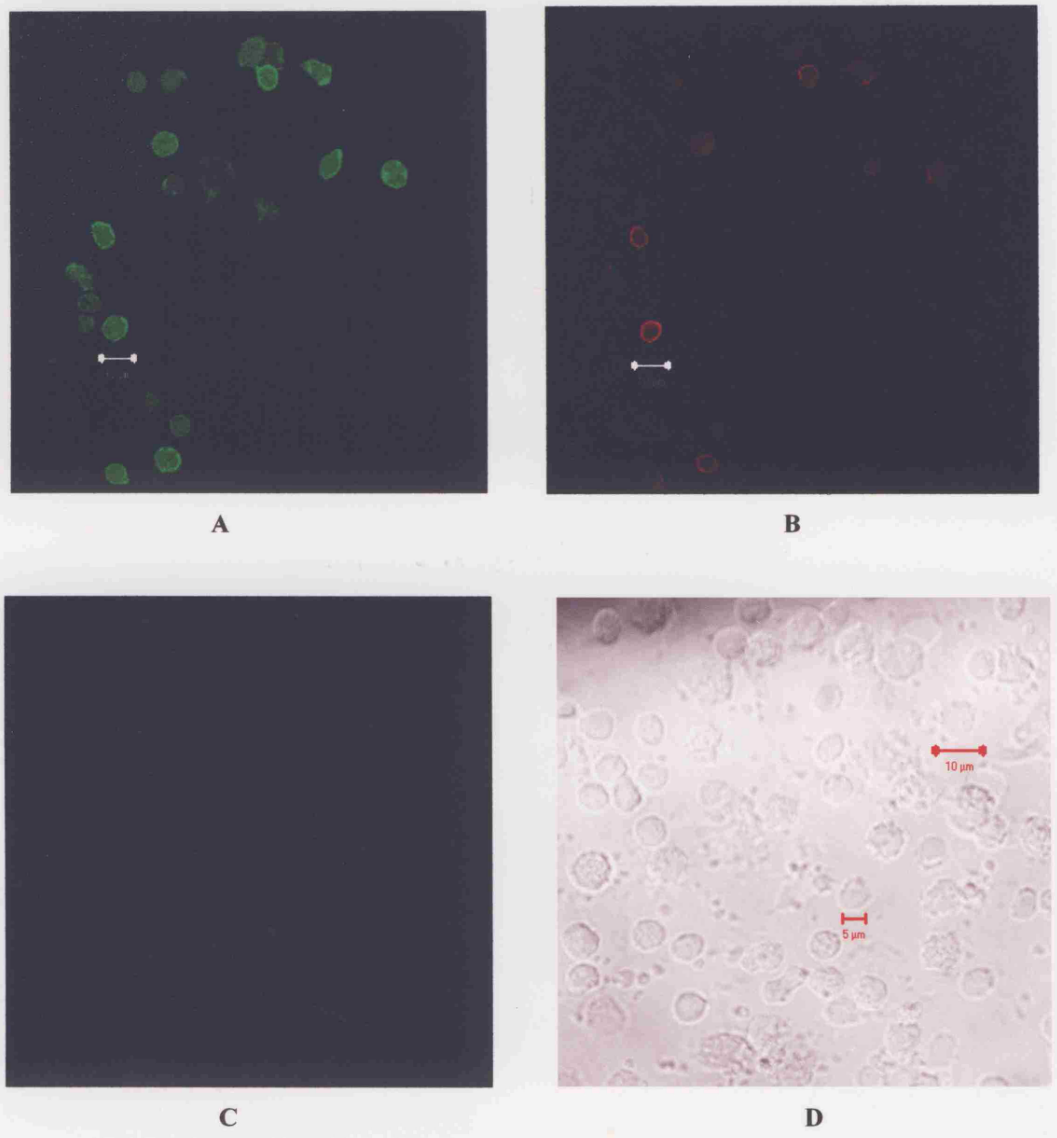

Figure 26: (A) Isolated human PBMCs labelled with $GABA_A$ anti-α_1 and FITC conjugated anti-rabbit IgG (B) PBMCs labelled with anti-CD19 and Texas Red conjugated anti-mouse IgG. (C) Negative control. PBMCs labelled with FITC conjugated anti-rabbit secondary antibody. (D) Cells in panel C viewed under transmitted light. Calibration bar 5 µm and 10 µm.

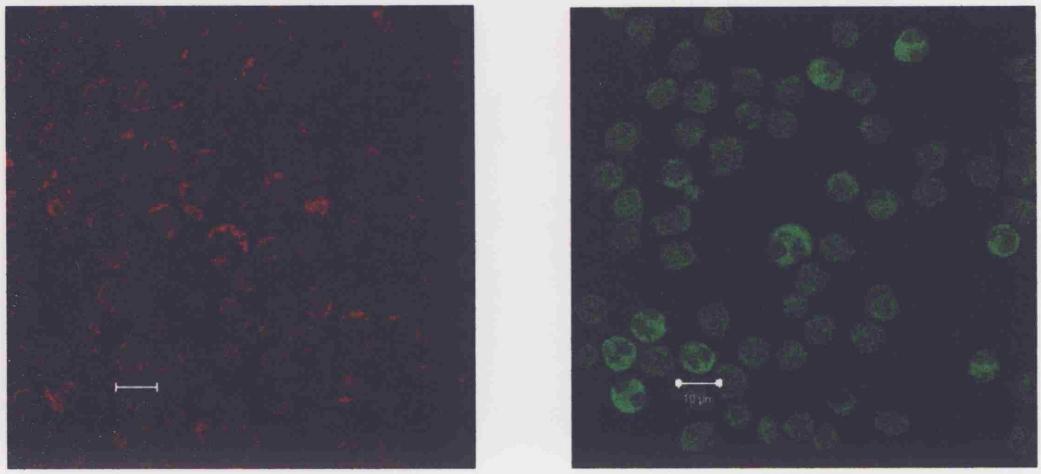

A B

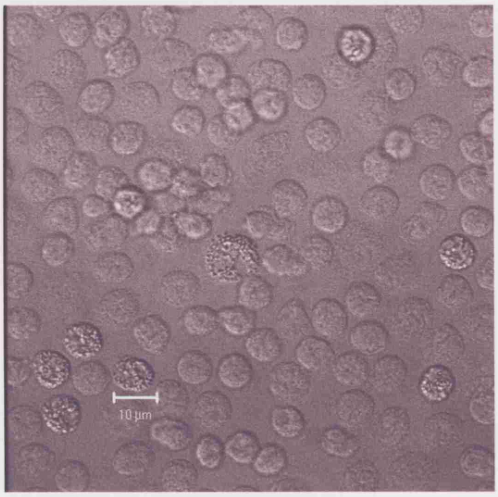

C

D E

Figure 27: (A) Isolated human neutrophils labelled with $GABA_A$ anti-α_1 and Texas Red conjugated anti-rabbit IgG. (B) Neutrophils labelled with anti-CD14 and FITC conjugated anti-mouse IgG (C) Cells in panels A and B viewed under transmitted light. (D) Negative control. Neutrophils labelled with FITC conjugated anti-mouse secondary antibody. (E) Neutrophils in panel D viewed under transmitted light. Calibration bar 10 µm.

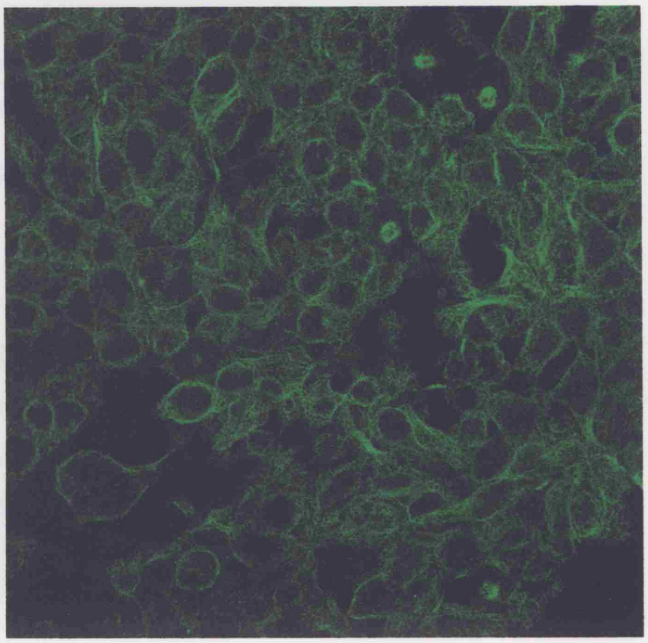

A

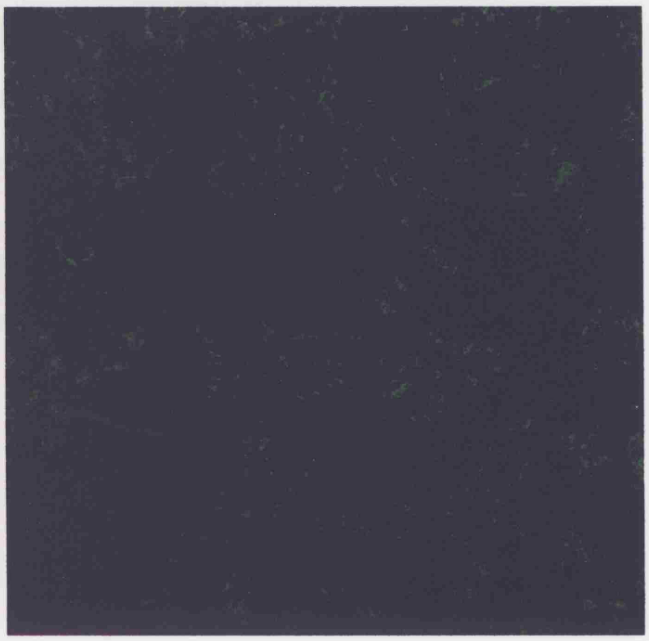

B

Figure 28: (A) HEK-293 cells labelled with anti-beta tubulin and FITC-conjugated anti-rat IgG. (B) HEK-293 cells labelled with anti-$GABA_A$ α1 and Texas Red conjugated anti-rabbit IgG.

4.2 – Discussion

Immunoblotting and immunofluorescence experiments showed that the $GABA_A$ receptor α_1 subunit protein is expressed at low levels in Jurkat cells, HL-60 cells and human PBMC, but are clearly absent from human neutrophils. The immunoblotting results showed that a band at ~ 50 kDa was observed in rat brain, Jurkat cells, HL-60 cells, human PBMC, human T-cells and BaF3 cells. This was close to the expected molecular weight of $GABA_A$ α_1 receptor subunit based on studies by Duggan & Stephenson (1989) and Aller *et al.* (2003), where the subunit was detected at 48 kDa (in bovine brain) and 51-53 kDa (in chicken brain) respectively. A band at 37 kDa was also present in all of the cells apart from PBMC and HEK-293 cells.

CD3 antigens are present on the plasma membrane of 60-80% of T-cells. CD4 antigens are present on the surface of helper T cells (CD4+ cells). Normal CD4+ cells make up 20-30% of lymphocytes. Immunofluorescence of both anti-CD3 and anti-CD4 was present around the plasma membrane which was as expected (Revy *et al.*, 2001). This confirms our results from the TaqMan studies which had shown that the α1 subunit mRNA could be detected in CD4+ cells. The CD14 antibody immunofluorescence was mainly present in the cytoplasmic (possibly azurophilic) granules in HL-60 cells and in most of the PBMCs. However, some cells in the PBMC preparation showed anti-CD14 staining only around the plasma membrane. This distinct pattern was only observed in about 10% of the cells, which showed a similar pattern of immunofluorescence for anti-$GABA_A$ α_1. This suggests that these cells may not be the more common T or B cells, which make up 90% of the PBMC preparation, but may be monocytes, which make up about 10-15% of the preparation. Also, CD14 antigens are known to be present on the plasma membrane of ~ 95% of monocytes (Rodeberg *et al.*, 1997). It has also been found on B cells and T cells (Labeta *et al.*, 1991; Terstappen *et al.* 1990). Therefore, the cells showing diffuse cytoplasmic staining could be T and B cells. CD14 antigens are found on the plasma membrane of 20 – 40% of human neutrophils (Ball *et al.*, 1982; Jayaram & Hogg, 1989), and in azurophilic granules (primary lysosomes) of human neutrophils (Rodeberg *et al.*, 1997). The neutrophils in these experiments

showed cytoplasmic staining, and the characteristic multi-lobed nucleus is very clear in a few cells, which also showed the most fluorescence.

The results, together with the qualitative and quantitative RT-PCR results clearly shows that the $GABA_A$ receptor $\alpha 1$ subunit can be detected at low levels in human PBMC at both the RNA and the protein level. Human PBMC, Jurkat, HL-60, T cells and BaF3 cells all show $\alpha 1$ subunit expression, while neutrophils do not. From these studies it can be suggested that any functional $GABA_A$ receptors present will contain the $\alpha 1$ subunit. Based on the RT-PCR results it had been suggested that $GABA_A$ receptor $\alpha 1$, $\alpha 3$ and $\beta 2$ subunits may form functional $GABA_A$ receptors on peripheral blood mononuclear cells, and the glycine receptor $\alpha 1$, $\alpha 2$ and β subunits may form any functional glycine receptors present. Therefore, immunoblotting and immunofluoresecence studies had also been carried out using antibodies to the $GABA_A$ $\alpha 3$, $\beta 2$ and $\beta 3$ subunits, and also the glycine $\alpha 1$, $\alpha 2$ and β subunit. Unfortunately these antibodies were all from commercial sources and resulted in high levels of non-specific staining.

Chapter 5

The effects of GABA and glycine on agonist induced $[Ca^{2+}]_i$ release in mammalian immune cells

5.1 – Glycine induced inhibition of intracellular free Ca^{2+} in rat neutrophils – published data.

Neutrophils are mobile phagocytic cells that are the central effector cells in human innate immune responses to microbial and inflammatory stimuli (see Section 1.2.2, Figure 3D). These cells are activated by several extracellular signals, including exposure to formylpeptides derived from bacterial proteins or disrupted cells and bacterial derived endotoxins such as lipopolysaccharides (Schiffman *et al.*, 1975; Forehand *et al.*, 1989; Troelstra *et al.*, 1999). The best studied member of the formylpeptide family is the chemotactic synthetic tripeptide, N-formyl-methionine-leucine-phenylalanine (fMLP), and specific receptors to this peptide have been identified on neutrophil plasma membranes (Tennenberg *et al.*, 1988; de Nardin *et al.*, 1991; Radel *et al.*, 1994). The human fMLP receptor is a seven-transmembrane-domain structure characteristic of the G-protein-coupled receptor superfamily (Boulay *et al.*, 1990), while LPS is recognized in mammals by a receptor complex composed of CD14, and Toll-like receptor 4 (TLR4) (Latz *et al.*, 2003).

The plasma membrane of mammalian cells contains two classes of calcium channels, which are either receptor-operated channels or voltage-operated channels. The opening of voltage-operated channels is dependent on the membrane potential of the plasma membrane which is a function of distribution of ions in the basal state. When fMLP or LPS bind to receptors on the neutrophil plasma membrane they cause a rapid depolarisation of the membrane potential. Interaction of fMLP or LPS with the receptor results in activation of phospholipase C (PLC) and specific guanine nucleotide regulatory proteins (G proteins) (Koo *et al.*, 1983; Guthrie *et al.*, 1984; Lad *et al.*, 1984; Rosoff *et al.*, 1985; Smith *et al.*, 1985; Prpic *et al.*, 1987), thereby degrading membrane-associated phosphatidylinositol-4,5-bisphosphate (PIP2) (Berridge and Irvine, 1984; Prentki *et al.*, 1984). This leads to the generation of second messengers such as diacylglycerol (DAG) and the intracellular messenger inositol 1,4,5-tris-phosphate (IP3). Interaction of IP3 with its receptor-operated Ca^{2+} channel in the ER results in rapid Ca^{2+} release from ER stores. This leads to depletion of ER Ca^{2+} stores and subsequently activates Ca^{2+} influx across the plasma membrane

(Bokoch and Gilman, 1984; Cockcroft *et al.*, 1984; Smith *et al.*, 1985, Forehand *et al.*, 1989; Krause *et al.*, 1993; Wheeler *et al.*, 2000; Chen and Jan, 2001).

Recent studies by Wheeler *et al.* (2000) have demonstrated that glycine blunts the response of rat neutrophils to LPS and to fMLP. They studied the effect of glycine on increases in $[Ca^{2+}]_i$ elicited either by fMLP or LPS in individual rat neutrophils using the calcium indicator Fura 2AM and fluorescence microscopy. Activated rat neutrophils were isolated, plated onto glass coverslips and then loaded with 5 mM Fura 2AM. The cells were incubated with 1mM glycine for 3 min before being exposed to either 1 μM fMLP or 100 μg/ml LPS. The results showed that the agonist effect was almost totally inhibited by 1 mM glycine.

They also measured radiolabeled chloride movement in the adherent neutrophils. The cells were incubated with $^{36}Cl^-$ and the tests showed that 1mM glycine caused a dose-dependent increase in $^{36}Cl^-$ influx. 1 μM strychnine, a glycine-gated chloride channel inhibitor (Ito and Cherubini, 1991; Ikejima *et al.*, 1997) strongly inhibited this glycine stimulated $^{36}Cl^-$ influx. Also, as activation of a glycine-gated chloride channel in the neutrophil would be dependent on the presence of extracellular chloride they substituted chloride with the impermeable anion, gluconate. This led to an almost complete prevention of the inhibitory effect of glycine on agonist-induced increases in $[Ca^{2+}]_i$. Also, Froh and Wheeler (2002) showed the expression of the glycine receptor α2, α4 and β subunit mRNAs in rat neutrophils. The glycine α1 subunit was detected in rat peritoneal neutrophils by immunoprecipitation and western blotting. Based on these studies, it was suggested that rat neutrophils contain a functional glycine-gated chloride channel similar to the glycine receptors expressed in neuronal tissues.

In order to explain these findings, Wheeler et al. (2000) hypothesised that when glycine binds to its receptor on the plasma membrane of the neutrophils, it activates its Cl- gated channel leading to an influx of Cl- that hyperpolarizes the cell membrane. These changes in membrane potential across both the cell and the endoplasmic reticulum membranes, decreases the open probability of the voltage-gated Ca2+ channels, therefore blocking movement of Ca2+ across the plasma

membrane and Cl^- induced Ca^{2+} release from intracellular stores after addition of fMLP or LPS (Langosch *et al.*, 1990). In addition, influx of chloride could also inactivate the IP3-gated Ca^{2+} channel on the ER, and therefore blunt the release of $[Ca^{2+}]_i$, resulting in an inhibition of neutrophil function. This proposed hypothesis is depicted in Figure 29.

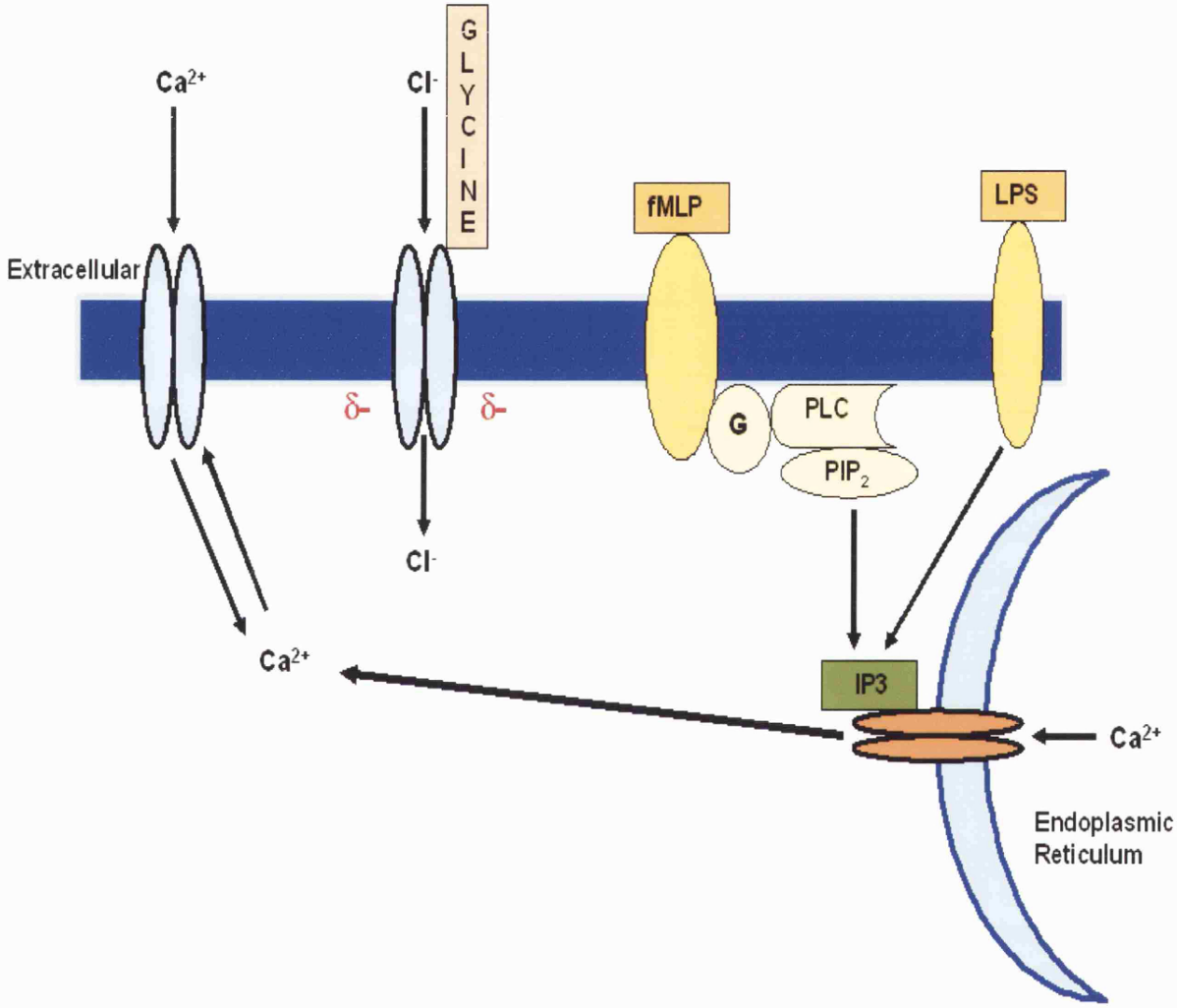

Figure 29: Proposed mechanism for inhibition of agonist-induced increases in $[Ca^{2+}]_i$ by glycine. Adapted from Wheeler *et al.*, 2000. When glycine enters the cell, it leads to an influx of Cl^-. This causes the plasma membrane to hyperpolarize, making opening of voltage-gated calcium channels on the cell surface more difficult, thereby diminishing responses to fMLP and LPS (as well as a variety of other agonists) that depolarise the cell membrane.

5.2 – Inhibition of $[Ca^{2+}]_i$ release from human neutrophils

Based on these results and the data obtained from real-time quantitative RT-PCR showing the detection of glycine α1, α2 and β subunits in human neutrophils (see Section 3.2.3; Figures 16 and 17), it was hypothesised that functional chloride-gated glycine receptors will also be present on human neutrophils. If functional inhibitory ligand gated ion channel receptors, such as glycine and $GABA_A$ receptors, are present on these cells, they could play an important role in modulating inflammatory cell responses.

Intracellular calcium in neutrophils was measured fluorometrically using the calcium indicator FLUO-3AM (Tef Labs), and the fluorescence imaging plate reader (FLIPR). The FLIPR is a high throughput screening system that is an extremely sensitive fluorescence detector (and therefore, ideally suited for kinetic, cell-based assays, including measuring changes in intracellular calcium levels). The FLIPR integrates a powerful argon laser to excite the fluorescent dye, a CCD (charged couple device) imaging camera and a programmable 96-well pipettor to perform fluorometric analyses on all 96 wells of a microplate simultaneously. This system generates real-time kinetic data by stimulating and reading all 96 wells in 1-second intervals.

FLUO-3AM is a visible light-excitable Ca^{2+} indicator that is essentially nonfluorescent unless bound to Ca^{2+}. It combines high fluorescence intensity upon Ca^{2+} binding with an absorption and emission spectrum very similar to that of fluorescein (Minta *et al.*, 1989). Its fluorescence intensity increases about 100-fold after binding of Ca^{2+} with 506 nm as the optimum excitation wavelength and 526 nm as the maximum emission wavelength. As the levels of $[Ca^{2+}]_i$ increase, the fluorescence of FLUO-3AM increases, leading to increased light output. The acetoxymethyl ester form of the dye was used as it is membrane permeate. After the FLUO-3AM is taken up by the cell, the ester is hydrolysed by an esterase in the cytoplasm to release the free acid form of the dye (FLUO-3), which then binds to Ca^{2+}. FLUO-3 has a low affinity for Ca^{2+} (Kd = 400 nM), and does not display

significant wavelength shifts after Ca^{2+} binding (Minta *et.al.*, 1989). This low affinity for Ca^{2+} makes it theoretically a more attractive compound for measuring transient $[Ca^{2+}]_i$ peaks than the UV light-excitable ratiometric Ca^{2+} indicator, Fura 2 (Kd = 224 nM), which was the probe used by Wheeler *et al.* (2000).

5.3 – Results

5.3.1 – Concentration-response curves for fMLP and LPS on increases in $[Ca^{2+}]_i$

The effect of various concentrations of fMLP (Figure 31) and LPS (Figure 32) on $[Ca^{2+}]_i$ in human neutrophils were carried out to determine the EC_{50} values for each agonist. Effects of fMLP were maximal at 1 nM with an EC_{50} of 0.42 μM. LPS increased $[Ca^{2+}]_i$ maximally at 1 mg/ml and had an EC_{50} of 35 μg/ml. In fact, the response curve for LPS indicates that the maximal response may be obtained at concentrations higher than 1 mg/ml.

Data were fit to the following equation:

$$y = Vmax\,[X^n / K^n + X^n)]$$

Where, y = the pharmacologic response of the drug concentration X
Vmax = is the maximum possible pharmacologic response
K = is the concentration of the drug at which y = ½ Vmax
n = the Hill coefficient.

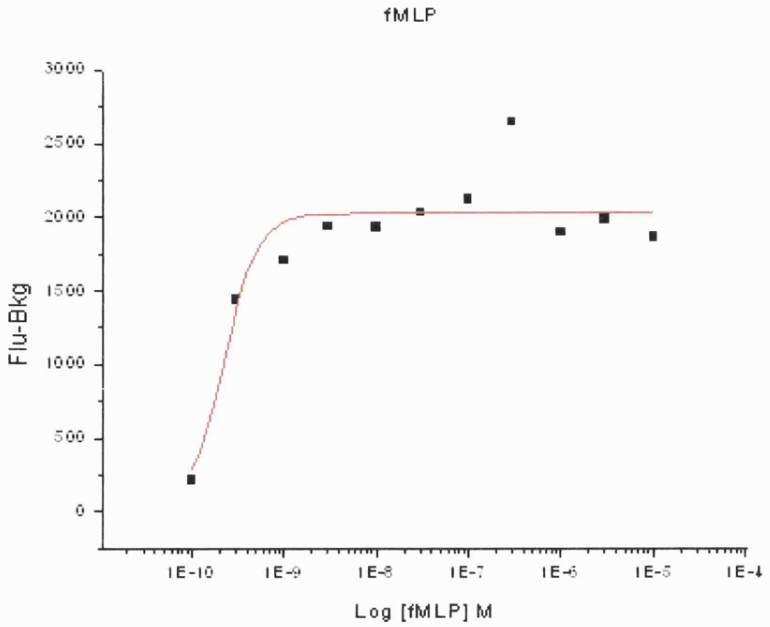

Figure 30: Concentration response curves for fMLP. Log of concentrations are plotted against background fluorescence. Maximal effects of fMLP were observed at 1 nM.

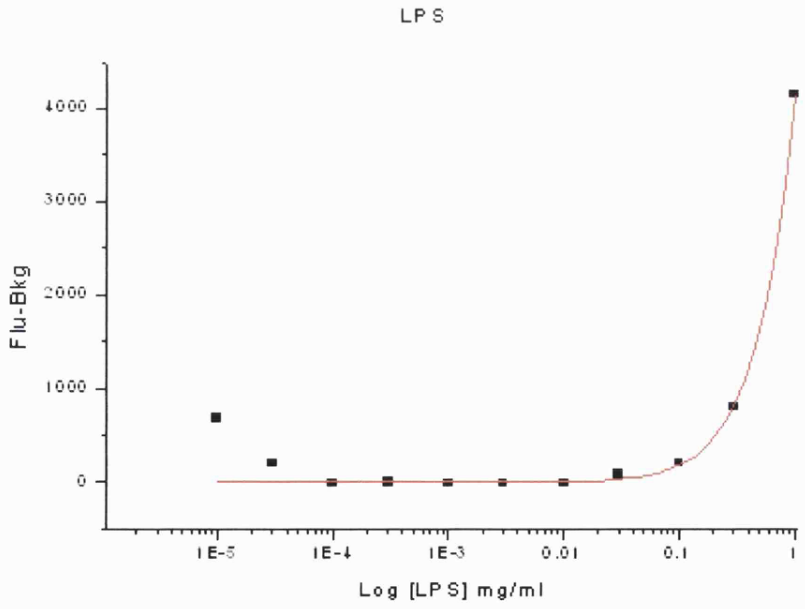

Figure 31: Concentration response curves for LPS. Log of concentrations are plotted against background fluorescence . The maximum dose of LPS used was 1mg/ml, and this showed the strongest response. However, the maximal effects obtained from LPS appears to require a higher concentration.

5.3.2 – Effects of fMLP on $[Ca^{2+}]_i$ levels in human neutrophils

$[Ca^{2+}]_i$ in human neutrophils was measured fluorometrically using the fluorescent Ca^{2+} indicator FLUO-3AM. Treatment with 1 nM fMLP caused a transient increase in $[Ca^{2+}]i$. Intracellular calcium was assessed by monitoring changes in fluorescence intensity of FLUO-3AM at excitation wavelengths of 506 nm with emission at 540 nm in the cells. This was measured every 2 seconds over 2 minutes. Figure 32 depicts a representative response to fMLP (1nM), where the agonist can be seen to cause a rapid increase in $[Ca^{2+}]_i$ within seconds followed by a gradual decrease, which reached a plateau and never returned to basal levels, confirming work by others (Wheeler *et al.*, 2000). This effect was inhibited by exposing the neutrophils to 100 μM sulfasalamide, which is known to inhibit the binding of fMLP to its receptor (Stenson *et al.*, 1984).

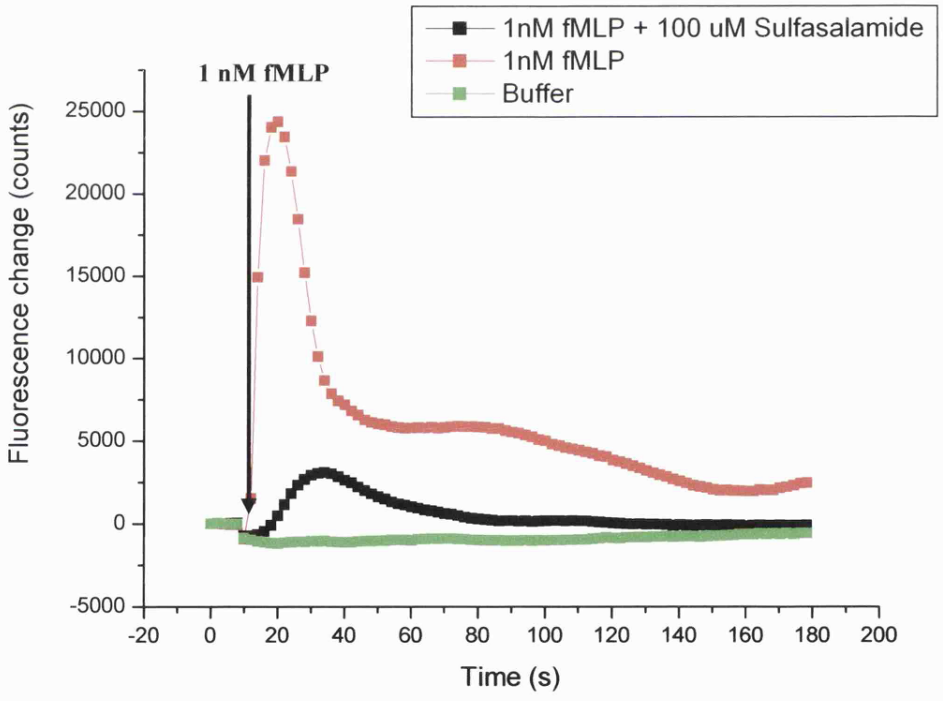

Figure 32: The effect of 1nM fMLP on $[Ca^{2+}]_i$ in human neutrophils. 100 μM sulfasalamide, a known fMLP blocker, is seen to inhibit this effect.

5.3.3 – Effects of GABA and glycine on agonist-induced increases in $[Ca^{2+}]_i$ in human neutrophils

Human neutrophils were incubated in assay buffer containing GABA or glycine (3 mM – 30 μM) for 5 min before and during the addition of the agonist. Figure 33 shows the effect of glycine and GABA at 1mM respectively on fMLP-induced increases in $[Ca^{2+}]_i$ in neutrophils. Neither compound had any significant effect on the levels of $[Ca^{2+}]_i$.

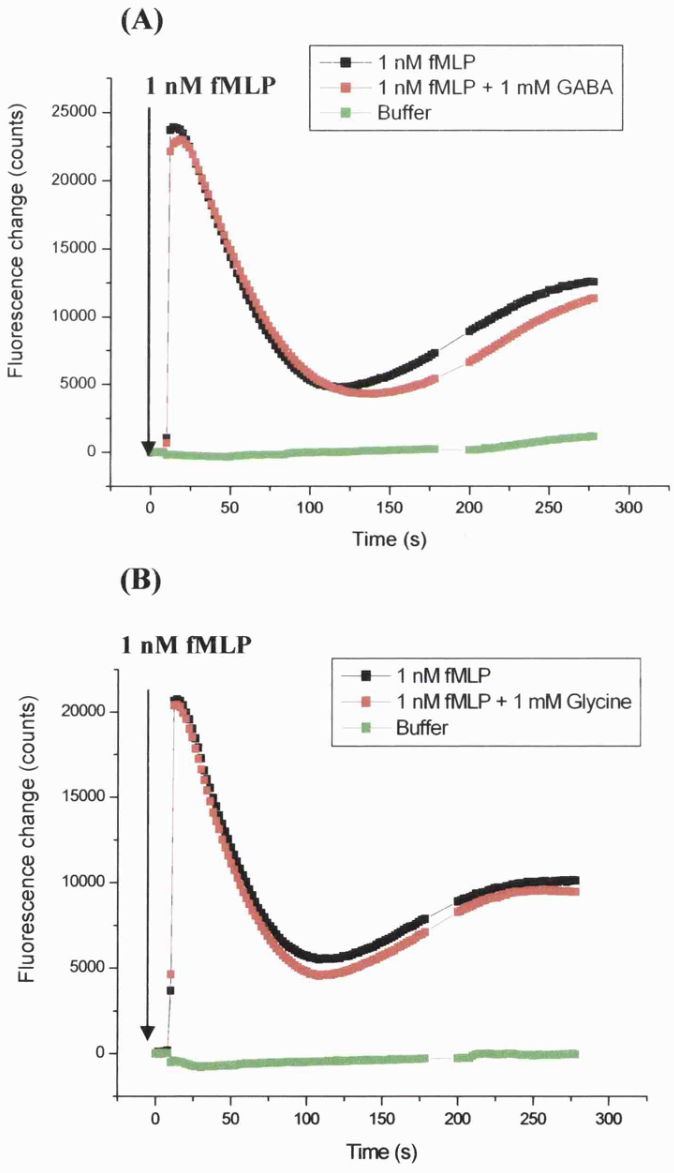

Figure 33 : The effect of 1 mM GABA (A) and 1mM glycine (B) on fMLP-induced increases in $[Ca^{2+}]_i$ in human neutrophils. Data shown are representative of experiments repeated 3-4 times.

1 mg/ml LPS was also used to induce release of intracellular calcium from neutrophils. Once again, this effect was not affected by exposure of cells to varying concentrations of GABA and glycine. Figure 34 shows the effect observed upon application of 1 mM GABA and glycine on LPS-induced increases in $[Ca^{2+}]_i$ in neutrophils.

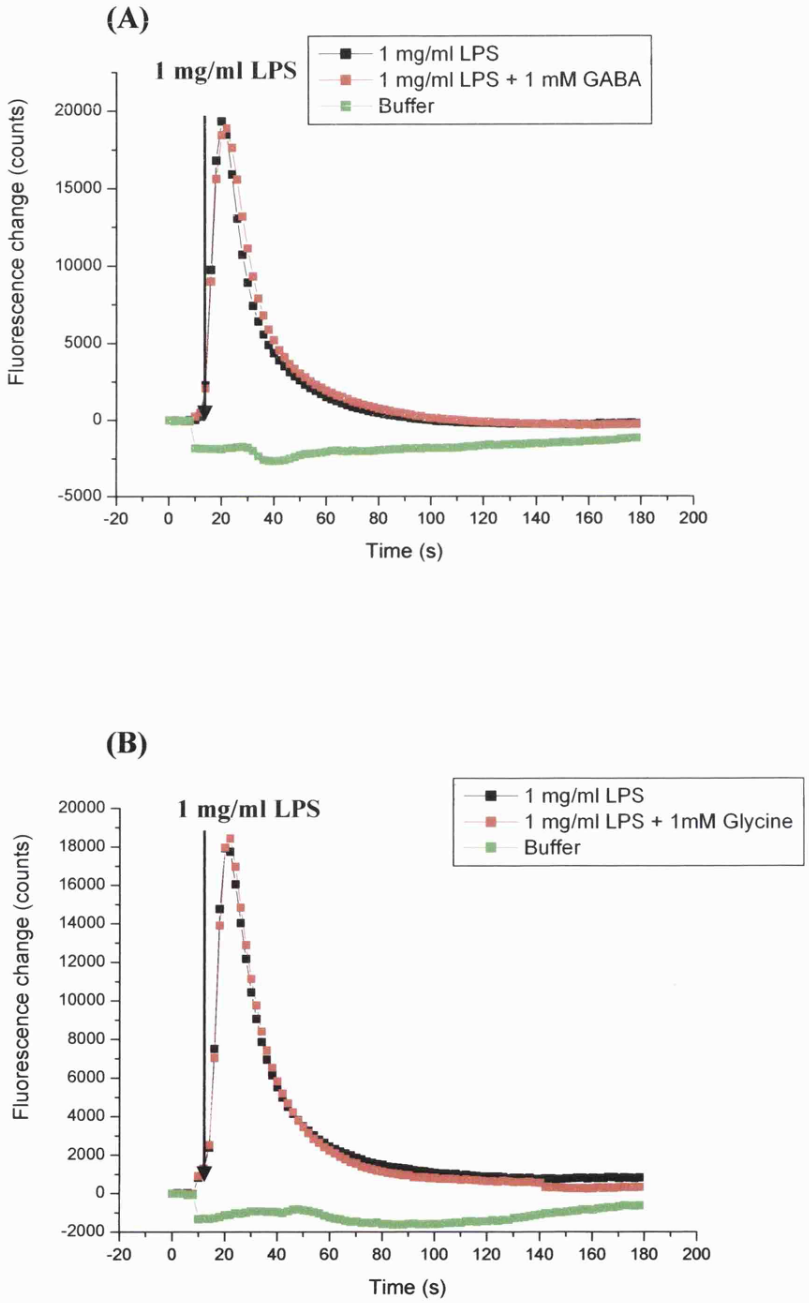

Figure 34: The effect of 1 mM GABA (A) and 1mM glycine (B) on LPS-induced increases in $[Ca^{2+}]_i$ in human neutrophils. Data shown are representative of experiments repeated 3-4 times.

5.4 – Flow cytometry analysis of $[Ca^{2+}]_i$ release

As the results obtained clearly showed that neither GABA nor glycine induced any changes in fMLP and LPS stimulated $[Ca^{2+}]_i$ release in human neutrophils, we carried out the experiment on rat neutrophils in an attempt to repeat the observations by Wheeler *et al.* (2000). However, due to a lack of similar equipment, and lower obtainable quantities of rat blood, we used flow cytometry via a FACS Vantage (Becton Dickinson) to measure any changes in fluorescence as a result of $[Ca^{2+}]_i$ release.

Flow cytometry involves the use of a laser beam projected through a continuous single-file liquid stream that contains cells, or other particles. The momentary pulse of fluorescence emitted as the cell crosses the beam is measured by a set of three photomultipliers at a 90° angle from the beam. The cytometer measures a number of factors based on scattering and emission of the light and uses this data to differentiate between and count the types of cells in the mixture. Some of the main aspects measured include low angle forward scatter intensity, which is approximately proportional to cell diameter; side (90 degree) scatter intensity, approximately proportional to the quantity of granular structures within the cell; and fluorescence intensities at several wavelengths. A histogram or dot plot of each cell can be created from these data.

5.4.1 – FACS analysis of release from rat and human immune cells

When the Ca^{2+} indicator FLUO-3AM penetrates the cells, a major spectral change can be measured at an excitation wavelength of 506 nm. In the following experiments, cells were loaded with 5 μm FLUO-3AM for 90 min at room temperature (see section 2.37.3) and then immediately run on the flow cytometer to obtain fluorescence histograms at an emission wavelength of 526 nm. Rat and human PBMCs were studied in addition to rat neutrophils, as RT-PCR data had

shown that a number of $GABA_A$ and glycine receptor subunits could be detected in human PBMCs (see table 11 and 13), and protein expression studies had shown the $GABA_A$ α1 subunit to be present at low levels in other immune cells (Figures 21 – 27).

Measurements of fluorescence after addition of the agonist were taken immediately, as the fMLP and LPS response occurs within seconds of addition. Data were collected on the FL1 channel (or 'green fluorescence' channel) as histograms of a log scale of intensity of fluorescence (X axis) against arbitrary fluorescence counts (Y axis) (see 2.37.3). Changes in fluorescence were estimated by a shift of the peak to the right (indicating increase of fluorescence) or left (decrease in fluorescence) along the X axis. In order to determine baseline fluorescence, readings were taken from unstimulated cells in assay buffer only (Figure 35, blue closed histogram). Neutrophils stimulated with 1 nM fMLP (Figure 35, green open histogram) showed a shift of the histogram to the right, indicating an increase in fluorescence due to $[Ca^{2+}]_i$ release. In order to confirm that increased fluorescence observed was due to the action of fMLP, 100 μM sulfasalamide was added to the cells 1 min before addition of 1nM fMLP. As expected, this led to inhibition of fMLP induced $[Ca^{2+}]_i$ release, thereby significantly reducing the fluorescence histogram shift to the right (Figure 35, pink open histogram).

Cells were incubated with GABA or glycine from 5s to 5 min. These different incubation times had no effects on fluorescence measured, and on cell viability (determined by trypan blue exclusion. See section 2.37.2). Figure 36 shows fluorescence from cells incubated with glycine for 5 min (Figure 36 A) before addition of 1 mg/ml LPS. The histograms are clearly superimposable, indicating that glycine had no effect on LPS stimulated $[Ca^{2+}]_i$ release. A similar result was observed upon application of GABA to rat neutrophils. However, when GABA was added to rat PBMCs for 5 s (Figure 36 B) before addition of fMLP, a small decrease in fluorescence could be observed. As PBMCs are a mixed population of cells (T cell, B cells and monocytes), it is likely that only one or two of the cell populations were responding to GABA treatment. From the histogram, it appears to be the population of cells giving rise to the smaller peak that were responding to

GABA treatment, while the larger peak remained unchanged with respect to fluorescence intensity. No such effect was observed upon application of GABA to LPS stimulated cells, and upon application of glycine to rat PBMCs stimulated with fMLP and LPS. Table 16 summarises the results obtained from rat neutrophils and PBMC.

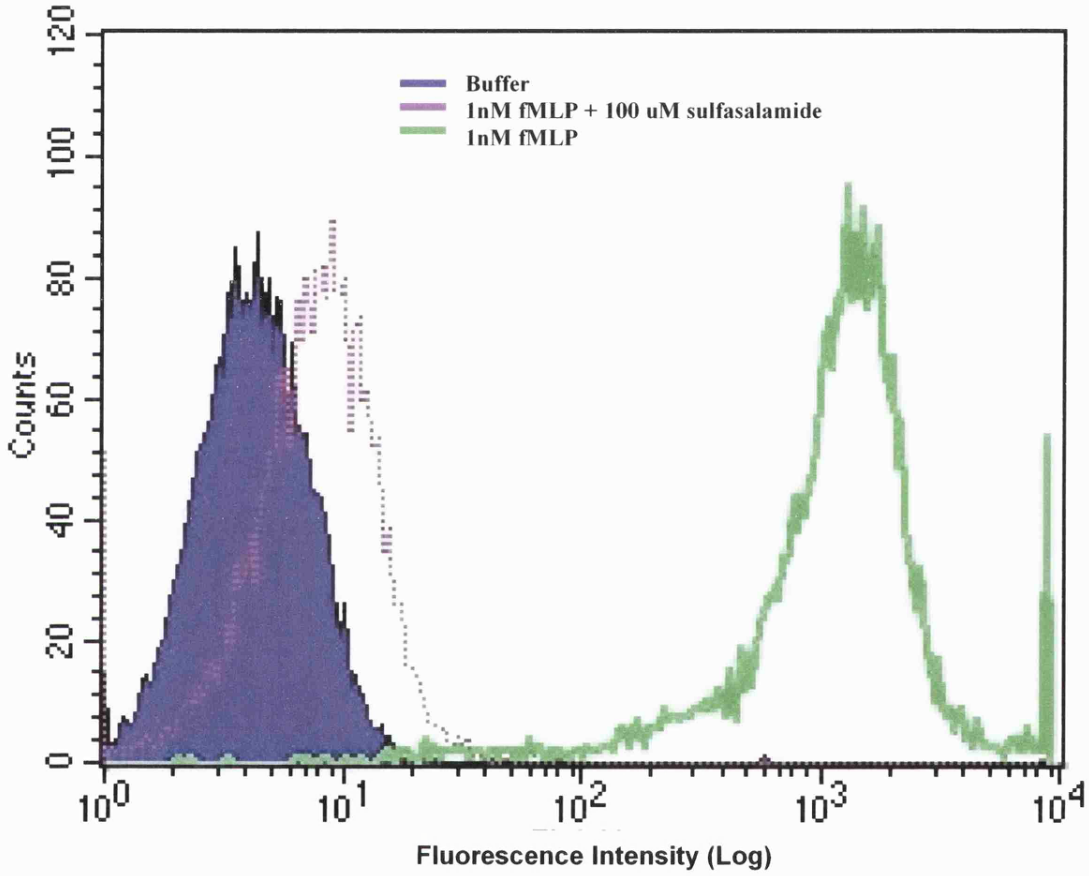

Figure 35: FL1 histograms showing changes in fluorescence in rat neutrophils. In order to determine baseline fluorescence, readings were taken from unstimulated cells in assay buffer only (blue closed histogram). Neutrophils stimulated with 1 nM fMLP (green open histogram) showed a shift (of the histogram) to the right, indicating an increase in fluorescence due to $[Ca^{2+}]_i$ release. When 100 μM sulfasalamide, was added to the cells (pink open histogram) fluorescence due to addition of fMLP was significantly reduced.

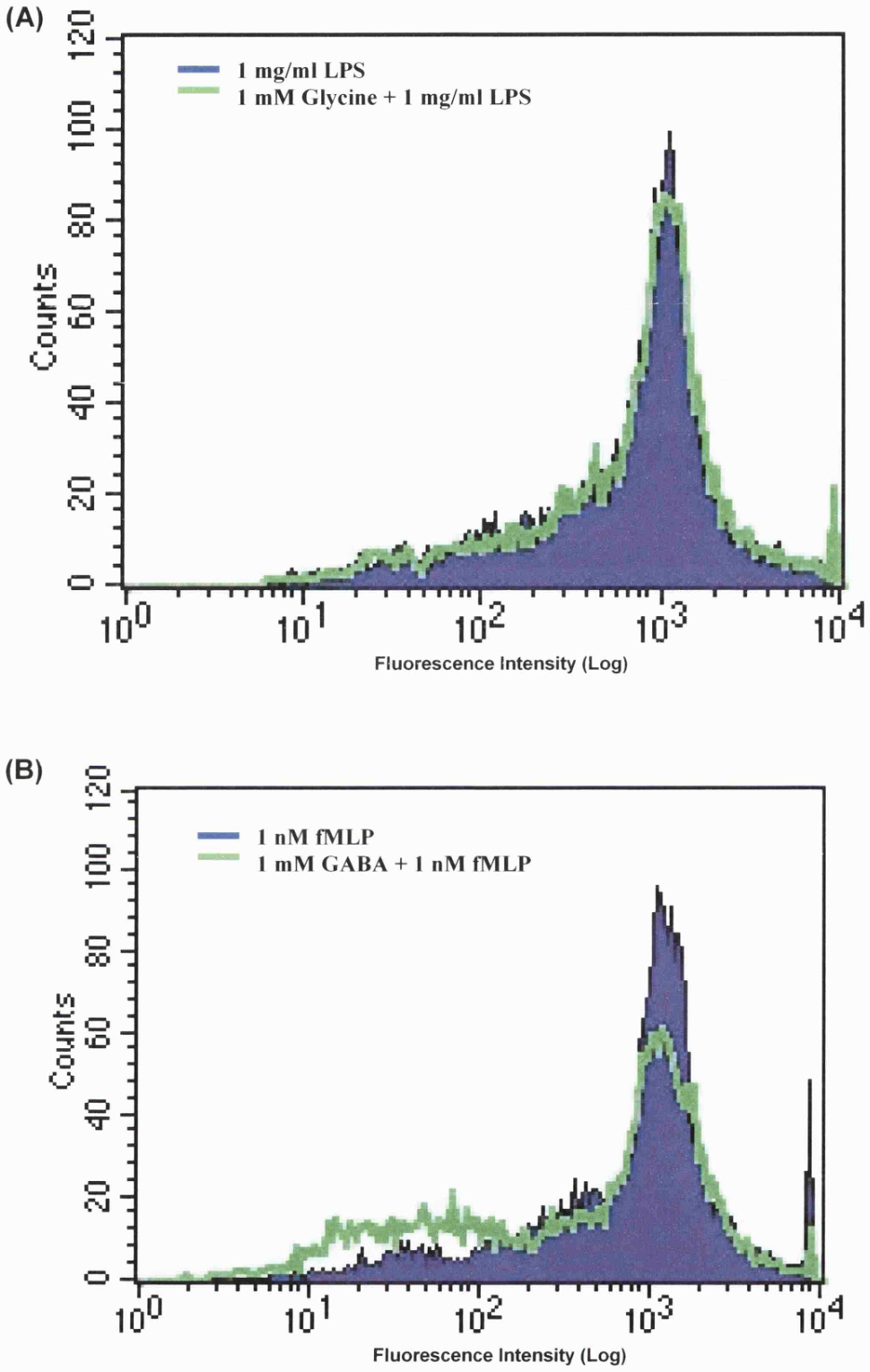

Fig 36: FL1 histograms of rat neutrophils (A) and rat PBMCs (B). In (A) neutrophils stimulated with 1 mg/ml LPS (blue closed histogram) caused an increase in fluorescence, which was not inhibited upon incubation of cells with 1 mM glycine (green open histogram). Similarly, PBMCs (B) stimulated with 1 nM fMLP (blue closed histogram) caused an increase in fluorescence. 1 mM GABA (green open histogram) leads to a small decrease of fMLP induced fluorescence.

Table 16: Average median values indicating changes in fluorescence intensities from rat neutrophils and PBMC.

Rat cell type	Agonist	Treatment	Incubation time (seconds), with antagonist	Median (Mean, ± SD) (n=3)
Neutrophils	1 nM fMLP	-	-	**100 (± 11)**
Neutrophils	1 nM fMLP	1mM GABA	5	**98 (± 35)**
Neutrophils	1 nM fMLP	1mM glycine	180	**102 (± 63)**
Neutrophils	1 nM fMLP	100 µM sulfasalamide	60	**47 (± 19)**
Neutrophils	1 mg/ml LPS	-	-	**99 (± 16)**
Neutrophils	1 mg/ml LPS	1mM GABA	5	**92 (± 41)**
Neutrophils	1 mg/ml LPS	1mM glycine	300	**91 (± 17)**
PBMCs	1 nM fMLP	-	-	**103 (± 15)**
PBMCs	1 nM fMLP	1mM GABA	5	**95 (± 24)**
PBMCs	1 nM fMLP	1mM glycine	120	**97 (± 28)**
PBMCs	1 nM fMLP	100 µM sulfasalamide	60	**39 (± 14)**
PBMCs	1 mg/ml LPS	-	-	**91 (± 19)**
PBMCs	1 mg/ml LPS	1mM GABA	5	**87 (± 48)**
PBMCs	1 mg/ml LPS	1mM glycine	300	**86 (± 44)**

In order to quantitate the fluorescence intensity, the median of the histograms were compared. The median refers to the middle of the population, i.e. the point at which there are 50% of the collected events on either side of the channel. It therefore gives a robust estimate of intensity characterising a population of cells. However, it must also be taken into account that PBMCs are a mixed population of cells, so median values can show variability between cell samples. From Table 16 it can be seen that only median values obtained from cells incubated with 100 µM sulfasalamide showed a significant decrease in fMLP stimulated fluorescence (neutrophils: 47 ± 19, n=3; PBMCs: 39 ± 14, n=3). Changes in median values from cells exposed to 1 mM glycine over various incubation times showed no significant change, which was also observed with 1mM GABA. However, rat PBMCs exposed to GABA over 5 seconds prior to addition of fMLP showed a small

decrease in fluorescence (87 ± 48, n=3). Similar experiments in human PBMCs were then carried out in order to compare these responses.

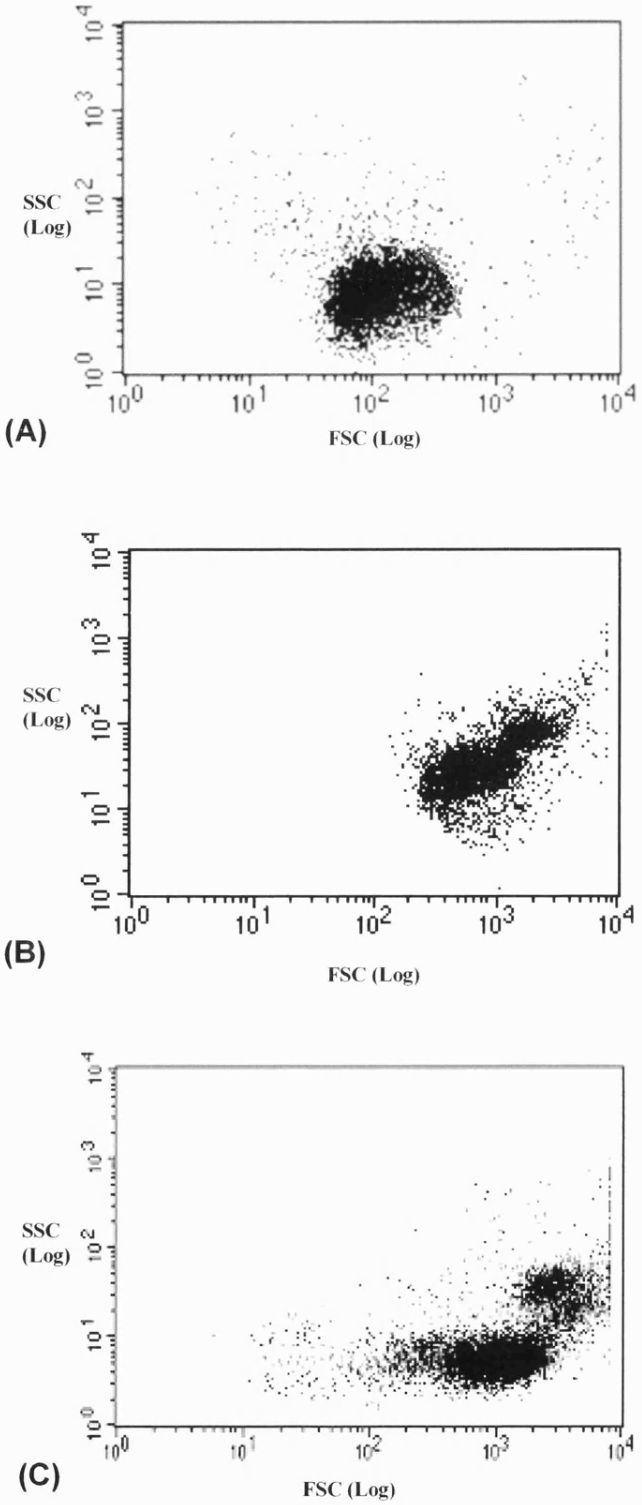

Figure 37: Comparison of representative dot plots of rat neutrophils (A) rat PBMCs (B) and human PBMCs (C). Each dot represents a single cell. Its position indicates its forward scatter (FSC) intensity value (cell size) on the X axis and its side scatter (SSC) intensity value (cell granularity) on the Y axis. Data were collected on the FL1 channel on a log scale.

The dot plots show unstimulated rat neutrophils (Figure 37A), rat PBMC (Figure 37B) and human PBMC (Figure 37C), where each dot represents a single cell. In Figures 37B and 37C, 2 distinct populations of cells can be seen, as opposed to one main population in A. This was expected as the PBMC preparation contains T and B cells as well as monocytes. Even though both rat PBMCs and human PBMCs display two main cell populations, this is more distinct in human PBMCs. Also, side scatter is higher in rat PBMCs reflecting that these cells are more granular than human cells. This is in agreement with findings that PBMC from animals such as rats, mice and rabbits tend to have a higher density than human PBMCs (Boyum *et al.*, 1991). Forward scatter for both rat and human PBMCs is very similar, indicating that the cells from the two main populations are of similar size.

As expected, addition of 1 nM fMLP (121 ± 16, n =3) and 1 mg/ml LPS (84 ± 17, n=3) to human PBMCs led to an increase in fluorescence (Figures 38A and 38B, blue closed histogram). Addition of 1 mM GABA to LPS stimulated cells splits the histogram into two distinct peaks (Figure 38B, green open histogram). The histogram also shifted slightly to the left indicating a decrease in fluorescence (76 ± 30, n =3). Addition of 1 mM glycine to human PBMCs for 2 min before addition of fMLP showed no change in fluorescence (114 ± 35, n =3), (Figure 38 A, green open histogram). In contrast, when PBMCs were treated with 1 mM GABA for 5 s prior to addition of fMLP (67 ± 23, n =3), the histogram shifts to the left and splits into two peaks (Figure 39 A), once again indicating that cell populations within the PBMC fraction differ in their response to GABA. This response was investigated further by gating the two main populations of cells (Figure 40). This showed that the population of cells corresponding to the larger peak responded to treatment with GABA by a reduction in fluorescence from $10^{2.5}$ to 10^{2} fluorescence units (log). However, the population of cells corresponding to the smaller peak showed no change in fluorescence. In order to determine if this GABA response was taking place via $GABA_A$ receptors, 100 μM muscimol, a $GABA_A$ receptor agonist was also added to the cells (Figure 39B, pink open histogram). Once again, the histogram spilts into two peaks and shifts to the left. However, in contrast to the GABA response, both peaks show a decrease in fluorescence intensity (55 ± 30, n =3). The $GABA_A$ receptor antagonist, bicuculline was also added to the cells at 30 μM for 5 min prior to addition of GABA (Figure 39B green open histogram). This

showed a reversal of the effects of GABA on fMLP stimulated cells, as the histogram showed no decrease in fluorescence (115 ± 20, n = 3), although a small spilt of the peak can be observed. Table 17 summarises the results obtained from human PBMCs.

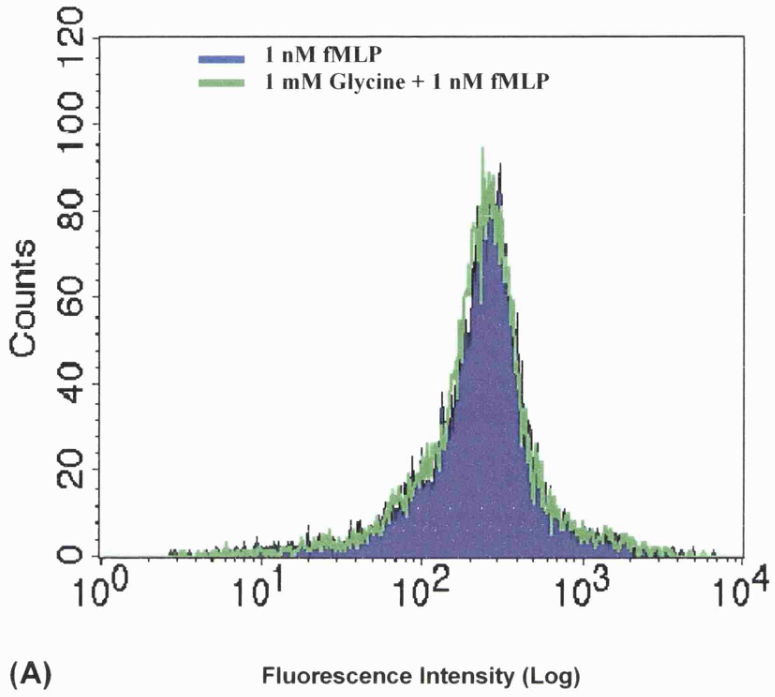

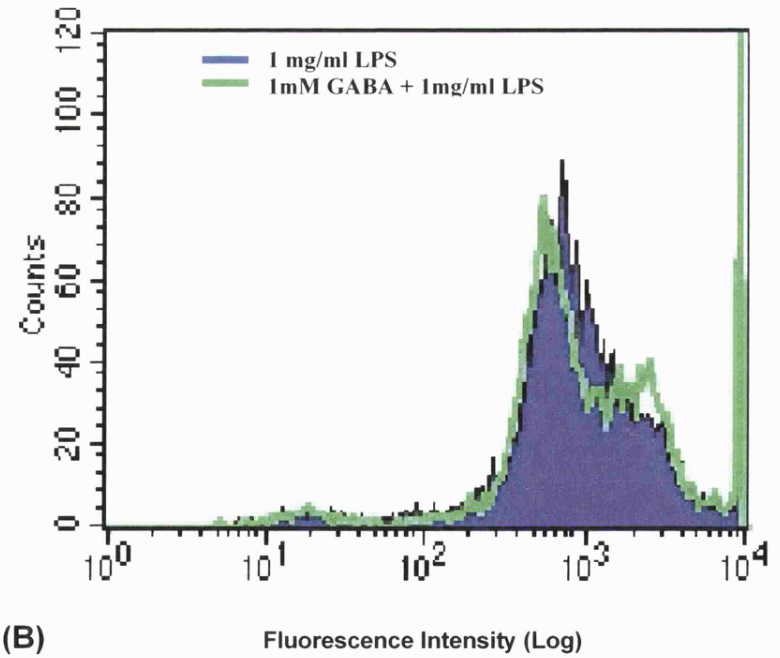

Figure 38: FL1 histograms demonstrating changes in fluorescence in human PBMCs. In (A) cells stimulated with 1 nM fMLP (blue closed histogram) caused an increase in fluorescence, which was not inhibited upon incubation of cells with 1 mM glycine (green open histogram). In (B) cells stimulated with 1 mg/ml LPS (blue closed histogram) caused an increase in fluorescence. Addition of 1 mM GABA (green open histogram) caused a small decrease in fluorescence and splits the peak into two.

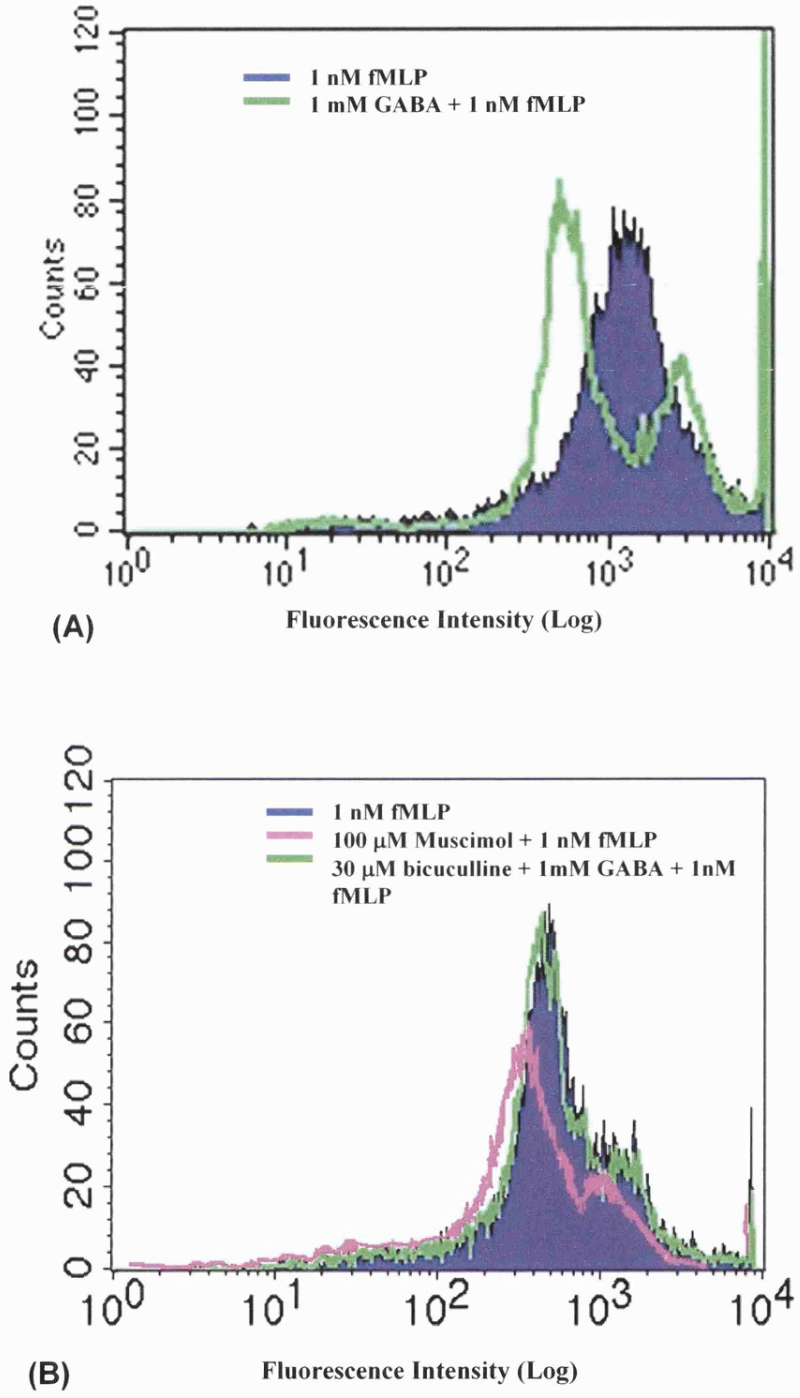

Figure 39: FL1 histograms demonstrating changes in fluorescence in human PBMCs stimulated with 1 nM fMLP (blue closed histogram). In (A) cells were incubated with 1mM GABA before addition of fMLP (green open histogram). In (B) cells were exposed to 100 µM muscimol. The decrease in fluorescence is reversed upon application of 30 µM bicuculline.

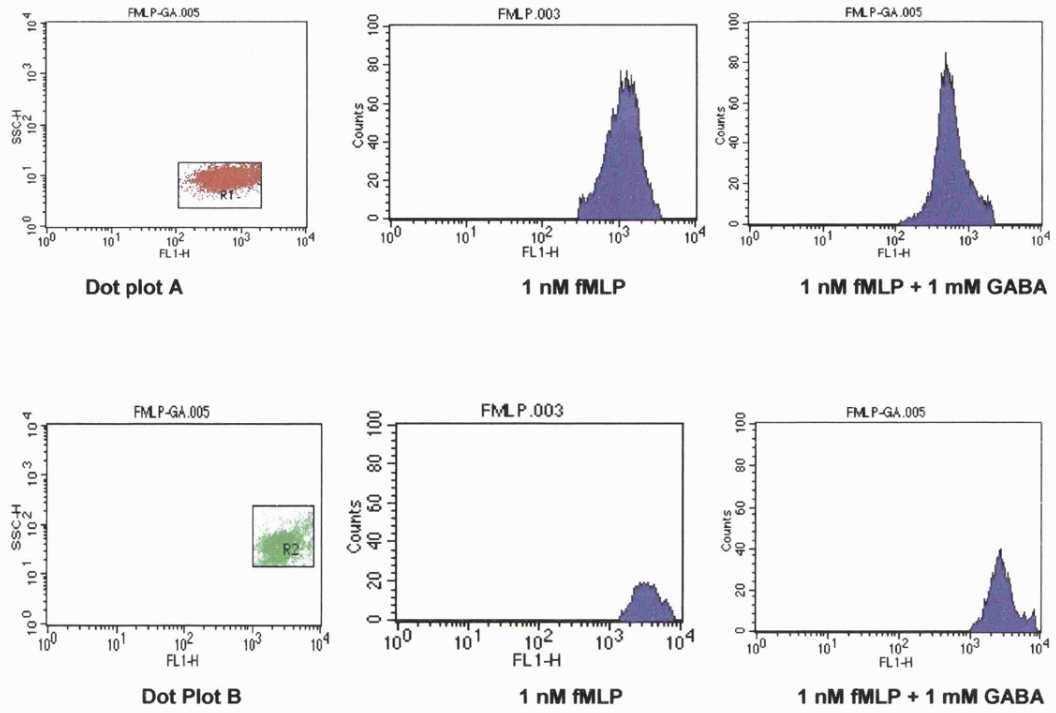

Figure 40 : Gating of PBMCs in figure 39A. The gated dot plots correspond to figure 37C. Only cell population (R1) shown in dot plot A, respond to addition of 1 mM GABA by shifting to the left. Cell population (R2), shown in dot plot B, remains unchanged.

Table 17: Average median values indicating changes in fluorescence intensities for human PBMCs.

Agonist	Treatment	Incubation time (seconds), with antagonist	Median (Mean, ± SD) (n=3)
1 nM fMLP	-	-	**121 (± 16)**
1 nM fMLP	1mM GABA	5	**67 (± 23)**
1 nM fMLP	100 µM muscimol	120	**55 (± 30)**
1 nM fMLP	1mM glycine	120	**114 (± 35)**
1 nM fMLP	100 µM baclofen	180	**119 (± 21)**
1 nM fMLP	30 µM bicuculline + 1 mM GABA	300 60	**115 (± 20)**
1 nM fMLP	100 µM sulphasalamide	60	**41 (± 18)**
1 mg/ml LPS	-	-	**84 (± 17)**
1 mg/ml LPS	1mM GABA	5	**76 (± 30)**
1 mg/ml LPS	1mM glycine	120	**78 (± 27)**

5.5 – Discussion

Activation of rat and human immune cells with 1 nM fMLP and 1mg/ml LPS clearly leads to a dose-dependent elevation of $[Ca^{2+}]_i$. fMLP caused a rapid increase in $[Ca^{2+}]_i$ within seconds followed by a gradual decrease, which reached a plateau and never returned to basal levels (Figure 32). This was similar to results found by others (Wheeler *et al.*, 2000; Jaconi *et al.*, 1988), where 1 μM fMLP was used to stimulate $[Ca^{2+}]_i$ release from rat neutrophils. This initial increase in calcium has been suggested to be from intracellular stores, whereas the sustained increase is the result of calcium influx from the extracellular space (Forehand *et al.*, 1989; Krause *et al.*, 1993; Wheeler *et al.*, 2000; Chen and Jan, 2001). These effects induced by fMLP were blunted by the addition of 100 μM sulfasalamide, which is a known to be able to block fMLP binding to human neutrophils (Stenson *et al.*, 1984), (Figure 32 and 35). Although LPS also leads to an increase in $[Ca^{2+}]_i$, relatively high concentrations were required to achieve this effect, and it is possible that the maximal response induced by LPS could lie at a higher concentration than 1 mg/ml (Fig 31). This was also higher than the concentration used by Wheeler *et al.* (2000) on rat neutrophils, where 100 μg/ml LPS was used to elicit $[Ca^{2+}]_i$ release.

The results from these experiments showed that unlike the effects observed by Wheeler *et al.* (2000), neither glycine nor GABA were seen to inhibit the fMLP and LPS induced increases in $[Ca^{2+}]_i$ in human neutrophils (Figure 33 and Figure 34). This was somewhat surprising as in the rat neutrophils studied in that paper, glycine had almost completely blunted the effects induced by both agonists. The fact that the response was so different in these experiments could be due to a number of reasons. Firstly, it could be hypothesised that rat neutrophils express a high number of glycine-gated chloride channels, compared to human cells, which is why Wheeler *et al.* (2000), were able to obtain strong responses. Also, Wheeler *et al.* had carried out single cell measurements on adherent neutrophils, unlike the method used in this project where calcium release was measured from a population of neutrophils in suspension. Studies have shown that adherence of neutrophils interferes with the characteristics of both calcium and O^{2-} generation, probably by

modifying the cytoskeleton structure (Dahinden *et al.*, 1983; Rebut-Bonneton *et al.*, 1988; Tanigawa *et al.*, 1993). This could lead to changes in neutrophil response to stimuli, and could account for some of the differences observed in the results obtained in this experiment.

The neutrophils used by Wheeler *et al.* had been isolated and cultured in a different way to the neutrophils we isolated from human blood (see section 2.6). Wheeler *et al.* had administered 1% glycogen to act as an inflammatory agent to the cells. These neutrophils were therefore activated and migrated to the peritoneum where they were collected by lavage. Studies have shown that although this technique elicits a 95% pure population of neutrophils, the cells display a phenotype that is dramatically different compared to quiescent neutrophils, for example with regard to their internal cytoskeletal arrangement and surface expression of adhesion molecules and receptors (Becker *et al.*, 1990; al-Mokdad *et al.*, 1997; Roussel and Gingras, 1997; Poon *et al.*, 1999; Wagner and Roth, 2000; Cotter *et al.*, 2001). Therefore, this exposure of the neutrophils to glycogen and the migration of the cells into the peritoneum could alter the activity of the neutrophils in the assay. It could be argued that the differences between the effects of glycine on the quiescent neutrophils used in this project, and the activated neutrophils used in Wheeler's study was due to the latter cells having already been engaged in an inflammatory response. Also, fMLP stimulation of neutrophils induces changes in the expression of surface receptors (Solomkin *et al.*, 1994; Videm and Strand, 2004), and it is possible that receptor expression in adherent neutrophils can be upregulated more readily than neutrophils in suspension (Balazovich *et al.*, 1996).

An additional point to add is that the $GABA_A$ receptors in particular, are fast-acting ligand-gated ion channels, and in the brain receptor activation is followed within milliseconds. Therefore, the incubation times used in this experiment for both transmitters of 30s-5 min could have led to desensitisation of any functional $GABA_A$ or glycine receptors present on the cells. However, Wheeler *et al.* had incubated the rat neutrophils with 1 mM glycine for 3 min before the addition of fMLP and LPS. Even though we had used both higher and lower incubation times than this, our results showed that the same concentration of glycine had no effect on $[Ca^{2+}]_i$ release from human neutrophils.

Having been unable to repeat Wheeler *et al.*'s findings in human neutrophils, I then used rat neutrophils (in suspension) to determine if glycine or GABA had any inhibitory effects on $[Ca^{2+}]_i$ release (Figure 36A). However, these studies also clearly showed that treatment with GABA or glycine had no effect on the agonist induced $[Ca^{2+}]_i$ release. In contrast, rat PBMCs showed a small decrease in fluorescence upon application of GABA to 1 nM fMLP stimulated cells (95 ± 24, n =3; Figure 36B). This effect was also observed in human PBMCs although the shift of the histogram peak to the left was of a higher magnitude when cells were exposed to 1 mM GABA prior to stimulation with 1 nM fMLP (67 ± 23, n = 3), (but not to stimulation with 1 mg/ml LPS; 76 ± 30, n = 3; Figure 39A). This effect was also reversed upon application of 30 μM of the $GABA_A$ receptor antagonist, bicuculline (115 ± 20, n =3). Addition of 100 μM of the $GABA_A$ receptor agonist muscimol (100 μM) also led to a small decrease in fluorescence (55 ± 30, n =3; Figure 39B), which was not observed upon application of the $GABA_B$ receptor agonist baclofen (100 μM; 119 ± 21, n =3). These results showed that the effects of GABA on human and rat PBMC was taking place via $GABA_A$ receptors and not $GABA_B$ receptors.

Another observation in responses from human PBMC was that the histogram split into two peaks upon application of GABA to fMLP stimulated cells, indicating that at least two different populations of cells were responding to GABA treatment in different ways (Figure 39A). Upon gating of each cell population (Figures 39A and 40), it was seen that only the cell group lying closest to the Y axis were showing a decrease in fluorescence in response to addition of 1 mM GABA. Addition of muscimol to fMLP stimulated PBMCs also led to a splitting of the histogram into two peaks, although this was not as distinctive as the effect seen with GABA. However, in contrast to the GABA response, the whole histogram shifts to the left, showing that all the cells in the PBMC fraction respond to application of muscimol. In the nervous system, muscimol is known to have a higher affinity for $GABA_A$ receptors than GABA (Baur and Sigel, 2003). Based on this, if functional $GABA_A$ receptors are present on immune cells, then muscimol may be able to bind to these receptors with a higher affinity which would explain why all the cells in the PBMC fraction respond to muscimol addition.

Bicuculline addition also caused the histogram to split into two peaks, although this effect was even smaller than that of muscimol (Figure 39B). Cells in the PBMC fraction are clearly responding to GABA in a different way to muscimol and bicuculline. One way to identify if these cells were T or B cells or monocytes, would be to label the PBMCs with fluorescent cell-type specific antibodies (e.g. anti-CD3, anti-CD19 and anti-CD14), and to then sort these cells according to the fluorescent dyes used. However, this could not be carried out as the responses to GABA and muscimol were somewhat variable. The cause for this is not entirely known, but one possible reason may be because as mentioned above $GABA_A$ receptors in particular, are fast-acting ligand-gated ion channels. Therefore, the incubation times for the transmitter could have led to desensitisation of any functional $GABA_A$ receptors present on the cells. Based on these points it seems evident that using the FACS for these experiments is perhaps not the best option, as compounds have to be added and mixed manually before placing the tube containing cells into the machine. This leaves room for human error in terms of keeping to exact times, etc. From the experiments carried out in the FLIPR, it was clear that the fMLP and LPS response took place within seconds of addition. Any delay on my part in placing the cells into the FACS after addition of both compounds led to a significant decrease in fluorescence readings.

The results from real-time quantitative RT-PCR showed that human neutrophils and PBMCs contained low level expression of mRNAs for $\alpha 1$, $\alpha 2$ and β glycine receptor subunits. However, no glycine receptor subunits could be detected in human PBMCs via qualitative RT-PCR. This is possibly because the high sensitivity of real-time RT-PCR had been able to detect the low level expression of these receptor subunits. Protein expression studies had also been carried out on human PBMCs and neutrophil using anti- $\alpha 1$, anti-$\alpha 2$ and anti-β glycine subunit antibodies. However, due to a high level of background staining, the presence of glycine receptor subunits on immune cells could not be shown. In the above experiments, addition of 1 mM glycine consistently had no significant effects on agonist induced $[Ca^{2+}]_i$ release from the human and rat neutrophils and PBMCs (Figures 36A and 38A).

Overall these studies clearly show that the presence of functional glycine receptors on human and rat neutrophils is unlikely. This is in contrast to data published by Wheeler *et al.* (2000), where the presence of functional glycine receptors on rat neutrophils was strongly suggested. However, functional $GABA_A$ receptors on human PBMCs and possibly also on rat PBMCs, may be present. Data from RT-PCR and protein expression studies showed the expression of a number of $GABA_A$ receptor subunits, in particular, the $GABA_A$ α1 subunit. GABA and muscimol also appear to modulate the immune cell response to inflammatory stimuli such as fMLP and LPS. Even though these effects were small, they were relatively consistent, although the magnitude of the response varied somewhat. This was probably because immune cells are subject to donor variation due to conditions such as cell activation as a result of a cold or an allergic reaction etc. Sometimes immune cells from the same donor showed variations in magnitude of response to addition of GABA or muscimol. This was particularly true if the donor was stressed or was suffering from a cold. In these cases, even though cell response to fMLP and LPS was relatively consistent, GABA and muscimol seemed to have a slightly stronger effect on reducing $[Ca^{2+}]_i$ release. Although these were casual observations, it could be explained by the fact that a cold or infection will lead to upregulation and activation of immune cells, which may lead to stronger responses to external stimuli. Also, studies have shown that fMLP stimulation of immune cells at low concentrations, selectively triggers directional movement and sustained $[Ca^{2+}]_i$ oscillations whereas higher concentrations initiates secretory functions (e.g. production of superoxide anions) which is concomitant with $[Ca^{2+}]_i$ release (Jaconi *et al.*, 1988). These dose-dependent changes in cell function could explain the limited effect of GABA in these assays, due to the maximal stimulation being given to the cells. Further tests should be performed to determine if GABA has a more potent effect on cells stimulated with lower doses of fMLP.

Conclusion

The qualitative and quantitative RT-PCRs and the immunoblotting and imunofluorescence experiments have all shown that the $GABA_A$ receptor α1 subunit mRNA and protein are present in human peripheral blood mononuclear cells. The RT-PCR results showed the presence of $GABA_A$ δ and ε subunits mRNAs. Neither γ2 or γ3 subunit mRNAs were detected in human PBMCs, an observation which agrees with findings by Bergeret *et al.* (1998) who reported that RT-PCR studies on P815 mast cells and H9 T cells showed no signals corresponding to γ1 and γ2 subunit mRNAs. These results suggest that $GABA_A$ receptors in immune cells would not exhibit benzodiazepine potentiation. The δ and ε subunits can replace γ subunits to form benzodiazepine-insensitive functional $GABA_A$ receptors (Shivers *et al.*, 1989; Sommer *et al.*, 1990; Davies *et al.*, 1997; Moss and Smart, 2001), and these receptors differ in their pharmacological profiles to γ containing receptors (Saxena and Macdonald, 1994; Mehta and Ticku, 1999; Sinkkonen *et al.*, 2000).

Studies of recombinant $GABA_A$ receptors report that the potency of inhibition by the external blocker, Zn^{2+}, is profoundly affected by the subunit composition of the receptor (Draguhn *et al.*, 1990; Smart *et al.*, 1991). $GABA_A$ receptors composed of αβγ subunits show markedly lower sensitivity to Zn^{2+} compared to αβδ and αβε receptors (Draguhn *et al.*, 1990; Smart *et al.*, 1991; Saxena and Macdonald, 1994; Saxena and Macdonald, 1996; Whiting *et al.*, 1997; Krishek *et al.*, 1998). Also, cells expressing α1β1ε $GABA_A$ receptors show reduced sensitivity to the anaesthetic 2,6-diisopropylphenol (propofol) and the benzodiazepine flunitrazepam (Whiting *et al.* 1997; Davies *et al.*, 2001), compared to cells containing α1β1γ2s $GABA_A$ receptors. Additionally, α1β1ε receptors exhibit rapid desensitization kinetics, as compared with α1β1 or α1β1γ2s $GABA_A$ receptors (Davies *et al.*, 2001), and α1β3ε receptors show increased potency and efficacy of direct activation by the barbiturate pentobarbital, neurosteroids and the partial $GABA_A$ agonists piperidine-4-sulphonic acid and thio-4-PIOL, as compared to α1β3γ2 $GABA_A$ receptors (Maksay *et al.*, 2003). These distinct pharmacological profiles

could be used to carry out further studies to test for the presence of δ and ε containing functional $GABA_A$ receptor subunits in human immune cells.

FLIPR and FACS methods were used in this project to study changes in $[Ca^{2+}]_i$ release from human and rat neutrophils and PBMCs, and the results clearly showed that functional glycine receptors are not present on immune cells. This is in contrast to the published work by Wheeler *et al* (2000), which in conjunction with studies on Kupffer cells (liver macrophages) and alveolar macrophages (Ikejima *et al.*, 1997; Wheeler and Thurman, 1999; Froh *et al.*, 2002), suggested that glycine has anti-inflammatory effects and could be useful in many disease states which are dependent on the activation of leukocytes and macrophages (Wheeler *et al.*, 1999b, Froh *et al.*, 2002). However, our data do not support such suggestions.

The data obtained from the FACS studies in this project showed that application of GABA and muscimol leads to a small inhibition of fMLP and LPS induced $[Ca^{2+}]_i$ release from human and rat PBMCs. Based on the mRNA and protein expression studies, any functional $GABA_A$ receptors present on the immune cells would contain the α1 subunit, and that the inhibition of $[Ca^{2+}]_i$ release could be taking place via the interaction of GABA and GABA agonists with these receptors. Various blood cells including lymphocytes have been shown to contain GABA and/or GABA related enzymes, and GABA-related metabolic enzymes have been involved in autoimmune diseases (Erdo and Wolff, 1990; Solimena *et al.*, 1990; Kaufman *et al.*, 1993; Tisch *et al.*, 1993; Schor *et al.*, 2001). Specific $GABA_A$ receptor binding sites have also been identified in platelet membranes (Oset-Gasque *et al.*, 1986; Bergeret *et.al.*, 1998), and GABA levels in the thymus have been shown to increase during an immune response (Hall *et al.*, 1985). Studies have also shown that proliferation of thymic cells and splenic lymphocytes is modulated by $GABA_A$ receptors (Pawlikowski *et al.*, 1987, Pawlikowski *et al.*, 1988).

GABA and GAD have also been shown to have inhibitory effects in the development of insulin-dependent diabetes mellitus, as the insulin producing β-cells also secrete GABA which may reach sufficient levels to down-regulate infiltrating effector T cells (Rorsman et al., 1989). Also, Wan *et al.* (1997) showed that insulin

can up-regulate neuronal $GABA_A$ receptor expression. Therefore, if insulin also increases $GABA_A$ receptors on islet-infiltrating T cells, it could enhance the immuno-inhibitory effect of GABA on T cell function. Bergeret *et al.* (1998) investigated a possible contribution of GABA to the physiology of immune competent cells, and reported that GABA modulates T cell-mediated cytotoxicity, probably via $GABA_A$ receptors, indicating that GABA can modulate immune cell functions. These findings agree with work published by Tian *et al.* (1999) showing that $GABA_A$ receptors can mediate inhibition of mouse T cell responses. Therefore, the presence of functional $GABA_A$ receptors on immune cells could provide new approaches to modulate leukocyte responses in inflammatory diseases.

References

Abbas, A. K., Lichtman, A.H., Pober, J.S. **CELLULAR AND MOLECULAR IMMUNOLOGY.** 2000. 4th edition **Publisher:** W B Saunders, London

Afan, A.M., Broome, C.S., Nicholls, S.E., Whetton, A.D. & Miyan, J.A. 1997. ***Bone marrow innervation regulates cellular retention in murine haemopoietic system.*** Br. J. Haematol. 98; 569-577

Akagi, H., Hirai, K. & Hishinuma, F. 1991. ***Cloning of a glycine receptor subtype expressed in rat brain and spinal cord during a specific period of neuronal development.*** FEBS Lett. 281; 160-166

Aller MI, Paniagua MA, Pollard S, Stephenson FA, Fernandez-Lopez A. 2003. ***The GABA(A) receptor complex in the chicken brain: immunocytochemical distribution of alpha 1- and gamma 2-subunits and autoradiographic distribution of BZ1 and BZ2 binding sites.*** J Chem Neuroanat. 25(1); 1-18.

Al-Mokdad, M., Shibata, F., Nakagawa, H. 1997. ***Effects of cytokine-induced neutrophil chemoattractants (CINCs) on shape change, adhesiveness and phagocytosis of rat neutrophils.*** Biol. Pharm. Bull. 20; 920-923

Amenta F, El-Assouad D, Mignini F, Ricci A, Tayebati SK. 2002. ***Neurotransmitter receptor expression by peripheral mononuclear cells: possible marker of neuronal damage by exposure to radiations.*** Cell Mol Biol. 48(4); 415-21.

Ando, T., Fujii, T & Kawashima, K. 1999. ***Expression of three acetylcholinesterase mRNAs in human lymphocytes.*** Jpn. J. Pharmacol. 79 (I), 289.

Aprison, M.H. and Werman, R. 1965. ***The distribution of glycine in cat spinal cord and roots.*** Life Sci. 4(21); 2075-83.

Aprison, M.H., and Daly, E.C. 1978. ***Biochemical aspects of transmission at inhibitory synapses: The role of glycine.*** In ADVANCES IN NEUROCHEMISTRY, 3rd edition. Agranoff, B.W., and Aprison, M.H. 203-294. Plenum publishing corporation, New York.

Aprison, M.H. 1990. ***The discovery of the neurotransmitter role of glycine.*** **In: Glycine neurotransmission.** Ottersen, O. & Storm-Mathisen, V. Eds. Wiley, Chichester, England. 1-23

Artico, M., Bosco, S., Cavallotti, C., Agostinelli, E., Giulliani-Piccari, G., Sciorio, S., Cocco, L. & Vitale, M. 2002. ***Noradrenergic and cholinergic innervation of the bone marrow.*** Int. J. Mol. Med. 10; 77-80

Backus KH, Arigoni M, Drescher U, Scheurer L, Malherbe P, Mohler H, Benson JA. 1993. ***Stoichiometry of a recombinant GABAA receptor deduced from mutation-induced rectification.*** Neuroreport. 5(3); 285-8.

Barker JL, McBurney RN, Mathers DA. 1983. ***Convulsant-induced depression of amino acid responses in cultured mouse spinal neurones studied under voltage clamp.*** Br J Pharmacol. 80(4); 619-29.

Ball, E.D., Graziano, R.F., Shen, L. & Fanger, M.W. 1982. ***Monoclonal antibodies to novel myeloid antigens reveal human neutrophil heterogeneity.*** Proc. Natl. Acad. Sci. USA. 79: 5374

Balazovich KJ, Suchard SJ, Remick DG, Boxer LA. 1996. ***Tumor necrosis factor-alpha and FMLP receptors are functionally linked during FMLP-stimulated activation of adherent human neutrophils.*** Blood. 88(2); 690-696.

Bany, U., Ryzewaki, J. and Maslinski, W. 1999. ***Relative amounts of mRNA encoding four subtypes of muscarinic receptors (m2-m5) in human peripheral blood mononuclear cells.*** J. Neuroimmunol. 97; 191-195

Barker JL, McBurney RN, Mathers DA. 1983. ***Convulsant-induced depression of amino acid responses in cultured mouse spinal neurones studied under voltage clamp.*** Br J Pharmacol. 80(4); 619-29.

Barnard, E.A., Darlison, M.G. and Seeburg, P. 1987. ***Molecular biology of the GABAA receptor: The receptor/channel superfamily.*** Trends Neurosci. 10; 502

Barnard EA, Skolnick P, Olsen RW, Mohler H, Sieghart W, Biggio G, Braestrup C, Bateson AN, Langer SZ. 1998. ***International Union of Pharmacology. XV. Subtypes of gamma-aminobutyric acidA receptors: classification on the basis of subunit structure and receptor function.*** Pharmacol Rev. 50(2); 291-313.

Bate, L. & Gardiner, M. 1999. ***Structure of a neuronal nicotinic acetylcholine receptor (nAChR).*** In EXPERT REVIEWS IN MOLECULAR MEDICINE. Cambridge University Press. http://www.ermm.cbcu.cam.ac.uk.

Baur, R., and Sigel, E. 2003. ***On high- and low-affinity agonist sites in GABAA receptors.*** J. Neurochem. 87; 325-332.

Bear, M.F., Connors, B.W., and Paradiso, M.A. 1996. **NEUROSCIENCE: EXPLORING THE BRAIN.** Williams and Wilkins, USA.

Becker, C.M., Hoch, W. & Bertz, H. 1988. ***Glycine receptor heterogeneity in rat spinal cord during postnatal development.*** EMBO J. 7; 3717-3726

Becker, E.L. 1990. ***The short and happy life of neutrophil activation.*** J. Leuko. Biol. 47; 378-389

Becker, C.M., Schmieden, V., Tarroni, P., Strasser, U., and Betz, H. 1992. ***Isoform-selective deficit of glycine receptors in the mouse mutant spastic.*** Neuron. 8; 283-289

Benke, D., Fritschy, J.M., Trzeciak, A., Bannwarth, W., and Möhler, H. 1994. ***Distribution, prevalence, and drug binding profile of γ–aminobutyric acid type A receptor subtypes differing in the β – subunit variant.*** J.Biol.Chem. 269; 27100-27107

Bergeret, M., Khrestchatisky, M., Tremblay, E., Bernard, A., Gregoire, A., and Chany, C. 1998. ***GABA modulates cytotoxicity of immunocompetent cells expressing GABAA receptor subunits.*** Biomed. and Phamacother. 52; 214-219

Berridge, M. J., and R. F. Irvine. 1984. ***Inositol trisphosphate, a novel second messenger in cellular signal transduction.*** Nature (Lond.). 312:315-321.

Betz, H., *et.al.* 1999. ***Structure and functions of inhibitory and excitatory glycine recptors.*** Ann. NY Acad. Sci. 868; 667-676

Bokoch, G. M., and Gilman, A. G. 1984. ***Inhibition of receptor-mediated release of arachidonic acid by pertussis toxin.*** *Cell* 39(2);301-308

Bongioanni, P. 1993. ***Neuroimmunomodulation. The bi- and unilateral correlations between the nervous system and the immune system.*** Minerva Med. 84 (7-8); 365-381

Bonnert, T.P., McKernan, R.M.., Farrar, S., Bourdelles, B.L., Heavens, R.P., Smith, D.W., Hewson, L., Rigby, M.R., Sirinathsinghji, D.J.S., Brown, N., Wafford, K.A and Whiting, P.J. 1999. ***θ, a novel $GABA_A$ receptor subunit.*** Proc. Natl. Acad. Sci. USA. 96; 9891-9896

Bormann, J. and Clapham, D.E. 1985. ***Gamma-Aminobutyric acid receptor channels in adrenal chromaffin cells: a patch-clamp study.*** Proc. Natl. Acad. Sci. USA. 82 (7); 2168-2172

Bormann, J. 1988. ***Electrophysiology of GABAA and GABAB receptor subtypes.*** TINS. 11(3); 112-116

Bormann, J. and Feigenspan, A. 1995. ***$GABA_C$ receptors.*** Trends Neurosci. 18; 515-519

Bormann, J. 2000. ***The 'ABC' of GABA receptors.*** Trends Pharmacol. Sci. 21; 16-19

Boulay, F., Tardif, M., Brouchon, L., and Vignais, P. 1990. ***Synthesis and use of a novel N-formyl peptide derivative to isolate a human N-formyl peptide receptor cDNA.*** Biochem. Biophys. Res. Commun.168;1103-1109.

Boyum, A., Lovhaug, D., Tresland, L. & Nordlie, E.M. 1991. ***Separation of leucocytes: improved cell purity by fine adjustments of gradient medium density and osmolality***. Scand. J. Immunol. 34(6); 697-712

Bradford, M.M. 1976. ***A rapid and sensitive method for the quantitation of microgram quantities of protein utilizing the principle of protein-dye binding.*** Anal. Biochem. 7(72); 248-254

Buchstaller, A., Adamiker, D., Fuchs, K., and Sieghart, W. 1991. ***N-Deglycosylation and immunological identification indicates the existence of β-subunit isoforms of the rat $GABA_A$ receptor***. FEBS Lett. 287; 27-30

Buchstaller, A., Fuchs, K., and Sieghart, W. 1991. ***Identification of α1 subunit, α2 subunit and α3 subunit isoforms of the $GABA_A$ benzodiazepine receptor in the rat brain***. Neurosci Lett. 120, 237-241

Burt DR, Kamatchi GL. 1991. ***GABAA receptor subtypes: from pharmacology to molecular biology.*** FASEB J. 5(14); 2916-23.

Callard RE, Rigley KP, Smith SH, Thurstan S, Shields JG. 1992. ***CD19 regulation of human B cell responses. B cell proliferation and antibody secretion are inhibited or enhanced by ligation of the CD19 surface glycoprotein depending on the stimulating signal used.*** J Immunol. 148(10) ; 2983-7.

Calvano JE, Agnese DM, Um JY, Goshima M, Singhal R, Coyle SM, Reddell MT, Kumar A, Calvano SE, Lowry SF. 2003. ***Modulation of the lipopolysaccharide receptor complex (CD14, TLR4, MD-2) and toll-like receptor 2 in systemic inflammatory response syndrome-positive patients with and without infection: relationship to tolerance.*** Shock. 20(5);415-9

Cavagnaro, J. 1986. ***Molecular basis for the bidirectional modulation of the neuroendocrine and the immune systems.*** Year. Immunol. 2, 303-322

Cavallotti C, Artico M, De Santis S. 1999. ***Occurrence of GABA-transaminase in the thymus gland of juvenile and aged rats.*** Eur J Histochem. 43(4); 293-9.

Chang Y, Wang R, Barot S, Weiss DS. 1996. ***Stoichiometry of a recombinant GABAA receptor.*** J Neurosci. 16(17); 5415-24.

Chebib M, Johnston GA. 1999. ***The 'ABC' of GABA receptors: a brief review.*** Clin Exp Pharmacol Physiol. 26(11); 937-40.

Chen LW, Jan CR. 2001. ***Mechanisms and modulation of formyl-methionyl-leucyl-phenylalanine (fMLP)-induced Ca2+ mobilization in human neutrophils.*** Int Immunopharmacol. 1(7):1341-1349

Cherubini E, Gaiarsa JL, Ben-Ari Y. 1991. ***GABA: an excitatory transmitter in early postnatal life.*** Trends Neurosci. 14(12);515-9.

Cherubini, E. & Conti, F. 2001. ***Generating diversity at GABAergic synapses.*** Trends. Neurosci. 24(3); 155-162

Cockcroft, S., Baldwin, J. M., and Allan, D. 1984. ***The Ca2+-activated polyphosphoinositide phosphodiesterase of human and rabbit neutrophil membranes.*** Biochem. J. 221(2); 447-482

Costa, P., Auger, C.B., Traver, D.J. and Costa, L.G. 1995. ***Identification of m3, m4 and m5 subtypes of muscarinic receptor mRNA in human blood mononuclear cells.*** J. Neuroimmunol. 60; 45-51

Cotter, M.J., Norman, K.E., Hellewell, P.G. & Ridger, V.C. 2001. ***A novel method for the isolation of neutrophils from murine blood using negative immunomagnetic separation***. Am. J. Path. 159(2); 473-481

Curtis, D.R. and Watkins, J.C. 1960. ***The excitation and depression of spinal neurones by structurally related amino acids.*** J Neurochem. 6; 117-41

Curtis, D.R., Hosli, L., Johnston, G.A.R. & Johnston, I.H. 1968. ***The hyperpolarisation of spinal motoneurones by glycine and related amino acids.*** Exp. Brain. Res. 5; 235-258

Curtis, D.R., Hosli, L. & Johnston, G.A.R. 1968. ***A pharmacological study of the depression of spinal neurones by glycine and related amino acids.*** Exp. Brain Res. 6; 1-18

Dahinden, C., Galanos, C., Fehr, J. 1983. ***Granulocyte activation by endotoxin. I. Correlation between adherence and other granulocyte functions, and role of endotoxin structure on biologic activity.*** J Immunol. 130(2):857-62

Dantzer R, and Wollman EE. 2003. ***Relationships between the brain and the immune system.*** J Soc Biol. 197(2);81-8.

Davidoff RA, Shank RP, Graham LT Jr, Aprison MH, Werman R. 1967. ***Association of glycine with spinal interneurones.*** Nature. 214(89);680-1.

Davidoff RA, Aprison MH. 1969. ***Picrotoxin antagonism of the inhibition of interneurons by glycine.*** Life Sci. 8(1); 107-12

Davies, P.A., Kirkness, E.F. and Hales, T.G. 2001. ***Evidence for the formation of functionally distinct αβγε GABAA receptors***. Journal of Physiology . 537.1; 101–113

Davies, P.A., Hanna, M.C., Hales, T.G. and Kirkness, E.F. 1997. ***Insensitivity to anaesthetic agents conferred by a class of $GABA_A$ receptor subunit.*** Nature. 385; 820-823

DeLorey TM, Olsen RW. 1992. ***Gamma-aminobutyric acidA receptor structure and function.*** J Biol Chem. 267(24); 16747-50.

de Nardin E, Radel SJ, Genco RJ. 1991. ***Isolation and partial characterization of the formyl peptide receptor components on human neutrophils.*** Biochem Biophys Res Commun. 174(1); 84-9.

de Rie MA, Schumacher TN, van Schijndel GM, van Lier RA, Miedema F. 1989. ***Regulatory role of CD19 molecules in B-cell activation and differentiation.*** Cell Immunol. 118(2); 368-81

Draguhn A, Verdorn TA, Ewert M, Seeburg PH, Sakmann B. 1990. ***Functional and molecular distinction between recombinant rat GABAA receptor subtypes by Zn2+.*** Neuron. 5(6); 781-8.

Duggan M.J, Stephenson F.A. 1989. ***Bovine gamma-aminobutyric acidA receptor sequence-specific antibodies: identification of two epitopes which are recognised in both native and denatured gamma-aminobutyric acidA receptors.*** J Neurochem. 53(1):132-9.

Duggan M.J, Stephenson F.A. 1990. ***Biochemical evidence for the existence of γ-Aminobutyrate$_A$ Receptor Iso-oligomers.*** J. Biol Chem. 265 (7); 3831-3835.

Erdo, S.L. 1984. ***Identification of GABA receptor binding sites in rat and rabbit uterus.*** Biochem Biophys Res Commun. 125(1);18-24.

Erdo, S.L. and Maksay, G. 1988. ***[35S]TBPS binding to membranes of the female sex organs: modulation of chloride ionophore by GABA and pentobarbital.*** Eur J Pharmacol. 147(2); 279-82.

Erdo, S.L., Ezer, E., Matuz, J., Wolff, J.R. and Amenta, F. 1989. ***GABA$_A$ receptors in the rat stomach may mediate mucoprotective effects.*** Eur J Pharmacol. 165(1);79-86.

Erdo, S.L. and Wolff, J.R. 1990. ***Gamma-aminobutyric acid outside the mammalian brain.*** J. Neurochemistry. 54; 363-372

Erdo, S.L. and Wekerle, L. 1990. ***GABA$_A$ type binding sites on membranes of spermatozoa.*** Life Sci. 47(13);1147-1151.

Erlander MG, Tobin AJ. 1991. ***The structural and functional heterogeneity of glutamic acid decarboxylase: a review.*** Neurochem Res. 16(3); 215-26.

Evans, R.H. 1978. ***Measurement of the antagonism of glycine by strychnine in the immature rat spinal cord in vitro [proceedings]*** Br J Pharmacol. 62(3); 431P-432P

Fajardo, O., Galeno, J., Urbina, M., Carreira, I., Lima, L. 2003. ***Serotonin, serotonin 5-HT (1A) receptors and dopamine in peripheral lymphocytes of major depression patients.*** Int. Immunopharmacol. 3 (9); 1345-52

Faraj BA, Olkowski ZL, Jackson RT. 1994. ***Expression of a high-affinity serotonin transporter in human lymphocytes.*** Int J Immunopharmacol. 16(7); 561-7.

Farrar, S.J., Whiting, P.J., Bonnert, T.P. and McKernan, R.M. 1999. ***Stoichiometry of a ligand-gated ion channel determined by fluorescence energy transfer.*** J. Biol. Chem. 274; 10100-10104

Fatani, J.A., Qayyum, M.A., Mehta, L., & Singh, U. 1986. ***Parasympathetic innervation of the thymus: a histochemical and immunocytochemical study.*** J. Anat. 147; 115-119

Felten, D.L., Felten, S.Y., Carlson, S.L., Olschowka, J.A. & Livnat, S. 1985. ***Noradrenergic and peptidergic innervation of lymphoid tissue.*** J. Immunol. 135; 755s-765s

Felten, S.Y., Felten, D.L., Bellinger, D.L., Carlson, S.L., Ackerman, K.D., Madden, K.S., Olschowka, J.A. & Livnat, S. 1988. ***Noradrenergic sympathetic innervation of lymphoid organs.*** Prog. Allergy. 43;14-36

Feng, D.F. & Doolittle, R.F. 1990. ***Progressive alignment and phylogenetic tree construction of protein sequences***. Methods Enzymol. 183; 375

Forehand, J.R., Pabstt M.J., Phillips,W.A. & Johnston, R.B. 1989. ***Lipopolysaccharide Priming of Human Neutrophils for an Enhanced Respiratory Burst Role of Intracellular Free Calcium***. J. Clin. Invest. 83; 74-83

Froh, M., Thurman, R.G., & Wheeler, M.D. 2002. ***Molecular evidence for a glycine-gated chloride channel in macrophages and leukocytes.*** Am. J. Physiol. Gastrointest Liver Physiol. 283; G856-G863

Fujii, T., Mori, Y., Tominaga, H., Hayasaka, I. and Kawashima, K. 1997. ***Maintenance of constant acetylcholine content before and after feeding in young chimpanzees.*** Neurosci. Lett. 227; 21-24

Fujii, T., Tajima, S., Yamada, S., Watanabe, Y., Sato, K.Z., Matsui, M., Misawa, H., Kasahara, T. and Kawashima, K. 1999. ***Constitutive expression of mRNA for the same choline acetyltransferase as that in the nervous system, an acetylcholine-synthesizing enzyme, in human leukemic T-cell lines.*** Neurosci. Lett. 259; 71-74

Fujii, T. and Kawashima, K. ***An independent non-neuronal cholinergic system in lymphocytes.*** 2001. Jpn. J. Pharmacol. 85; 11-15

Germain RN, Stefanova I, Dorfman J. 2002. ***Self-recognition and the regulation of CD4+ T cell survival.*** Adv Exp Med Biol. 512; 97-105.

Ghosh M.C, Mondal A.C, Basu S, Banerjee S, Majumder J, Bhattacharya D, Dasgupta P.S. 2003. ***Dopamine inhibits the cytokine release and expression of tyrosine kinases, Lck and Fyn in activated T cells.*** Int. Immunopharmacol. 3 (7); 1019-1026

Gilon P, Reusens-Billen B, Remacle C, Janssens de Varebeke P, Pauwels G, Hoet JJ. 1987. ***Localization of high-affinity GABA uptake and GABA content in the rat duodenum during development.*** Cell Tissue Res. 249(3):593-600.

Goetzl, E.J., Adelman, C., and Sreedharan, S.P. 1990. ***Neuroimmunology.*** Advances in immunology. 48; 161

Gordon, J. & Barnes, N.M. 2003. ***Lymphocytes transport serotonin and dopamine: agony or ecstasy.*** Trends Immunol. 24 (8); 438-443.

Grenningloh G, Rienitz A, Schmitt B, Methfessel C, Zensen M, Beyreuther K, Gundelfinger ED, Betz H. 1987. ***The strychnine-binding subunit of the glycine receptor shows homology with nicotinic acetylcholine receptors.*** Nature. 328 (6127); 215-220

Grenningloh G, Pribilla I, Prior P, Multhaup G, Beyreuther K, Taleb O, Betz H. 1990a. ***Cloning and expression of the 58 kd beta subunit of the inhibitory glycine receptor.*** Neuron. 4(6); 963-70.

Grenningloh G, Schmieden V, Schofield PR, Seeburg PH, Siddique T, Mohandas TK, Becker CM, Betz H. 1990b. ***Alpha subunit variants of the human glycine receptor: primary structures, functional expression and chromosomal localization of the corresponding genes.*** EMBO J. 9(3); 771-6.

Guthrie, L. A., L. C. McPhail, P. M. Henson, and R. B. Johnston, Jr. 1984. ***Priming of neutrophils for enhanced release of oxygen metabolites by bacterial lipopolysaccharide.*** J. Exp. Med. 160; 1656-1671.

Hadingham KL, Wingrove PB, Wafford KA, Bain C, Kemp JA, Palmer KJ, Wilson AW, Wilcox AS, Sikela JM, Ragan CI. 1993. ***Role of the beta subunit in determining the pharmacology of human gamma-aminobutyric acid type A receptors.*** Mol Pharmacol. 44(6);1211-8.

Hadingham KL, Garrett EM, Wafford KA, Bain C, Heavens RP, Sirinathsinghji DJ, Whiting PJ. 1996. ***Cloning of cDNAs encoding the human gamma-aminobutyric acid type A receptor alpha 6 subunit and characterization of the pharmacology of alpha 6-containing receptors.*** Mol Pharmacol. 49(2); 253-9.

Hall NR, Suria A, Goldstein AL. 1985. ***Elevated levels of gamma amino butyric acid (GABA) in the thymus gland during the immune response.*** Lymphokine Res. 4(4); 339-41.

Halper JP, Mann JJ, Weksler ME, Bilezikian JP, Sweeney JA, Brown RP, Golbourne T. 1984. ***Beta adrenergic receptors and cyclic AMP levels in intact human lymphocytes: effects of age and gender.*** Life Sci. 35(8); 855-63.

Handford CA, Lynch JW, Baker E, Webb GC, Ford JH, Sutherland GR, Schofield PR. 1996. ***The human glycine receptor beta subunit: primary structure, functional characterisation and chromosomal localisation of the human and murine genes.*** Brain Res Mol Brain Res. 35(1-2); 211-9.

Hedblom, E. and Kirkness, E.F. 1997. ***A novel class of $GABA_A$ receptor subunit in tissues of the reproductive system.*** J. Biol. Chem. 272;15346-15350

Heid, C.A., Stevens, J., Livak, K.J. and Williams, P.M. 1996. ***Real time quantitative PCR.*** Genome Res. 6; 86-94

Hiemke, C., Stolp, M., Reuss, S., Wavers, A., Reinhardt, S., Maelicke, A., Schlegel, S. and Schroder, H. 1996. ***Expression of alpha subunit genes of nicotinic receptors in human lymphocytes.*** Neurosci Lett. 214; 171-174

Hills JM, Jessen KR, Mirsky R. 1987. ***An immunohistochemical study of the distribution of enteric GABA-containing neurons in the rat and guinea-pig intestine.*** Neuroscience. 22(1); 301-12.

Hills JM, King BF, Mirsky R, Jessen KR. 1988. ***Immunohistochemical localisation and electrophysiological actions of GABA in prevertebral ganglia in guinea-pig.*** J Auton Nerv Syst. 22(2);129-40.

Hosie AM, Dunne EL, Harvey RJ, Smart TG. 2003. ***Zinc-mediated inhibition of GABA(A) receptors: discrete binding sites underlie subtype specificity.*** Nat Neurosci. 6(4):362-9.

Hu JH, He XB, Wu Q, Yan YC, Koide SS. 2002. ***Subunit composition and function of GABAA receptors of rat spermatozoa.*** Neurochem Res. 27(3);195-9.

Ikejima K, Iimuro Y, Forman DT, Thurman RG. 1996. ***A diet containing glycine improves survival in endotoxin shock in the rat.*** Am J Physiol. 271(1 Pt 1);G97-103.

Ikejima, K., Qu, W., Stachlewitz, R.F. and Thurman, R.G. 1997. ***Kupffer cells contain a glycine-gated chloride channel.*** Am. J. Physiol. 272; G1581-G1586

Ito, S. and Cherubini, E. 1991. ***Strychnine-sensitive glycine responses of neonatal rat hippocampal neurones.*** J Physiol. 440; 67-83.

Jaconi, E.E.M., Rivest, R.W., Schlegel, W., Wollheim, C.B., Pittet, D.P. and Lew, D. 1988. ***Spontaneous and chemoattractant-induced oscillations of cytosolic free calcium in single adherent human neutrophils.*** J.Biochem. 263(22); 10557-10560

Jayaram, Y., & Hogg, N. 1989. ***Expression of CD14 molecules by human neutrophils.*** Tissue Antigens. 33; 199

Kastrup J, Pedersen LO, Dietrich J, Lauritsen JP, Menne C, Geisler C. 2002. ***In vitro production and characterization of partly assembled human CD3 complexes.*** Scand J Immunol. 56(5); 436-42.

Kaufman DL, Clare-Salzler M, Tian J, Forsthuber T, Ting GS, Robinson P, Atkinson MA, Sercarz EE, Tobin AJ, Lehmann PV. 1993. ***Spontaneous loss of T-cell tolerance to glutamic acid decarboxylase in murine insulin-dependent diabetes.*** Nature. 366(6450); 69-72.

Kawashima, K., Fujii, T., Watanabe, Y. and Misawa, H. 1998. ***Acetylcholine synthesis and muscarinic receptor subtype mRNA expression in T-lymphocytes.*** Life sciences. 62(17/18), 1701-1705

Kawashima, K., and Fujii, T. 2000. ***Extraneuronal cholinergic system in leukocytes.*** Pharmacology and Therapeutics. 86; 29-48

Koning F, Maloy WL, Coligan JE. 1990. ***The implications of subunit interactions for the structure of the T cell receptor-CD3 complex.*** Eur J Immunol. 20(2); 299-305.

Koo, C., Lefkowitz, R. J., and R. Snyderman. 1983. ***Guanine nucleotides modulate the binding affinity of the oligopeptide chemoattractant receptor of human polymorphonuclear leukocytes.*** J. Clin. Invest. 72; 748-753.

Krause, K., Demaurex, N., Jaconi, M., and Lew, D.P. 1993. ***Ion channels and receptor-mediated Ca2+ influx in neutrophil granulocytes.*** Blood cells. 19; 165-173

Krishek BJ, Moss SJ, Smart TG. 1998. ***Interaction of H+ and Zn2+ on recombinant and native rat neuronal GABAA receptors.*** J Physiol. 507 (Pt 3); 639-52.

Kuhse, J., Schmieden, V. & Bertz, H. 1990a. ***A single amino acid exchange alters the pharmacology of neonatal rat glycine receptor subunit.*** Neuron. 5; 867-873

Kuhse, J., Schmieden, V. & Bertz, H. 1990b. ***Identification and functional expression of a novel ligand binding subunit of the inhibitory glycine receptor.*** J. Biol. Chem. 265; 22317-22320

Kuhse J, Laube B, Magalei D, Betz H. 1993. ***Assembly of the inhibitory glycine receptor: identification of amino acid sequence motifs governing subunit stoichiometry.*** Neuron. 11(6);1049-56.

Labeta, M.O., Landmann, R., Obrecht, J.P. & Obrist.R. 1991. ***Human B cells express membrane bound and soluble forms of the CD14 myeloid antigen.*** Mol. Immunol. 28; 115-122

Lad, P. M., Glovsky, M. M., Richards, J. H., Learn, D. B., Reisinger, D. M., and P. A. Smiley. 1984. ***Identification of receptor regulatory proteins, membrane glycoproteins, and functional characteristics of adenylate cyclase in vesicles derived from the human neutrophil.*** Mol. Immunol. 21:627-639.

Langosch, D., Thoma, L., and Betz, H. 1988. ***Conserved quaternary structure of ligand-gated ion channels: the postsynaptic glycine receptor is a pentamer.*** Proc. Natl. Acad. Sci. USA. 85; 7394-7398

Langosch, D., Becker, C.M., and Betz, H. 1990. ***The inhibitory glycine receptor: a ligand gated chloride channel of the central nervous system.*** Eur. J. Biochem. 194; 1-8

Lanier, L.L. and Phillips, J.H. 1996. ***Inhibitory MHC class 1 receptors on NK cells and T cells.*** Immunol. Today. 17; 86-91

Laszlo A, Villanyi P, Zsolnai B, Erdo SL. 1989. ***Gamma-aminobutyric acid, its related enzymes and receptor-binding sites in the human ovary and fallopian tube.*** Gynecol Obstet Invest. 28(2); 94-7

Latz, E., Visintin, A., Lien, E., Fitzgerald, K.A., Espevik, T. and Golenbock D.T. 2003. ***The LPS receptor generates inflammatory signals from the cell surface.*** J. End. Res. 9(6); 375-380

Laurie, D.J., Seeburg, P.H. and Wisden, W. 1992. ***The distribution of 13 GABAA receptor subunit mRNAs in the rat brain. II. Olfactory bulb and cerebellum.*** J. Neurosci. 12. 1063-1076

Lima, L. and Urbina, M. 2002. ***Serotonin transporter modulation in blood lymphocytes from patients with major depression.*** Cell Mol Neurobiol. 22(5-6); 797-804.

Link, H., Xu, Z.Y., Melms, A., Kalbacher, H., Sun, J.B., Wang, Z.Y., Fredrikson, S., Olsson, T. 1992. ***The T-cell repertoire in myasthenia gravis involves multiple cholinergic receptor epitopes***. Scand. J. Immunol. 36; 405-414

Lüscher, B. 2002. ***GABAA and GABAC receptors: regulation of assembly, localisation, clustering and turnover.*** In: RECEPTOR AND ION-CHANNEL TRAFFICKING-CELL BIOLOGY OF LIGAND-GATED AND VOLTAGE-SENSITIVE ION CHANNELS. Editors: Moss, S.J. and Henley, J. Molecular and Cellular Neurobiology Series. Series Advisors: Davies, R.W., Collingridge, G.L. and Hunt, S.P. OXFORD UNIVERSITY PRESS

Macdonald, R.L. and Olsen, R.W. 1994. ***$GABA_A$ receptor channels.*** Annu. Rev. Neurosci. 17; 569-602

Macdonald, R.L. & Twyman, R.E. 1991. ***Biophysical properties and regulation of GABAA receptor channels.*** Sem. Neurosci. 3; 219

Majewska MD, Vaupel DB. 1991. ***Steroid control of uterine motility via gamma-aminobutyric acidA receptors in the rabbit: a novel mechanism?*** J Endocrinol. 131(3); 427-34.

Maksay G, Thompson SA, Wafford KA. 2003. ***The pharmacology of spontaneously open alpha 1 beta 3 epsilon GABA A receptor-ionophores.*** Neuropharmacology. 44(8); 994-1002.

Maslinski W. 1989. ***Cholinergic receptors of lymphocytes.*** Brain Behav Immun. 3(1); 1-14.

Maslinski W, Laskowska-Bozek H, Ryzewski J. 1992. ***Nicotinic receptors of rat lymphocytes during adjuvant polyarthritis.*** J Neurosci Res. 31(2); 336-40.

Mehta AK, Ticku MK. 1999. ***An update on GABAA receptors.*** Brain Res Brain Res Rev. 29(2-3); 196-217.

McKenna F, McLaughlin PJ, Lewis BJ, Sibbring GC, Cummerson JA, Bowen-Jones D, Moots RJ. 2002. ***Dopamine receptor expression on human T- and B-lymphocytes, monocytes, neutrophils, eosinophils and NK cells: a flow cytometric study.*** J. Neuroimmunol. 132 (1-2); 34-40

McKernan, R.M., Quirk, K., Prince, R., Cox, P.A., Gillard, N.P., Ragan, C.I., and Whiting, P. 1991. ***$GABA_A$ receptor subtypes immunopurified from rat brain with α subunit-specific antibodies have unique pharmacological properties.*** Neuron. 7; 667-676

McKernan, R.M. and Whiting, P.J. 1996. ***Which $GABA_A$-receptor subtypes really occur in the brain?*** Trends Neurosci. 19; 139-143

Michalik, M. and Erecinska, M. 1992. ***GABA in pancreatic islets: metabolism and function.*** Biochem Pharmacol. 44(1); 1-9.

Mignini, F., Streccioni, V., & Amenta, F. 2003. ***Autonomic innervation of immune organs and neuroimmune modulation.*** Autonomic and Autacoid Pharmacology. 23. 1-25

Mihovilovic, M. & Roses, A.D. 1991. ***Expression of mRNAs in human thymus coding for the α3 subunit of a neuronal acetylcholine receptor.*** Exp. Neurol. 111; 175-180

Mihovilovic, M. & Roses, A.D. 1993. ***Expression of α3, α5, and β4 neuronal acetylcholine receptor subunit transcripts in normal and myasthenia gravis thymus.*** J. Immunol. 151; 6517-6524

Miller GW, Lock EA, Schnellmann RG. 1994. ***Strychnine and glycine protect renal proximal tubules from various nephrotoxicants and act in the late phase of necrotic cell injury.*** Toxicol Appl Pharmacol. 125(2); 192-7.

Minta, A., Kao, J.P.Y. & Tsien, R.Y. 1989. ***Fluorescent indicators for cytosolic calcium based on rhodamine and fluorescein chromophores.*** J.Biol. Chem. 264, 8171-8178

Morris, M.R., Doull, I.J.M. and Hallet, M.B. 2001. ***Osmotically induced cytosolic free Ca2+ changes in human neutrophils.*** Biochimica et Biophysica Acta. 1538; 20-27

Moss, S.J. and Smart, T.G. 2001. ***Constructing inhibitory synapses***. Nat. Neurosci. 2(4); 240-250

Nio, D.A., Moylan, R.N. and Roche J.K. 1993. ***Modulation of T lymphocyte function by neuropeptides.*** J. Immunology. 150 (12); 5281-5288

Niiro H, Clark EA. 2002. ***Regulation of B-cell fate by antigen-receptor signals.*** Nat Rev Immunol. 2(12); 945-56.

Nussler AK, Wittel UA, Nussler NC, Beger HG. 1999. ***Leukocytes, the Janus cells in inflammatory disease.*** Langenbecks Arch Surg. 384(2); 222-32.

Olsen R.W. and Tobin A.J. 1990. ***Molecular biology of $GABA_A$ receptors.*** FASEB Journal. 4 (5); 1469-1480

Olsen RW, Sapp DM, Bureau MH, Turner DM, Kokka N. 1991a. ***Allosteric actions of central nervous system depressants including anesthetics on subtypes of the inhibitory gamma-aminobutyric acidA receptor-chloride channel complex.*** Ann N Y Acad Sci. 625; 145-54.

Olsen RW, Bureau M, Endo S, Smith G, Deng L, Sapp D, Tobin AJ. 1991b. ***GABAA-benzodiazepine receptors: demonstration of pharmacological subtypes in the brain.*** Adv Exp Med Biol. 287; 355-64.

Ong, J., and Kerr, D.I.B. 1982. ***GABAA- and GABAB-receptor-mediated modification of intestinal motility.*** Eur. J. Pharmacol. 86 (1); 9-17

Ong, J. and Kerr, D.I.B. 1984. ***Potentiation of GABAA-receptor-mediated responses by barbiturates in the guinea-pig ileum.*** Eur J. Pharmacol. 103 (3-4); 327-332

Oset-Gasque, M.J., Launay, J.M., Gonzalez, M.P. 1986. ***GABAergic mechanisms in blood cells: their possible role.*** In: GABAERGIC MECHANISMS IN THE MAMMALIAN PERIPHERY. Eds: Erdo, S.L., Bowery, N.G. Publisher: Raven Press, New York . pp: 305

Owens, T. 1988. ***A noncognate interaction with anti-receptor antibody-activated helper T cells induces small resting murine B cells to proliferate and to secrete antibody.*** Eur J Immunol. 18(3); 395-401.

Owens, T. 1991. ***A role for adhesion molecules in contact-dependent T help for B cells.*** Eur J Immunol. 21(4); 979-83

Paldi-Haris P, Szelenyi JG, Nguyen TH, Hollan SR. 1990. ***Changes in the expression of the cholinergic structures of human T lymphocytes due to maturation and stimulation.*** Thymus. 16(2); 119-22.

Parducz A, Dobo E, Wolff JR, Petrusz P, Erdo SL. 1992. ***GABA-immunoreactive structures in rat kidney.*** J Histochem Cytochem. 40(5):675-80.

Pawlikowski M, Stepien H, Mroz-Wasilewska Z, Pawlikowska A. 1987. ***Effects of diazepam on cell proliferation in cerebral cortex, anterior pituitary and thymus of developing rats.*** Life Sci. 40(11); 1131-5.

Pawlikowski M, Lyson K, Kunert-Radek J, Stepien H. 1988. ***Effect of benzodiazepines on the proliferation of mouse spleen lymphocytes in vitro.*** J Neural Transm. 73(2); 161-6.

Persohn E, Malherbe P, Richards JG. 1992. ***Comparative molecular neuroanatomy of cloned GABAA receptor subunits in the rat CNS.*** J Comp Neurol. 326(2);193-216.

Pfeiffer, F. & Betz, H. 1981. ***Solubilisation of the glycine receptor from rat spinal cord.*** Brain Res. 226; 273-279

Pfeiffer, F., Graham, D. & Betz, H. 1982. ***Purification by affinity chromatography of the glycine receptor of rat spinal cord.*** J. Biol. Chem. 257; 9389-9393

Poon, B.Y., Ward, C.A., Giles, W.R. & Kubes, P. 1999. ***Emigrated neutrophils regulate ventricular contractility via alpha4 integrin.*** Circ. Res. 84; 1245-1251

Prentki, M., C. B. Wollheim, and P. D. Lew. 1984. ***Ca2+ homeostasis in permeabilized human neutrophils. Characterization of Ca2+-sequestering pools and the action of inositol 1,4,5-trisphosphate.*** J. Biol. Chem. 259:13777-13782.

Prpic, V., J. E. Weiel, S. D. Somers, J. DiGuiseppi, S. L. Gonias, S. V. Pizzo, T. A. Hamilton, B. Herman, and D. 0. Adams. 1987. ***Effects of bacterial lipopolysaccharide on the hydrolysis of phosphatidylinositol-4,-5-bisphosphate in murine peritoneal macrophages.*** J. Immunol. 139; 526-533.

Qian, H. & Ripps, H. 1999. ***Response kinetics and pharmacological properties of heteromeric receptors formed by coassembly of GABA rho- and gamma 2-subunits.*** Proc. R. Soc. Lond. B.Biol. Sci. 266;2419-2425

Rabow, L.E., Russek, S.J., and Farb., D.H. 1995. ***From ion currents to genomic analysis, recent advances in $GABA_A$ receptor research.*** Synapse. 21; 189-274

Radel SJ, Genco RJ, De Nardin E. 1994. ***Structural and functional characterization of the human formyl peptide receptor ligand-binding region.*** Infect Immun. 62(5); 1726-32.

Rajendra S, Lynch JW, Schofield PR. 1997. ***The glycine receptor.*** Pharmacol Ther. 73(2); 121-46.

Razin, E., Pecht, I. and Rivera, J. 1995. ***Signal transduction in the activation of mast cells and basophils.*** Immunol. Today. 16; 370-373

Rebut-Bonneton C, Bailly S, Pasquier C. 1988. ***Superoxide anion production in glass-adherent polymorphonuclear leukocytes and its relationship to calcium movement.*** J Leukoc Biol. 44(5):402-10

Reth, M. 1995. ***The B-cell antigen receptor complex and co-receptors.*** Immunol Today. 16(7); 310-3.

Revy P, Sospedra M, Barbour B, Trautmann A. 2001. ***Functional antigen-independent synapses formed between T cells and dendritic cells.*** Nat Immunol. 2(10); 925-31.

Ricci A, Chiandussi L, Schena M, Schiavone D, Veglio F, Amenta F. 1995. ***Dopamine D5 receptor expression is unchanged in peripheral blood lymphocytes in essential hypertension.*** Clin Exp Hypertens. 17 (8); 1157-72.

Rinner, I. and Schauenstein, K. 1991. ***The parasympathetic nervous system takes part in the immuno-neuroendocrine dialogue.*** J Neuroimmunol. 34(2-3); 165-72.

Rodeberg, D.A., Morris, R.E. & Babcock, G.F. 1997. ***Azurophilic granules of human neutrophils contain CD14.*** Infection and Immunity. 65(11); 4747-4753

Roitt, I.M., Brostoff, J. and Male, D. 1998. **IMMUNOLOGY**. 5th edition. **Publisher**: Mosby, London

Rorsman P, Berggren PO, Bokvist K, Ericson H, Mohler H, Ostenson CG, Smith PA. 1989. ***Glucose-inhibition of glucagon secretion involves activation of GABAA-receptor chloride channels.*** Nature. 341(6239); 233-6.

Rosoff, P. M., and L. C. Cantley. 1985. ***Lipopolysaccharide and phorbol esters induce differentiation but have opposite effects on phosphatidylinositol turnover and Ca2l mobilization in 70Z/3 pre-B lymphocytes.*** J. Biol. Chem. 260;9209-9215.

Roussel, E. and Gingras, M.C. 1997. ***Transendothelial migration induces rapid expression on neutrophils of granule-release VLA6 used for tissue infiltration.*** J. Leukoc. Biol. 62; 356-362

Saha B, Mondal AC, Majumder J, Basu S, Dasgupta PS. 2001. ***Physiological concentrations of dopamine inhibit the proliferation and cytotoxicity of human CD4+ and CD8+ T cells in vitro: a receptor-mediated mechanism.*** Neuroimmunomodulation. 9(1); 23-33.

Sato, E., Koyama, S., Okubo, Y., Kubo, K. and Sekiguchi, M. 1998. ***Acetylcholine stimulates alveolar macrophages to release inflammatory cell chemotactic activity.*** Am. J. Physiol. 274; L970-L979

Saxena, N.C. and Macdonald, R.L. 1994. ***Assembly of GABAA receptor subunits: role of δ subunit.*** J.Neurosci. 14(11);7077-7086

Schiffman, E., Corcoran, B. A., and Wahl, S. M. 1975. ***N-formylmethionyl peptides as chemoattractants for leukocytes.*** Proc.*Natl. Acad. Sci. U. S.* A. 72,1059-1062

Schor DS, Struys EA, Hogema BM, Gibson KM, Jakobs C. 2001. ***Development of a stable-isotope dilution assay for gamma-aminobutyric acid (GABA) transaminase in isolated leukocytes and evidence that GABA and beta-alanine transaminases are identical.*** Clin Chem. 47(3); 525-31.

Schmid G, Bonanno G, Raiteri L, Sarviharju M, Korpi ER, Raiteri M. 1999. ***Enhanced benzodiazepine and ethanol actions on cerebellar GABA(A) receptors mediating glutamate release in an alcohol-sensitive rat line.*** Neuropharmacology. 38(9):1273-9.

Schmieden, V., Grenningloh, G., Schofield, P.R. & Betz, H. 1989. ***Functional expression in Xenopus oocytes of the strychnine binding 48 kd subunit of the glycine receptor.*** EMBO J. 8;695

Shivers, B.D., Killisch, I., Sprengel, R., Sontheimer, H. and Kohler, M. 1989. ***Two novel GABAA receptor subunits exist in distinct neuronal subpopulations.*** Neuron. 3; 327

Sieghart, W. 1995. ***Structure and pharmacology of gamma-aminobutyric acidA receptor subtypes.*** Pharmacol. Rev. 47 (2); 181-234

Sieghart, W. 2000. ***Unraveling the function of $GABA_A$ receptor subtypes.*** Trends Pharmacol.Sci. 21; 411-413

Sigel, E. 2002. ***Mapping of the benzodiazepine recognition site on GABA(A) receptors.*** Curr Top Med Chem. 2(8); 833-839

Sinkkonen ST, Hanna MC, Kirkness EF, Korpi ER. 2000. ***GABA(A) receptor epsilon and theta subunits display unusual structural variation between species and are enriched in the rat locus ceruleus.*** J Neurosci. 20(10); 3588-95.

Skok, M.V., Kalashnik, E.N., Koval, L.N., Tsetlin, V.I., Utkin, Y.N., Changeux, J-P & Grailhe, R. 2003. ***Functional nicotininc acetylcholine receptors are expressed in B lymphocyte-derived cell lines.*** 64(4); 885-889

Smart TG, Moss SJ, Xie X, Huganir RL. 1991. ***GABAA receptors are differentially sensitive to zinc: dependence on subunit composition.*** Br J Pharmacol. 103(4); 1837-9.

Smith, C. D., Lane, B. C., Kusaka , I., Verghese, M. W. and Snyderman, R.. 1985. ***Chemoattractant receptor-induced hydrolysis of phosphatidylinositol 4,5-bisphosphate in polymorphonuclear leukocyte membranes. Requirement for a guanine nucleotide regulatory protein.*** J. Biol. Chem. 260;5875-5878.

Solimena M, Folli F, Aparisi R, Pozza G, De Camilli P. 1990. ***Autoantibodies to GABA-ergic neurons and pancreatic beta cells in stiff-man syndrome.*** N Engl J Med. 322(22); 1555-60.

Solomkin JS, Tindal CJ, Cave CM, Zemlan F. 1994. ***Regulation of TNF-alpha receptor expression on human neutrophils by various cell activating factors.*** J Surg Res. 56(3); 261-6.

Sommer, B., Poustka, A., Spurr, N.K. and Seeburg, P.H. 1990. ***The murine GABAA receptor delta gene: Structure and assignment to human chromosome 1.*** DNA Cell Biol. 9; 561

Sontheimer, H., Becker, C-M., Pritchett, D.B., Schofield, P.R., Grenningloh, G., Kettenmann, H., Betz, H., & Seeburg, P.H. 1989. ***Functional chloride channels by mammalian cell expression of rat glycine receptor subunit.*** Neuron. 2;1491

Spits, H. 2002. ***Development of alphabeta T cells in the human thymus.*** Nat Rev Immunol. 2(10); 760-72.

Spittler A, Reissner CM, Oehler R, Gornikiewicz A, Gruenberger T, Manhart N, Brodowicz T, Mittlboeck M, Boltz-Nitulescu G, Roth E. 1999. ***Immunomodulatory effects of glycine on LPS-treated monocytes: reduced TNF-alpha production and accelerated IL-10 expression.*** FASEB J. 13(3); 563-71.

Springer, T.A. 1994. ***Traffic signals for lymphocyte recirculation and leukocyte emigration: the multistep paradigm.*** Cell. 76; 301-314

Stefulj J, Jernej B, Cicin-Sain L, Rinner I, Schauenstein K. 2000. ***mRNA expression of serotonin receptors in cells of the immune tissues of the rat.*** Brain Behav Immun. 14(3); 219-24.

Stenson, W.F., Mehta, J. and Spilberg, I. 1984. ***Sulfasalazine inhibition of binding of N-formyl-methionyl-leucyl-phenylalanine (fMLP) to its receptor on human neutrophils.*** Biochem. Pharmacol. 33 (3); 407-412

Stephenson, F.A. 1988. ***Understanding the $GABA_A$ receptor: a chemically gated ion channel.*** Biochem. J. 249 (1); 21-32

Stephenson, A. 1995. ***The $GABA_A$ receptors***. Biochem J. 310. 1-9

Szelenyi J, Paldi-Haris P, Hollan S. 1987. ***Changes in the cholinergic system of lymphocytes due to mitogenic stimulation.*** Immunol Lett. 16(1); 49-54.

Tabarowski, Z., Gibson-Berry, K. & Felten, S.Y. 1996. ***Noradrenergic and peptidergic innervation of the mouse femur bone marrow.*** Acta Histochem. 98; 453-457

Tanaka, C. 1985. ***gamma-Aminobutyric acid in peripheral tissues.*** Life Sci. 37(24); 2221-35.

Tanigawa T, Kotake Y, Reinke LA. 1993. ***Spin trapping of superoxide from glass adherent polymorphonuclear leukocytes induced by N-formylmethionyl-leucyl-phenylalanine.*** Free Radic Res Commun. 19(2); 101-10.

Tayebati, S.K., El-Assouad, D., Ricci, A. and Amenta, F. 2002. ***Immunochemical and immunocytochemical characterization of cholinergic markers in human peripheral blood lymphocytes.*** 132; 147-155

Tennenberg SD, Zemlan FP, Solomkin JS. 1988. ***Characterization of N-formyl-methionyl-leucyl-phenylalanine receptors on human neutrophils. Effects of***

isolation and temperature on receptor expression and functional activity. J Immunol. 141(11); 3937-44.

Terstappen, L.W.M.M., Hollander, Z., Meiners, H. & Loken, M.R. 1990. ***Quantitative comparison of myeloid antigens on five lineages of mature peripheral blood cells.*** J. Leukocyte Biol. 48; 138-148

Tian, J., Chau, C., Hales, T.G. and Kaufman, D.L. 1999. ***$GABA_A$ receptors mediate inhibition of T cell responses.*** J NeuroImmunology. 96; 21-28

Ticku, M.K. 1991. ***Ethanol interactions at the gamma-aminobutyric acid receptor complex.*** Ann N Y Acad Sci. 625; 136-44.

Tisch, R., Yang, X.D., Singer, S.M., Liblau, R.S. Fugger, L., Mcdevitt, H.O. 1993. ***Immune response to glutamic acid decarboxylase correlates with insulitis in non-obese diabetic mice.*** Nature. 366; 72

Tissot, M., Pradelles, P. and Giroud, J.P. 1988. ***Substance P-like levels in inflammatory exudates.*** Inflammation. 12; 25

Topilko A, Caillou B. 1985. ***Acetylcholinesterase in human thymus cells.*** Blood. 66(4); 891-5.

Toyabe, S., Iiai, T., Fukada, M., Kawamura, T., Suzuki, S., Uchiyama, M. and Abo, T. 1997. ***Identification of nicotinic acetylcholine receptors on lymphocytes in the periphery as well as thymus in mice.*** Immunology. 92; 201-205

Tretter V, Ehya N, Fuchs K, Sieghart W. 1997. ***Stoichiometry and assembly of a recombinant GABAA receptor subtype.*** J Neurosci. 17(8); 2728-37.

Troelstra A, de Graaf-Miltenburg LA, van Bommel T, Verhoef J, Van Kessel KP, Van Strijp JA. 1999. ***Lipopolysaccharide-coated erythrocytes activate human neutrophils via CD14 while subsequent binding is through CD11b/CD18.*** J Immunol. 162(7); 4220-5.

Tyndale, R., Olsen, R.W., Tobin, A.J. 1995. ***$GABA_A$ receptors.*** In: HANDBOOK OF RECEPTORS AND CHANNELS: LIGAND AND VOLTAGE GATED ION CHANNELS. Boca Raton, FL: CRC Press. 261-286

Valerio A, Tinti C, Spano P, Memo M. 1992. ***Rat pituitary cells selectively express mRNA encoding the short isoform of the y2 GABAA receptor subunit.*** Brain Res Mol Brain Res. 13(1-2); 145-50.

Vernallis, A.B., Conroy, W.G. & Berg, D.K. 1993. ***Neurons assemble acetylcholine receptors with as many as three kinds of subunits while maintaining subunit segregation among receptor subtypes.*** Neuron. 10; 451

Videm, V. and Strand, E. 2004. ***Changes in neutrophil surface-receptor expression after stimulation with FMLP, endotoxin, interleukin-8 and activated complement compared to degranulation.*** Scand J Immunol. 59(1); 25-33.

Wagner S, Castel M, Gainer H, Yarom Y. 1997. ***GABA in the mammalian suprachiasmatic nucleus and its role in diurnal rhythmicity.*** Nature. 387(6633); 598-603.

Wagner, J.G. and Roth, R.A. 2000. ***Neutrophil migration mechanisms, with an emphasis on the pulmonary vasculature.*** Pharmacol. Rev. 52; 349-374

Wan Q, Xiong ZG, Man HY, Ackerley CA, Braunton J, Lu WY, Becker LE, MacDonald JF, Wang YT. 1997. ***Recruitment of functional GABA(A) receptors to postsynaptic domains by insulin.*** Nature. 388(6643); 686-90.

Wang, T. and Brown, M.J. 1999. ***mRNA quantification by real time TaqMan polymerase chain reaction: Validation and comparison with RNase protection.*** Anal. Biochem. 269; 198-201

Wang, H., Yu, M., Ochani, M., Amella, C.A., Tanovic, M., Susarta, S., Li, J.H., Wang, H., Yang, H., Ulloa, L., Al-Abed, Y., Czura, C.J. and Tracey, K.J. 2002 (22 Dec). ***Nicotinic acetylcholine receptor α7 subunit is an essential regulator of inflammation.*** Nature. doi:10.1038/nature01339. www.nature.com/nature

Wardlaw AJ, Moqbel R, Kay AB. 1995. ***Eosinophils: biology and role in disease.*** Adv Immunol. 60; 151-266.

Werman, R., Davidoff, R.A. & Aprison, M.H. 1967. ***Inhibition of motoneurons by ionophoresis of glycine.*** Nature. 214; 681-683

Werman R, Davidoff RA, Aprison MH. 1968. ***Inhibitory of glycine on spinal neurons in the cat.*** J Neurophysiol. 31(1):81-95.

Wessler, I., Kilbinger, H., Bittinger, F., and Kirkpatrick, C.J. 2001. ***The biological role of non-neuronal acetylcholine in plants and humans.*** Jpn. J. Pharmacol. 85; 2-10

Wessler I, Kilbinger H, Bittinger F, Unger R, Kirkpatrick CJ. 2003. ***The non-neuronal cholinergic system in humans: expression, function and pathophysiology.*** Life Sci. 72(18-19); 2055-61.

Wilsden, W., Laurie, D.J., Monyer, H., and Seeburg, P.H. 1992. ***The distribution of 13 $GABA_A$ receptor subunit mRNAs in the rat brain.*** J. Neuroscience. 12; 1040-1062

Wheeler, M.D., Seabra, V., and Thurman, R.G. 1999a. ***Molecular evidence for glycine-gated chloride channel in Kupffer cells.*** In CELLS OF THE HEPATIC SINUSOID. Wisse, E., Knook, D.L. and Wake, K. The Kupffer cell foundation, Leiden, The Netherlands

Wheeler, M.D., Ikejima, K., Enomoto, N., Stachlewitz, R.F., Seabra, V., Zhong, Z., Schemmer, P., Rose, M.L., Rusyn, I., Bradford, B.U., and Thurman, R.G. 1999b.